# D4.2 | Technology transfer report

**Author(s): Francisco López, Rubén González, Elizabeth Goiri**

**Delivery date: 31.05.2021**

**Version: 1.0**

| | |
|---|---|
| Project Acronym: | SUPERTED |
| Project Full Title: | Thermoelectric detector based on superconductor-ferromagnet heterostructures |
| Call: | H2020-FETOPEN-2016-2017 |
| Topic: | FETOPEN-01-2016-2017 |
| Type of Action: | RIA |
| Grant Number: | 800923 |
| Project URL: | https://superted-project.eu/ |
| Editor: | ADVACAM |
| Deliverable nature: | R |
| Dissemination level: | PU |
| Contractual Delivery Date: | 31.05.2021 |
| Actual Delivery Date : | 31.05.2021 |
| Number of pages: | 177 |

*This project has received funding from the European Union´s Horizon 2020 research and innovation programme under grant agreement No 800923.*

| | |
|---|---|
| **Keywords** | Thermoelectric Detector (TED), Superconducting sensors, Technology Transfer, Applications |
| **Authors** | Francisco López (BIHUR/ADVACAM), Ruben González (BIHUR), Elizabeth Goiri (BIHUR) |
| **Contributors** | Alessandro Monfardini (NEEL), Elia Strambini (CNR), Ilari Maasilta (JYU), Celia Rogero (CSIC), Max Ilin (CSIC), Tero Heikkila (JYU), Juha Kalliopuska (ADVACAM), Sami Vahanen (ADVACAM) and Jouni Ruoppa (ADVACAM) |
| **External Contributors** | Francesc Monrabal (Ikerbasque), Carlos Peña (Laboratorio Subterraneo Canfranc) |


**Abstract**

Project SUPERTED is focused on the first demonstration of a new type of Thermo Electric Detectors - TED, which take advantage of the giant thermoelectric effect for detecting radiation in a wide range of wavelengths, from X-rays up to THz/GHz.

Although TED technology finds itself at an early stage of development, the SUPERTED Consortium has the ambition to push it as fast as possible towards applications, and eventually towards a successful commercial exploitation.

This effort is summarised in this report, which is constituted by three different parts:

- **Technological Landscape:** in order to asses the competitiveness of TED technology, we have gathered a large amount of information related to: 1) other competing technologies, 2) applications in which the technology can be used, 3) markets and actors present in them, and 4) benchmarking data.
- **Collaborative Platforms:** describes the initiatives which are being set in place for testing the TED technology in environments as realistic as possible, related to main applications. These test activities are open to interaction with other researchers from outside the Consortium.
- **Management of Technology Transfer:** describes the actions taken to organise and ease the technology transfer process, as well as the efforts taking for pushing key outcome of the project towards markets.


*This project has received funding from the European Union´s Horizon 2020 research and innovation programme under grant agreement No 800923.*

# Contents

*This project has received funding from the European Union ´s Horizon 2020 research and innovation programme under grant agreement No 800923.*

*This project has received funding from the European Union´s Horizon 2020 research and innovation programme under grant agreement No 800923.*

# Part I

# The Technological Landscape

# 1
# *Introduction*

The detection of electromagnetic radiation is the fundamental physical principle underpinning a wide range of applications. In a zero-order approach, all applications fall into three categories:

*Inspection:* The analysis of how an object interacts with electromagnetic radiation allows to remotely gather information about this object. This is the core of applications like (in order of market share) medical diagnose, security screening or industrial inspection, but also the basis for some of the most powerful techniques for probing the universe from cosmological down to atomic scale. These techniques are at the core of frontier science.

*Transmission:* Controlled emission, transmission and detection of electromagnetic radiation can be used to encode and transfer information between two geometrically separated points. Modern transmission networks rely in this principle, as well as the flow of information through logical circuits in emerging (photonic and quantum) technologies.

Both types of applications have been born and developed mainly through the XX century. In the case of inspection, the use of $X-$rays in medical radiology has been both the starting and driving force. In the case of transmission, the deployment of modern optical and satellite information networks is possibly the most relevant example so far.

While scientific applications in domains like astrophysics and material sciences are niches of much lesser importance in the economical plane, they have played a mayor role in discovery, development and optimisation of many of the related technologies.

The detecting technologies had enabling character in all of these applications, but it would be incorrect to think that the technical performance is the main and/or only determining factor. Once the technical solution makes its way into a market, a much larger and

complex set of parameters will define if it would be able compete against other existing or emerging solutions. A non-exhaustive list of these parameters could be the following:

*Cost:* this factor ultimately determines which type of actors will be able to afford the solutions, and will define the financial structure of the market. While high cost is not necessarily a negative factor, it will expel from the market customers with small financial capacity unless alternative business models (renting, rather than purchase, for instance) are adopted . On the other hand, low cost solutions may lead to small margins that will make the solution viable only for very large volumes.

*Maintenance* Cost: this factor is often underestimated because, while technical solutions are developed, the effect of intensive use is not properly taken into account. Servicing of the system is generally required for supplying consumables, preventively replacing parts or repairing. On top of this, the down-service time generates extra costs linked to the rest of the structure (staff, depreciation of complementary equipment, etc) which are kept idling while the system is put back to work.

*Logistics:* manufacture, install and maintenance of a technically complex solution involves very large supply chains. This multiplies the risks of delays in the supply of critical components and consumables, and of appearance of vulnerabilities due to scarcity of resources.

*Safety:* the intensive use of a system implies a very significant increase in the time exposure of users to potential dangers. This may come from the very own nature of the electromagnetic radiation (X-rays, for instance, carry enough energy to break chemical bond and so they can incur damage to critical biomolecules such as DNA), but also from secondary elements such as high voltage power sources, dangerous liquids and/or gases, etc. A given solution will not be deployed unless safe protocols could be set in place.

*Usability:* complex technical solutions makes it difficult for end users to have enough background regarding the fundamental technologies involved and how they can be set up and controlled. Often such knowledge must be replaced by training of strict usage protocols, and the adoption of a solution largely depends on the ability to be run under a simplified regime where many of the operating parameters are preset or controlled automatically.

*This project has received funding from the European Union´s Horizon 2020 research and innovation programme under grant agreement No 800923.*

*Maturity/Reliability:* the time, effort and resources invested on a technology have a direct impact on its reliability. Improvement often comes from exposure to real conditions, when several usability issues become apparent during operation. Once the solution has successfully entered a market, the number of users, and therefore the amount of feedback, grows rapidly. Not only the maturity of the technology, but also that of the manufacturing processes required to fabricate it, plays an important role.

Because of all these reasons, new technologies have a vulnerability against already adopted ones. The transferring of a new technology, such as Thermo - Electric Detectors - TED, from its laboratory embrionary stage towards the applications (and thus its economical exploitation) will follow a well known process, often described by means of the TRL index.

Along the SUPERTED project, the technology has evolved from TRL1 towards TRL3. In the following TRL levels, the technology will have to be progressively adapted taking into account more and more constraints defined by the applications. The choice of technical solutions, because of the influence of all the aforementioned factors, will definitively have an impact on its fate, as it will determine who will be the competing technologies, and how it will be positioned against them.

On the financial side, funding of the technological development will also find a different landscape. As TRL augments, the possibility to rely on institutional R&D funds will fade away, and only way of funding the activity will depend on a reliable exploitation plan that will ensure a return over investment for the financial players.

For the case of very new technologies, the task is often delegated onto entrepreneurs. Very typically, this individuals will (understandably) have some gaps in their background: either they will come from the technological disciplines (and thus have a sallower knowledge about business development and management) or from business background (with a limited capability to understand very complex technologies). Result from this is that the entrepreneurial projects very often run on inflated expectations, triggering unrealistic audiences, or underestimating the position and actions of other solutions.

In order to have any chance of success, completing the process of technology transfer will require intelligence, i.e. information gathered from reliable sources, and possibly analysed by experts with enough understanding of the relevant knowledge. This information should then be used to make the right technical, strategical and financial decisions.

The purpose of this first chapter is to provide the basis for this kind of analysis. This can be used as a starting point for anybody

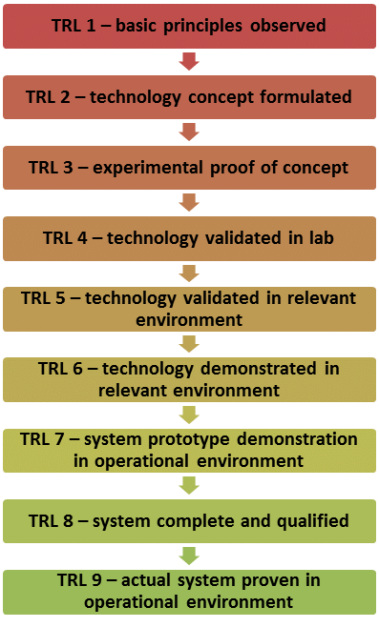


Figure 1.1: **Technology Readiness Level:** This classification (originally developed by NASA) is currently accepted in the H2020 program as a standard for understanding the degree of maturity of an emerging technology.

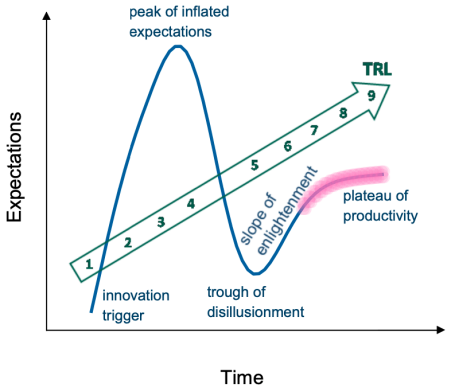


Figure 1.2: **The Gartner hype cycle** analyses the evolution of the expectations through the maturing cycle of a technology. Source: (18).

*This project has received funding from the European Union´s Horizon 2020 research and innovation programme under grant agreement No 800923.*

interested in adopting and making evolve the TED technology.

In order to structure the information, we will analyse separately three areas:

- Competing Technologies.
- Applications range and needs.
- Main Actors present in the markets linked to each application.

The sum of this blocks will provide a picture of the technological landscape. This should allow to reach an understanding about what could be the TED technology competitive advantages and weaknesses, as compared to other alternatives. This refers not only to technical performance but also to more operational issues, like what business models are being adopted, and whether any of the solutions is already at a stage where economical exploitation is taking place.

The last important point to mention is prejudice. Sometimes the potential of a technology is involuntarily biased by the imagination of its developers which, on turn, largely depends on their training and (limited) knowledge. While successful ways of transferring the technology can go through small application niches, maybe not economically significant but with less competition, in most cases developers keep focused in the largest applications, where the economical gain and societal impacts look more attractive. In order to mitigate, and ideally avoid, such situation the intelligence report must be constructed in following a systematic procedure that will start by keeping a large 360º view of the applications landscape, and can try to spot there opportunities where the technology may show a competitive edge. This is the exercise that we have tried to do in this document.

*This project has received funding from the European Union´s Horizon 2020 research and innovation programme under grant agreement No 800923.*

# 2
# *Competing technologies:*

## *2.1 Introduction*

Currently, the workhorses for particle or photon detectors are semiconductor based CCD and CMOS arrays. While these type of sensors are used intensively for high energy particles and photons, they are especially dominant for light within the ultraviolet, visible and near infrared ranges.

The reason for the success of this technology is that devices for this range use Silicon as core material. This choice is not only related to technical performance, but also manufacturability and economy. Silicon has also been the material of choice of microelectronics. This industry has sustained a half-a century long and coordinated effort to improve both material purification and processing technologies. As a consequence, any device which is manufactured relying on this value chain can achieve unpreceded levels of integration and cost competitiveness. This is the case for both CCD and CMOS sensors.

These types of semiconductor detectors are based in the principle of exciting charge carriers across the semiconductor band gap. This band gap defines the detector's basic characteristics, but it is also responsible for significant limitations. The band gap in Si is around 1.1 eV, thus any photon to be detected with a Si-based CCD needs at least this 1.1 eV of energy (equivalent to a 1088 nm wavelength) to excite one electron. Even a photon with just a little below twice this energy still results in the same signal. Semiconductor-based CCDs therefore can only achieve energy resolution on a single pixel basis at energies that are significantly higher than their band gap.

For this reason, small band gap semiconductors like, for instance, HgCdTe, have been used for lower photon energies in the infrared - IR. Nevertheless, practical limitations for their smallest achievable band gaps still restrict their energy resolution and low energy cut-off.

An intriguing option to build on and extend the tremendous success of semiconductor- based detectors is to instead use the much

smaller band gaps found in superconductors. These has triggered several interesting concepts, all leading to the development of sensors which, in many cases, have established the current upper limits of performance in many aspects such as sensitivity and energy resolution.

Superconducting state is characterised by the appearance of coupled pairs of electrons (Cooper pairs) are formed thanks to electron-phonon interaction, once the temperature of the material is below a transition temperature $T_c$. A Cooper-pair has the minimum binding energy $E_g = 2\Delta(T)$, where $\Delta(T)$ is the energy gap of the superconducting material, which is sensitive to T. When $T << T_c$, $Eg = 2\Delta(0) = 3.528 k_B T_c$, where $k_B = 1.381 \times 10^{-23}$ J/K is the Boltzmann constant.

If radiation hits a superconducting material, energy of the incoming photon will cause breaking of a certain amount of Cooper pairs, and appearance of a fraction of electrons that are not in Cooper pairs. These unpaired electrons are often referred to as quasiparticles. Any photon with an energy $hf > 2\triangle$, if absorbed, will break apart Cooper pairs resulting in an excess quasiparticle population $\left(N_{qp} \approx \frac{\eta h\nu}{\triangle}\right)$ where $\eta$ reflects the efficiency of the process of conversion of photons into quasiparticles ($\eta$ will be less that one since some of the energy of the photon will excite phonons in the material lattice). In principle, the amount of broken Cooper pairs will be proportional to the ratio between the energy of the photon $E(\lambda)$ and the superconducting gap energy$E_g$.

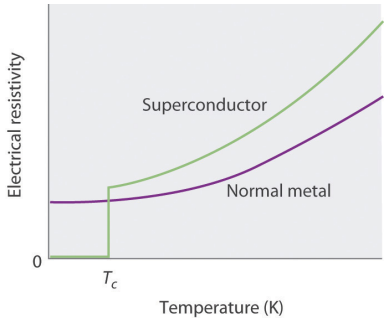


Figure 2.1: **Superconducting state is characterised,** among other things, by a sudden drop of the DC resistance of the material when it reaches the transition temperature $T_c$.

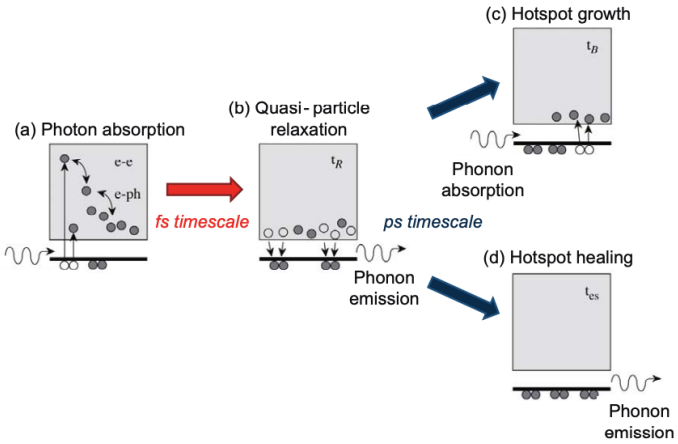


Figure 2.2: **Photo-induced avalanche process in a superconductor.** Adapted from (152).

The chain of processes that take place at atomic scale (also schematiced in Figure 2.2) is the following:

a) A photon with an energy $\omega >> 2\Delta$ breaks up a Cooper pair whilst creating a highly excited quasi-particle and a low energy quasi-particle. The hot electron breaks up additional Cooper pairs

*This project has received funding from the European Union´s Horizon 2020 research and innovation programme under grant agreement No 800923.*

on a fs timescale via electron-electron ($e^- - e^-$) scattering and, subsequently via electron-phonon ($e^-$-ph) interaction.

a) During this thermalisation process the temperature of the electron subsystem $T_e$ rises above $T_C$ leading to a local resistive area. Quasiparticles begin to recombine while emitting phonons at an energy equal to $2\Delta$.

a) These phonons have enough energy to break up additional Cooper pairs resulting in hotspot growth taking place on a ps-timescale.

a) At the same time, thermal phonons escape from the film into the substrate causing hotspot healing and restoration of superconductivity.

All types of superconducting sensors present very low levels of noise and very high sensitivity, efficiency and energy resolution. All these characteristics arise from the intrinsic suppression of thermal noise, due to the ultra-low operating temperatures, and the small energy gaps which are characteristic of the superconducting state.

The sensing technology developed within SUPERTED project falls naturally into the family of superconducting sensors, and will exhibit also very high levels of performance, but also the intrinsic limitations, such as the complexity and cost of the cryogenics needed to reach the superconducting state. It is therefore worth analysing in detail these technologies, in order to understand which are the properties where TED technology shows better performance than the rest.

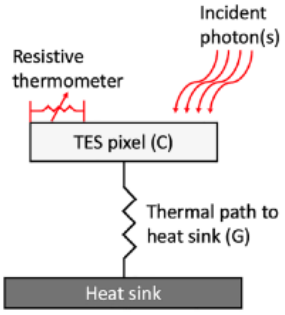


Figure 2.3: **Transition Edge Detector.** On top, schematic representation of the system.

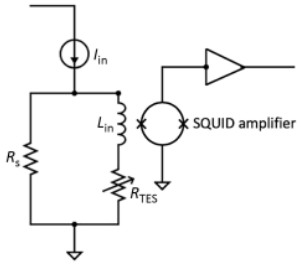


Figure 2.4: **Negative Feedback Circuit and SQUID readout.** When TES resistance increases it causes a drop in TES current. As the Joule power in turn drops the device is cooled back to its equilibrium state in the self-biased region. used for stable operation of the TES. Changes in TES current manifest as a change in the input flux of the SQUID, whose output can then be adequately processed.

## 2.2 *Transition Edge Sensors – TES*

The transition between superconducting and normal state is characterised by a sudden drop of DC resistance at a given temperature ($T_c$). This provides a straightforward detection principle, by which if a material is held at $T_c$, small changes in temperature will cause drastic changes in DC resistance, which can be accurately quantified[1].

For the purpose of radiation detection (see Figure 2.3), the detector consists of a thermal mass of heat capacity $C$ at a temperature $T_0$, isolated from a thermal bath at temperature $T_b$ across a thermal link with conductance $G$. The thermometer measures the temperature of the isolated thermal mass, which can consist of electrons or electrons and phonons. This type of device was proposed along the 1940s, as sensors for infrared radiation first, and alpha-particles later (245). Original devices turned out to be unstable and difficult to use due to the technical difficulty of stabilising operation temperature of

[1] A comprehensive description of TES technology can be found in ref. (148). A very detailed discussion regarding limitations and deviations from ideal behaviour of TES technology can be found in ref (139).

*This project has received funding from the European Union´s Horizon 2020 research and innovation programme under grant agreement No 800923.*

the detector within the superconducting transition range. This difficulty was solved with the introduction of the negative electrothermal feedback(244). Under this configuration, the device is operated at near-constant voltage bias to stabilise the device in the superconducting transition via negative electrothermal feedback. A shunt resistor whose resistance is much smaller than the TESs at its operating point is typically used to achieve voltage bias. The shunt resistance value, in conjunction with the device and bias circuit inductance, sets the electrical time constant.

This structure can be operated both as a calorimeter (for measurement of a discrete deposition of energy), if $\tau_0 = \frac{C}{G} \ggg T$, or as a bolometer (for measurement of quasistatic power dissipated by a flux of photons) if $\tau_0 \lll T$.

In practice, calorimeters are mainly employed for detection of high energy radiation ($\alpha-$particles, $\gamma-$ray and X-ray), and bolometers for detection of microwave, sub-mm, THz and far infrared radiation.

When compared to some available sensing technologies (specially in the optical and mid-IR range), like avalanche photodiodes, TES have been found to be slow devices. Typically, TES have jitter within the range of 100 ns (in comparison, avalanche photodiodes have jitter within the 10 picoseconds range), and single-photon spikes could last in the order of microseconds(231).

In what concerns read-out, several strategies like cross-correction circuits(243) were employed in early experiments, and tried to overcome the difficulty of extracting signal from a very small impedance system. Such schemes were difficult to scale up to many pixel systems. The adoption of SQUID amplifiers(244) has solved many noise related issues and, most importantly, has paved the way for the construction of multiplexed devices, essential for imaging. Time division multiplexing - TDM(242), frequency-division multiplexing FDM , code-division multiplexing (CDM) and microwave SQUID multiplexing ($\mu$MUX) have been already demonstrated. TDM technology, probably the most mature, has been succesfully applied in complex astrophysics projects(241). Similarly, FDM has been applied both in grond based(239) and air borne (240) experiments. CDM technology has prooven to suppress $\frac{1}{f}$ noise to below 20 mHz (238). Finally, $\mu$MUX, in principle, allows for much larger multiplexing factors, compared with all other techniques, because it takes advantage of the change in inductance of the disipationless SQUID for modulating the resonance frequencies of microwave resonators(237). This transducing mechanism allows to remove electronic components from the vicinity of the sensors, thus eliminating sources of thermal noise and leaving room for higher density of detectors. This technology has also recently been deployed for astrophysics applications(236).

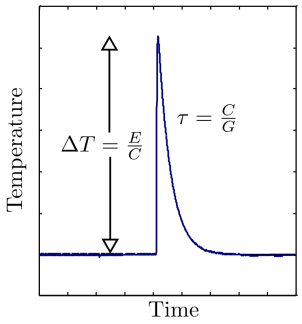


Figure 2.5: **Thermal Behavior** of the TES detector, which is characterised by the heat capacity of the absorber (C) and the thermal path to the heat sink (G).

*This project has received funding from the European Union´s Horizon 2020 research and innovation programme under grant agreement No 800923.*

TESs have been adapted for detection of virtually all relevant ranges of the electromagnetic spectrum. Feed horns coupled with lithographic orthomode transducers (235) and with spiderweb structures (234) have been used for detection in the GHz, THz and far-infrared range(235). Sensors for near-IRm optical and UV range with very efficient absorption (97%) have been constructed using anti-reflective coatings and a gold reflector placed below the TES(233). In the $X-$ray and $\gamma-$ray range resonant structures cannot easily be constructed (due to the very short wavelength of this radiation), but it is often sufficient to use absorbers with high stopping power, like Bi, Sn or HgTe layers in direct contact with the sensor(232).

As what concerns astrophysics, TES-based bolometers have been the dominant technology for detecting continuum radiation in the sub-millimetre region of the spectrum on ground based and space-based instruments. Although these instruments have been very successful, there is an inherent difficulty in scaling these detectors to arrays with more than $10^4$ pixels - as the cost of the cryogenic cooling systems to ensure sufficient removal of thermal signals and to keep the arrays uniformly cooled becomes prohibitive. There are also issues remaining with the scaling of TES arrays to larger than 100 pixels, while still allowing for precise, single photon detection. These issues are still unresolved, though hybridised arrays have been proposed using current amplifier based on nonlinear-kinetic inductance to read the TES current (123). This approach, on top of better scalability, allows to reach operating temperatures of 4.2 K which simplify the cryogenics of the system. A new architecture (Hydra Design), where each TES can handle signals from as many as 25 absorbers, have opened the route for very large scale integration (prototype contains 86,400 pixels) (43). Very recent work has shown how engineering of the device at the nanoscale level allows to achieve substantial increase of sensitivity in the GHz band (23).

The bottom line about TES technology is that it is a mature, well understood solution, which has received attention from scientific community since the early days of superconductivity. Practical demonstrations in all relevant fields of application have been already presented. Several landmark experiments integrate this technology and commercial products are available in the market (see Section 4).

## 2.3 *Hot Electron Bolometers - HEB*

In principle, HEB are quite similar to TES. A film is biased near its superconducting transition, so that its resistance is strongly influenced by the small temperature changes caused by the absorption of radiation. The main difference between HEBs and ordinary bolo-

*This project has received funding from the European Union´s Horizon 2020 research and innovation programme under grant agreement No 800923.*

meters is the speed of their response: HEBs should be fast enough to allow GHz output bandwidths.

High speed is achieved by allowing the radiation power to be directly absorbed by the electrons in the superconductor (as compared to TES bolometers, which uses a separate radiation absorber for allowing the energy to flow to the superconducting material via phonons). When a photon is absorbed in a metal, a single electron initially receives the photon energy $h\nu$. This energy is rapidly shared with other electrons, producing a slight increase in the electron temperature. The electron temperature subsequently relaxes to the bath temperature, usually through the emission of phonons.

A HEB takes advantage of this effect, as near $T_C$, the superconductor's resistance is sensitive to the electron temperature. The thermal relaxation time $\tau$ of the electrons can be made fast by choosing a material with a large electron-phonon interaction, such as NbN , and using very thin films so that the phonons can escape into the substrate before being reabsorbed by the electrons. Alternatively, $\tau$ can be made rapid using electron out diffusion. For a fixed $\tau$ , the heat capacity sets the required local oscillator power and can be minimised by using a very small volume $\left(< 10^{-2}\mu m^3\right)$ of superconducting material. This type of devices (often named mixers) are used in a heterodyne setups[2] and work as as frequency downconverters with high spectral resolution $\left(\frac{\lambda}{\Delta\lambda} > 10^3\right)$.

Historically, HEBs were first developed using semiconductors (and played a role in early sub-millimetre astronomy) but this technology was replaced by other technologies[3]. However, the development of superconducting versions led to very sensitive devices at frequencies in the THz region where they outperform their competitors such as superconductor-insulator-super- conductor SIS tunnel junctions and Schottky diodes.

Coupling to the device is rat straightforward, since the RF impedance is essentially resistive, and can be done either with waveguide or quasi-optical techniques.

Both phonon-cooled and diffusion-cooled devices have been operated at 2.5 THz and above, with IF bandwidths of several gigahertz. The performance of these devices has been steadily improving, and have reached resolution below 1 K/GHz. The phonon-cooled NbN devices generally outperform the diffusion-cooled type. Most of the HEB measurements at higher frequencies are performed using far-IR gas lasers, which have high output power at discrete frequencies, allowing the use of very weakly reflecting beamsplitters for local oscillator injection. An early experiment at 1.5 THz using a waveguide NbN mixer showed that this is indeed possible, achieving a DSB noise temperature around 1500 K with $\backsim 1\mu W$ of local oscillator

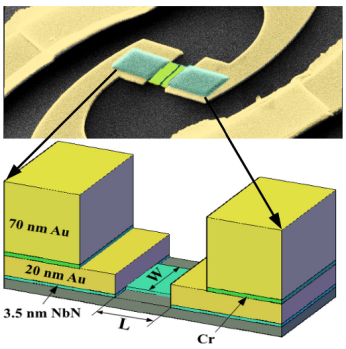


Figure 2.6: **Structure of a Hot Electron Bolometer.** Source: (70).

[2] In heterodyne receivers a RF signal picked up by an antenna at frequency $\nu_{RF}$ and the sine-wave output of a "local" oscillator at frequency $\nu_{LO}$ are combined in a nonlinear device known as a mixer, which generates the beat frequency which generates the beat frequency $\nu_{BF} = |\nu_{RF} - \nu_{LO}|$. The BF signal may then be further down converted or demodulated, and its spectrum is a replica of the original RF spectrum. Very high spectral resolution is possible, since $\nu_{IF} \lll \nu_{BF}$.

[3] A detailed presentation of this technology can be found in ref (73).

*This project has received funding from the European Union 's Horizon 2020 research and innovation programme under grant agreement No 800923.*

power.

Despite the seeming simplicity of the concept, with the HEB device essentially presented by a superconducting micro-bridge imprinted in between the two metallic leads, theoretical description of the HEB physics is quite complicated due to the presence of superconductivity in the leads intended to remain normal(70).

To date, the HEB technology has been successfully employed for a spaceborne mission Herschel (onboard ESA) (72), airborne stratospheric SOFIA experiment (69; 71). The operation of the HEB detectors was also demonstrated in the FIR wave range, where the semiconductor detectors limited by the photoelectric threshold are no longer an option.

## 2.4 *Superconducting Tunnelling Junctions - STJ*

Tunnelling junctions are thee-dimensional structures consisting in two layers of superconducting material separated by a thin insulating layer[4]. Quantum tunnelling allows current to flow through such device. Typical superconducting materials used in the fabrication of STJs are Nb, Tn or Hf separated by a thin insulating layer.

When the STJs are cooled well below the critical temperature $T_c$ of the superconductor material electrons are organised in Cooper pairs, with a binding energy $2\Delta$ (Where $\Delta$ the superconductor energy band gap) which is inversely proportional to $T_c$ . When this is heated due to photon absorption a fraction of the Cooper pairs are broken into quasiparticles, by the continuous pair breaking by phonons with energies greater than $2\Delta$ and the recombination of quasiparticles with the emission of a phonon. The recombination rates for the Cooper pairs is material dependent and tends to happen more slowly on materials with lower $T_c$. Under this situation of perturbation of the equilibrium state of the tunnelling barrier, if a magnetic field is used to suppress the Josephson current and the junction is biased at a nonzero voltage, excess quasiparticles tunnel through the insulating barrier, producing a current pulse which is proportional to the energy of the incoming radiation.

The number of quasiparticles produced is $N_{qp} = E/\epsilon$, where $\epsilon$ is the average energy required to produce a quasiparticle, and $E$ is the energy of the incoming photon. For most superconductors, $\epsilon \approx 1.7\triangle$ where $\triangle$ is the superconducting energy gap. Quasiparticle can tunnel back and forth through the barrier of an STJ detector and this multiple tunnelling can increase the measured signal. The tunnelling rate is inversely proportional to the barrier thickness and the thickness of the superconductor. The barrier can be only so thin before it becomes leaky, allowing resistive current flow and excess noise

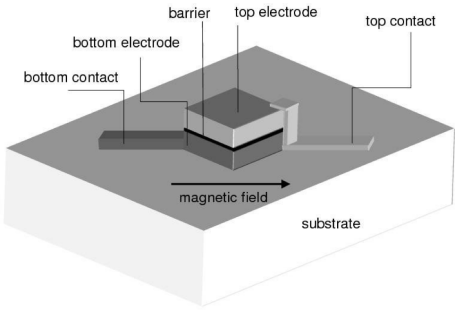


Figure 2.7: **Structure of a STJ sensor.**

[4] A comprehensive description of STJ technology can be found in ref. (147)

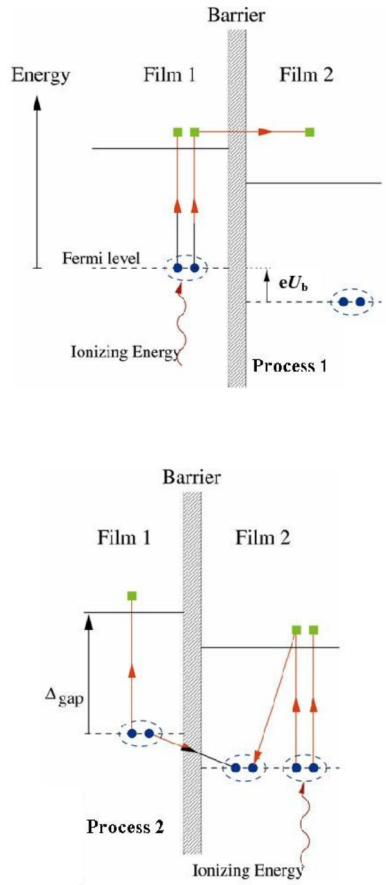


Figure 2.8: **Schematic representation of the possible tunnel processes that can occur in an STJ.** The vertical scale represents energy.

*This project has received funding from the European Union´s Horizon 2020 research and innovation programme under grant agreement No 800923.*

(on top of this, the sensor may have very low absorption efficiency if used for detecting high energy radiation, like X-rays). The tunnelling will stop when the quasiparticles recombine into Cooper pairs, and the $2\Delta$ phonons released by the recombination escape from films to substrates.

Main advantages or STJs are:

a) If appropriated material is selected, the level of cooling required can be easier to handle than that used for bolometers (300mK for STJs vs. 50mK for TES);

a) STJs are grown using epitaxial growth (for instance, and very typically, niobium on a sapphire substrate) and do not require complex micro-machining or lithography techniques;

a) the time constants for STJs are much lower than the thermal relaxation time constants which detectors like TESs rely on; and

a) the fundamental noise due to the random generation and recombination of thermal quasi-particles decreases exponentially with temperature, as $\exp\left(-\frac{\Delta}{\kappa_B T}\right)$. In contrast, bolometric detectors convert the incoming radiation into heat rather than quasiparticle excitations, and their sensitivity exhibits a slower power-law dependence with temperature. However, since the photo-produced quasi-particles are in a sea of Cooper pairs, one needs a method to measure their presence or to separate them out.

In practice, STJ detectors can achieve high energy resolution and high time resolution. In X-ray detectors, for instance, a mean energy resolution of $6.7 \pm 1.0$ eV for 400 eV and time resolution ($< 1$ μs) has been reported(194).

On the other hand, the most critical issue with arrays of STJs is the application of a consistent and exacting magnetic field to suppress the junction current, which has to be uniform across the array. The scalability of arrays is also limited due to the wiring connections of large arrays which lead to lower pixel fill factors as array size increases. These larger arrays also need to be multiplexed to the readout stage, thus increasing the readout time as the array scales.

Although adoption of techniques such as as Distributed Read-Out Imaging Devices (DROID) have tried to overcome these issues, and despite a significant investment of resources (see, for instance, the SCAM program by the European Space Agency), attention from the application developers has slowly faded away, JTSs seem to be displaced by other alternative technologies.

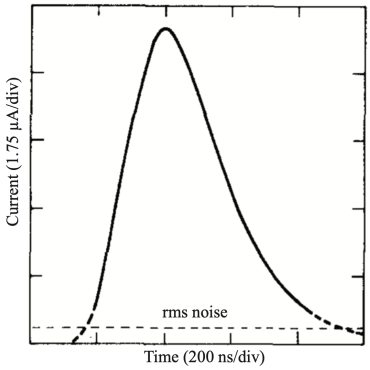


Figure 2.9: **Output pulse induced by an α-particle traversing an STJ.** Dotted line represents the rms (root-mean-square) noise output from the amplifiers.

*This project has received funding from the European Union´s Horizon 2020 research and innovation programme under grant agreement No 800923.*

## 2.5 *Superconducting Nanowire Single Photon Detectors - SNSPD*

This type of sensors are built as a thin and narrow wire (typically about 5 nm wide, and 100 nm long) made of superconducting material. For sensing applications, the wire is arranged in a meander structure, as to maximise the detection area. Basic operation is schematically represented in Figure 2.10.

If the nanowire is maintained below $T_c/2$ and persistently biased by a transport current just below the superconducting critical current $I_c$ (i in the Figure), when a photon with an energy higher than $2\Delta$ impacts on the nanowire, Cooper pairs will be broken into quasiparticles, and the generated quasiparticles form a localised 'hotspot' (ii).

As a consequence, the supercurrent will flow around the hotspot resistive region (iii). This, on turn, will lead to an increase of the current density beyond the critical current density in the sidewalks (iv), creating a resistive barrier across the width of the nanowire (v). The sudden increase in resistance from zero to a finite value generates a measurable voltage pulse across the nanowire. Eventually, due to continuous cooling, the energy dissipates into the substrate by the phonon in the superconductor (vi) and SNSPD recovers to superconducting state (i).

Compared with other single photon detectors, SNSPD possesses higher detection efficiency and a lower dark count rate. In addition, the recovery time and jitter time of SNSPD are faster than those of existing single-photon detectors(192).

For practical applications, another great advantage is related to cooling. Although the operating temperature of SNSPD is below $\frac{T_c}{2}$, the $T_c$ of the materials typically employed can be higher than that of superconducting materials employed in the construction of other types of sensors. SNSPD have been demonstrated above boiling point of liquid helium, which is an obvious advantage, as much simpler cryogenics is required(193).

Taking into account all these features, SNSPDs are a promising alternative for time-correlated single-photon counting, mainly at at infrared wavelengths, offering single-photon sensitivity combined with low DCR[5], low timing jitter $\Delta t$ (tens of ps), short recovery time, and free-running operation. In contrast with all other types of superconducting detectors, which have been mainly developed with sensing applications in mind, SNSPDs are being applied to new emerging, but important applications quantum key distribution (QKD), optical quantum computing, characterisation of quantum emitters, space-to-ground communications, integrated circuit testing, fibre sensing and time- of-flight ranging(190; 193).

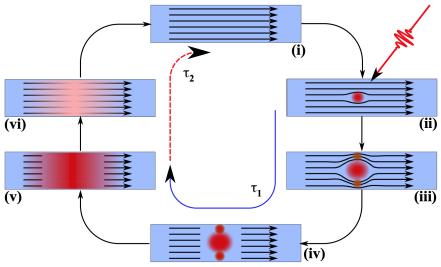


Figure 2.10: **Basic operation principle of the SNSPD.** See text for description. Source:(193)

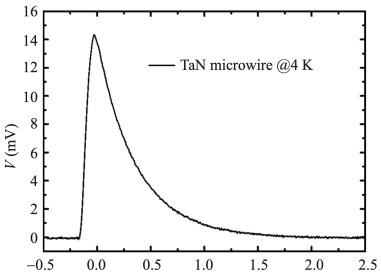


Figure 2.11: **Response pulse of a SNSPD** made of TaN, when exposed to a $Fe^{55}$X-ray source.

[5] DCR: DC resistance of an inductor.

*This project has received funding from the European Union 's Horizon 2020 research and innovation programme under grant agreement No 800923.*

Because of this different orientation of this technology towards applications, the focus on the development efforts has also been different. Efficient integration of the detectors with waveguides, and mainly for IR range, has been demonstrated recently (191). SNSPDs have also found applications in unconventional scientific uses like detection of multi-photon signals, photon counting in strong magnetic fields, detection of signals from massive particles ( from keV-range energy ions and electrons up to MeV charged particles) and detection of neutrons(2).

## 2.6 *Microwave Kinetic Inductance Detectors - MKID*

The Microwave Kinetic Inductance Detector (MKID) concept was originally proposed as an AC method[6] of measuring the relative fraction of paired and unpaired electrons in superconductors.

An electric field applied near the surface of a superconductor causes the Cooper pairs to accelerate, allowing energy storage in the form of kinetic energy. Because the supercurrent is non-dissipative, this energy may be extracted by reversing the electric field. Similarly, energy may be stored in the magnetic field inside the superconductor, which penetrates only a short distance from the surface($\lambda \approx 50nm$). The overall effect is that a superconductor has a surface inductance $L_s = \mu_0\lambda$, due to the reactive energy flow between the superconductor and the electromagnetic field. The surface impedance $Zs = Rs + i\omega L_s$ also includes a surface resistance $R_s$, which describes a.c. losses at angular frequency $\omega$ caused by the appearance of quasiparticles. For temperatures T much lower than $T_c$, $R_s << \omega L_s$.

When applied to sensing, the device will provide information regarding the change in quasiparticle population within the volume of a superconducting film upon photon absorption. These quasiparticles will prevent the Cooper pairs from occupying some of the electron states (through the exclusion principle), which modifies the effective pairing energy and reduces the density of pairs. The result of this event is to alter the complex impedance of the film by increasing the kinetic inductance ($L_s$).

The fundamental energy resolution of the detector is limited by the statistical fluctuation of the number of remaining quasiparticles, given by $\sigma_N = \sqrt{FN_{qp}}$, where F is the Fano factor. The maximum energy resolution of the detector $R = \frac{E}{\delta E}$ is then $R = \frac{1}{2.355}\sqrt{\frac{\eta h\nu}{F\triangle}}$. The Fano factor[7] accounts for the fact that the variance in the number of quasiparticles created is not $N_{qp}$, but is in fact smaller$\left(FN_{qp}\right)$ . This occurs because the energy cascade that takes the original photon's energy and converts it into quasiparticles and phonons is highly correlated, as quasiparticles and phonons interact with each other.

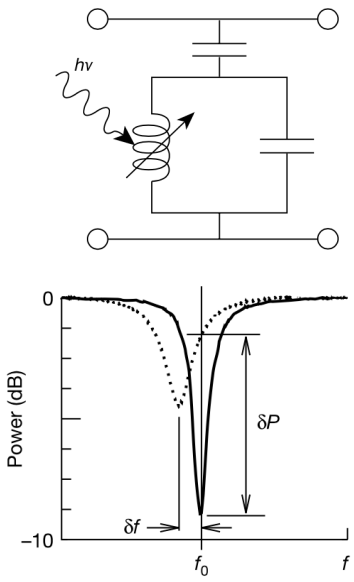


Figure 2.12: **Basic circuit of a MKID.** The quasiparticles produced by the photons will cause shifts the resonance to lower frequency and makes the dip broader and shallower (as shown on bottom, see text for details).

[6] While a superconductor has zero resistance for d.c. electrical current, it has a nonzero impedance for a.c. currents.

[7] Fano factor results from the energy loss in a collision not being purely statistical. The process giving rise to each individual charge carrier is not independent as the number of ways an atom may be ionized is limited by the discrete electron shells. The net result is a better energy resolution than predicted by purely statistical considerations. The Fano factor is material specific (calculated values, as an example, give Si: 0.115; Ge: 0.13; GaAs: 0.12) Source: (17).

*This project has received funding from the European Union´s Horizon 2020 research and innovation programme under grant agreement No 800923.*

The changes in surface impedance, although very small, can be accurately measured by making the strip of superconductor part of a microwave resonant LC circuit, and by monitoring the phase of a microwave signal transmitted through (or past) the resonator. The effect of the surface inductance $L_s$ is to increase the total inductance $L$, while the effect of the surface resistance $R_s$ is to make the inductor slightly lossy (equivalent to adding a series resistance). When at resonance, the LC circuit loads the through line, producing a dip in its transmission. As the quasiparticles produced by the photon increase both $L_s$ and $R_s$, the resonance will be displaced towards lower frequency (due to $L_s$) and makes the dip broader and shallower (due to $R_s$). Both of these effects contribute to changing the amplitude (c) and phase (d) of a microwave probe signal transmitted past the circuit.

This choice of circuit design, which has high transmission away from resonance, is intrinsically very well suited for frequency-domain multiplexing(146). Because in the quarter wave coplanar waveguide - CPW resonator transmission away from the resonance frequency is nearly perfect, multiple resonators can be engineered for operation at slightly different frequencies coupled to the same through line. A single cryogenic HEMT (high electron mobility transistor) amplifier is then capable of amplifying the output signals from a large number of detectors, as many as $10^3$–$10^4$, depending on the amplifier bandwidth and the detector frequency spacing. This depends on the resonator quality factor $Q = f_0/\triangle f$ and the lithographic control of the resonances. An array of synthesisers and quadrature receivers at room temperature can then be used as final section of the read-out system (this technology also applies to, and has been mainly developed for, wireless communications). This approach means as many as 10 000 devices can be read out using only two coaxial lines connected to the detector array.

The mainstream read out procedure described above has some drawbacks. Each element of a KID array must be individually characterised under precisely controlled conditions. A second, even greater challenge is that the response of each KID element changes with temperature, thus requiring in-system re- calibration. Finally, current KIDs require 4-stage cryo-coolers in order to operate at mK temperatures, which are very challenging implementations for many applications. New stimulation and detection approaches for arrays of high- temperature (~4K) KID sensors are being investigated to simplify the electronics required for the source signal and reduce the impact of even small changes in temperature(122).

For practical realisation, it is important to achieve efficient coupling of photons or quasiparticles into the sensitive end of the reson-

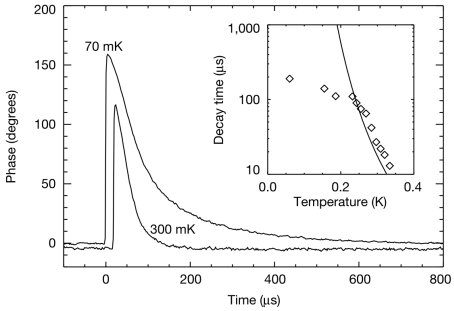


Figure 2.13: **Single-photon X-ray pulses** measured at 70 and 300 mK. Source: (146)

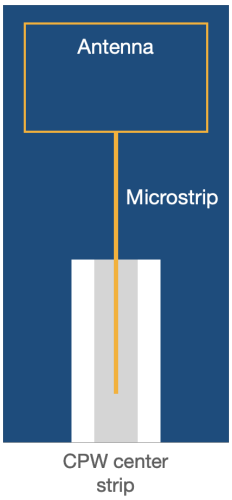


Figure 2.14: **Typical Structure of a MKID adapted for detection of millimetre and sub millimetre photons.** Typical material choices are Nb for antenna and micro strip, and Al for superconducting ground plane.

*This project has received funding from the European Union´s Horizon 2020 research and innovation programme under grant agreement No 800923.*

ators. This task necessarily requires engineering different solutions in depending of the wavelength/energy range of the radiation to be detected. Demonstrations for X-ray(143), UV/visible/IR (204)and sub millimeter and millimeter ranges (146) were quickly developed. The adaptations for the different ranges are, basically:

- Planar antennas with microstrip lineswork well at millimetre and sub millimetre wavelengths, and coupling millimetre or sub millimetre photons to a quarter wave - CPW resonator may be achieved by using an antenna to absorb the incoming radiation and send it down a micro strip. The gap frequency of the material forming the micro strip will define the upper limit of the frequency transmitted through it. Radiation above the gap frequency will break Cooper pairs in the superconductor and result in a lossy transmission line. Running this micro strip over a superconducting ground plane (in this case, the centre strip of a quarter wave resonator) will cause the radiation to break Cooper pairs in the ground plane since the radiation is above the gap frequency of superconductor. This will cause a quasiparticle excess that the resonator can detect.

- Sensors for optical/ultraviolet/X-ray will require the integration of absorbers, i.e. materials with good quantum efficiency and stopping power. Historically, Tantalum has been a usual choice, because of its density ($\rho \approx 16 \frac{g}{cm^3}$), high atomic number ($Z = 73$) and high transition temperature $T_c \approx 4.5K$. This provides this material with high X-ray stopping power and good quantum efficiency in the optical/UV. It can be grown in epitaxial form on r-plane sapphire, leading to a high residual resistance ratio[8] - RRRand a good diffusion constant. Diffusion and quasiparticle trapping allow the separation of absorber and detector functions, which provides considerable flexibility for detector optimisation(145). Other alternatives, like single layer implanted AlMn devices have shown good transmission of quasiparticles at optical thicknesses, and in principle avoid the trapping issues which appear at two-level interface (like Ta/Al, in this case). Detectors based on this approach, but using TiN/Ti structures have reported photon-noise limited sensitivity(136). Geometry of the absorber and structure of the device play a significant role. Strip detectors, for instance, are built so that photons are absorbed in a rectangular strip creating quasiparticles, which diffuse to either end of the strip where they are sensed by MKIDs. If the MKIDs are made of a lower gap material than the absorbing strip, the quasiparticles quickly emit a phonon and fall below the gap of the absorber, preventing diffusion out of the MKID. Since the response of the detector is proportional to the density of quasiparticles in the MKID, quasiparticle trapping

[8] Residual Resistance Ratio - RRR is usually defined as the ratio of the resistivity of a material at room temperature and at 0 K. Since the RRR can vary quite strongly for a single material depending on the amount of impurities and other crystallographic defects, it serves as a rough index of the purity and overall quality of a sample. In superconductors, the diffusion constant is proportional to RRR.

*This project has received funding from the European Union´s Horizon 2020 research and innovation programme under grant agreement No 800923.*

allows for sensitive detectors while still maintaining large volume absorbers with high absorption efficiency(196).

- Adaptations to particles physics setups, like neutron detection, implement a superconducting $MgB_2$ meanderline(140). This detector is based on the nuclear reaction of $^{10}B$ in $MgB_2$ with neutrons, which releases a huge amount of nuclear energy (2.3 MeV). The nuclear reaction energy breaks some Cooper pairs in the superconducting $MgB_2$ thin wire and causes a change $\Delta L_k$.

There are variants of the MKID technology, which try to overcome certain issues appearing at the original device (LC resonator circuit and direct coupling to antenna or absorber).:

- TKIDs (Thermal Kinetic Inductance Detectors) are bolometers whose thermometer exploits the temperature dependence of the kinetic inductance effect (142). As in a direct absorber kinetic inductance detector, the resonant frequency of an LC resonator shifts in response to the quasiparticle density in a superconducting inductor. However, in a TKID, rather than directly breaking pairs, photons are absorbed on a suspended island shared by the inductor and quasiparticles are produced thermally. Like KIDs, TKIDs can be frequency multiplexed by assigning each detector a different resonant frequency, and weakly coupling the resonators to a shared readout transmission line. The potential advantage of TKIDs is engineering freedom. In a KID, the function of electromagnetic absorption, conduction of optical power out of the detector and to the bath, and low frequency readout are performed by the kinetic inductor which must be simultaneously optimised for all three functions. In a TKID, these functions can be separated into a load resistor, a membrane (typically made of silicon nitride), and superconducting inductor, which can be independently optimised, at the cost of a many layer fabrication process.

- LEKIDs (Lumped Element Kinetic Inductance Detectors) are based on a series LC circuit inductively coupled to a micro-strip feed line(141). Such device shows no current variation along its length and can be arranged into a photon absorbing area coupled to free space and therefore requiring no antennas or quasi-particle trapping. This is specially indicated for work at wavelengths shorter than around 500 μm where antenna coupling can introduce a significant loss of efficiency.

- CBKIDSs (Current Biased Kinetic Inductance Detectors) is a variation in which the detector (140) is fed by a bias current $I_b$ through a bias resistor, and therefore the voltage $V$ across the

*This project has received funding from the European Union´s Horizon 2020 research and innovation programme under grant agreement No 800923.*

detector depends both in magnetic inductance $L_m$ and surface inductance $L_s$, while the former is larger than the later, but independent of time. Signal amplitude is scalable by tuning the bias current. When a variation of $L_s$ occurs in a period of $\Delta t$, the voltage across the sensor under current-biased conditions is given by $V = I_b \frac{dL_k}{dt} \backsimeq I_b \frac{\Delta L_k}{\Delta t}$, where the change in the bias current $\Delta I_b$ should be negligibly small at temperatures much lower than $T_c$. This can be used as a method to sense quasiparticle excitations directly and hence should be very fast (in the order of nano or even pico-seconds, (178)) in response time compared to MKID (order of microseconds). We believe that a resonance technique in an LC tank circuit in the MKID would elongate the overall response time while the quasiparticle dynamics could be very fast, presumably on the order of picoseconds.). Also, the operating temperature is not limited to the very narrow regime near $T_c$ (which is a major limitation of the TES technology).

The fundamental noise limit in any KID devices arises from generation and recombination of quasi-particles $\left(NEP_{qp} = 2\Delta\sqrt{\frac{n_{qp}}{\tau_{qp}}}\right)$. This is the theoretical limit and will depend heavily on the film quality, which ultimately determines the number of quasiparticles at a given temperature $\left(n_{qp}\right)$ and the quasi-particle life time at that temperature $\left(\tau_{qp}\right)$. By working at low temperatures this noise is reduced by minimising the number of quasi-particles in the and increasing the quasi-particle lifetime. Stray light creates quasi-particles and reduces responsiveness, so should be reduced to a minimum. Early KID devices demonstrated an excess noise. This noise was attributed to the microwave field of the resonator exciting two level systems -TLS on the surface of the superconductor. This causes a fluctuation in the dielectric constant of the oxide on the surface of the film causing the capacitance to fluctuate. This can be mitigated by choosing a capacitor geometry such that the electric field lines mainly exist outside of the TLS region[9].

The factors that make MKID attractive are:

- They provide a clear path towards effective and relatively straightforward scale up of arrays with very large number of pixels. As opposed to other types of superconducting sensors, the implementation of the frequency multiplexing technique does not cause problems of thermal instability or loss of effective sensing area (due to presence of elements of the read out system around the pixel area).

- MKIDs can in principle be manufactured using a single step lithographic process. The ease of processing is in striking contrast with

[9] Introductions to KID technology can be found in refs: (138) and (121). A very detailed discussion regarding limitations and deviations from ideal behaviour of KID technology can be found in ref: (139).

*This project has received funding from the European Union´s Horizon 2020 research and innovation programme under grant agreement No 800923.*

competing detector technologies such as Transition Edge Sensors (TES) which require multiple fabrication steps.

- The fact that read-out system is largely available and at low cost (due to the fact that the technology has been developed for wireless communications) makes the overall cost of the system rather price competitive (this, of course, does not refer to the cost of the cryogenics, which remains the real limiting factor in many applications).

The bottomline for this technology is that it is relatively young, as compared to other superconducting sensing technologies, but has quickly gained attention in applications where dense arrays are required. This includes both astrophysics(158) and spectroscopic set ups(143). Currently, several KID arrays are being tested for integration into space borne missions, and also being tested for particle physic experiments related to dark matter and neutrino detection(28).

## 2.7 *Other superconducting sensing technologies.*

Apart from the technologies described in detail in the previous sections, several other concepts have been proposed and developed up to a certain degree. At present, these are not considered to be main competitors, for a number of reasons:

- Some of the technologies, like magnetically coupled micro-calorimeters are well understood and have received considerable attention, but present intrinsic difficulties which make it difficult to adapt them for the requirements of the main applications.

- Some other technologies, like graphene based devices, are just too young, and research activity is at incipient stage, with very few groups focusing effort on them. While showing potential, it is unlikely that disruptive concepts arising from these technologies will emerge with enough force as to displace more mature technologies in the short- and mid- term, although they may become interesting solutions looking a a further horizon.

- Finally, we wanted to show some other concepts, like superheated superconducting granules, that where developed under the basis of relatively easy fabrication, which is certainly an advantage for competing in commercial applications. This condition, is however clearly insufficient, as the technical difficulties that have emerged from the lack of control at manufacturing stage have lead to dead-ends that will be difficult to overcome.

*This project has received funding from the European Union´s Horizon 2020 research and innovation programme under grant agreement No 800923.*

This list is by no means comprehensive. The scientific literature is bast and it will be impossible (even for a much larger effort than the one we could make during this project) to collect information about all alternative technologies which are being conceived and explored at research level.

### 2.7.1 *Magnetically Coupled Micro-calorimeters*

These devices utilise the temperature dependence of the magnetisation of a paramagnetic material in a weak magnetic field to detect the temperature rise resulting from the absorption of a photon or energetic particle[10]. Gold doped with a small amount of erbium (Au:Er) is an effective sensor material. The temperature rise from an absorbed photon causes a change of magnetisation $(M \propto \frac{1}{T})$of the Er spins, which is measured as a flux change in a SQUID magnetometer. Several configurations are possible:

- In Metallic magnetic calorimeters - MCC the magnetic sensor is positioned inside a superconducting loop of wire connected to the input coil of a SQUID in a closed superconducting loop; in operation the total flux threading this loop remains constant. An external magnetic field (H) is required to produce a magnetisation of the paramagnetic system. When the magnetisation of the sensor changes, the resulting change in flux within the loop generates a change in current through the input coil of a highly sensitive SQUID am- meter. A weak thermal link to a heat bath provides a means for the temperature of the MMC to return to its base temperature.

- In Magnetic penetration thermometers - MPT are read out in an almost identical way, except that the paramagnetic sensor is replaced by a Type-I superconducting metal, which becomes a near-perfect diamagnet below its transition temperature. In comparison with MMC, the MPT has a stronger dependence on temperature in the steepest part of the transition region, which makes even higher energy resolution possible.

Magnetic calorimeters are very well understood, as they have been under development for over 20 years targeting a wide variety of different applications that require very high resolution spectroscopy. They have proven to be highly suitable detectors for various applications including high-resolution X-ray spectroscopy in atomic and nuclear physics(133) nuclear forensics(132), radiation metrology(131), direct neutrino mass determination(130), searches for neutrinoless double beta decay(129) and mass spectrometry(128).

[10] A rather complete description of these technology can be found in (185).

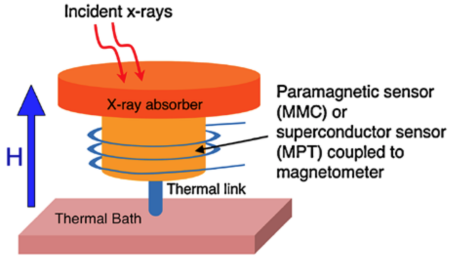


Figure 2.15: **Magnetic Calorimeters.**

*This project has received funding from the European Union´s Horizon 2020 research and innovation programme under grant agreement No 800923.*

Both MMCs and MPTs have intrinsic properties that are highly desirable for increasingly larger x-ray micro-calorimeter arrays. First, no heat is dissipated in the calorimeter when measuring the magnetisation with a superconducting SQUID loop. Thus, very large-format focal-plane arrays can be built without the difficulty of removing large amounts of heat from the detector array. Second, they can both be operated with unprecedented energy sensitivity for an energy dispersive detector. For example, they have the potential to meet the demands of the ideal x-ray camera for astrophysics, having more than a million pixels, and providing an energy resolution of better than 1 eV for energies up to 10 keV. They can be made using standard vapour-deposition techniques.

The read-out of large arrays of such devices remains a significant challenge, and appears to be more difficult than other micro-calorimeter technologies. Individual two-stage dc-SQUIDs are mostly used for reading out single channel detectors or small detector arrays. In principle, this approach could be scaled up to allow reading out large arrays. However, the linear scaling of the system complexity, the parasitic heat load as well as cost with the number of detectors N makes this very hard or even impossible. In TDM the white noise level of a multiplexed pixel increases with $\sqrt{N}$ due to aliasing of wide band SQUID noise, and the fast signal rise time of MMCs can't be maintained due to the small effective bandwidth per channel. In contrast, microwave SQUID multiplexing appears to be much better suited for MMC readout since the fast signal rise time can be maintained by allocating sufficient bandwidth per channel, and the white noise level is independent of N. State of the art demonstrations of this approach had produced a 64 pixel layout, although the achieved energy resolution is not yet compatible with state-of-the-art single-channel MMCs (186). While promising, this milestone is still very far from the demonstrated scaling capability of other technologies, and specially MKID.

### 2.7.2 *SIN Junction Cold Electron Bolometers - CEB*

In this devices a tunnel junction one of the electrodes is a normal metal. In order for an electron to tunnel from the normal metal into the superconductor, it must have an energy above the Fermi level of at least $\Delta - eV_b$, where $\Delta$ is the gap width of the superconductor and $V_b$ is the junction bias voltage. The junction current therefore probes the tail of the Fermi distribution of electrons in the normal metal, and is exponentially sensitive to the electron temperature $T_c$, scaling as $\exp\left[-\frac{\Delta - eV_b}{k_B T_e}\right]$.

This working principle allows accurate probing of the electron

*This project has received funding from the European Union´s Horizon 2020 research and innovation programme under grant agreement No 800923.*

temperature in a normal metal. This property was exploited for developing hot-electron micro-bolometers, in which the absorbed radiation heats the electrons in the normal metal, and the increase in is measured using the SIN junction. Such devices have a negative feedback effect, as the tunnelling electrons also carry away heat from the normal metal. Because of this characteristic, these devices have been sometimes named as Cold Electron Bolometers - CEB(49).

The theory and experimental characterisation of antenna-coupled detectors has been already presented(51; 50). Some studies suggested that TES base bolometers have at least one order better (lower) noise equivalent power (NEP) in comparison with a single SIN-junction with micro-bolometer with similar dimensions(54), although it is likely that progress in understanding and manufacturing has been done since.

With the aim of expanding the range of application of these devices through integration onto focal plane arrays, dc SQUID readout have been proposed(53), but junction field effect transistor read-out has been used instead for the only application of this type of devices for OLIMPO airborne telescope(52).

Very recently, a theoretical minimum of the electron temperature experimentally down to 65 mK at 300 mK phonon temperature has been demonstrated in this kind of devices. This sets a technological milestone because such temperature because can be reached in $^3He$ cryostats. Electron cooling from 256 mK (which can be reached in two-stage$^3He$ cryostats) to 48 mK is also demonstrated in the same work (48).

### 2.7.3 *Graphene Bolometers*

While this is not a superconducting material, its very special characteristics allow, in principle, to achieve remarkable performance. Graphene has unique combination of a record small electronic heat capacity and a weak electron–phonon coupling. These unique thermal properties and its broadband photon absorption from the UV to GHz frequencies make graphene a promising platform for ultra-sensitive and ultrafast hot electron bolometers, calorimeters and single-photon detectors for low-energy photons.

So far, most experiments have employed graphene on a $SiO_2$ substrate with a slow d.c. transport readout. In order to achieve a high response, graphene's weak temperature-dependent resistance $\frac{\Delta R(T_e)}{\Delta T_e}$ had to be artificially increased by introducing disorder, patterning, nano-structures or opening a band gap in bilayer graphene. However, disorder introduces charge fluctuations at the charge neutrality point - CNP, limiting the detector's response, as the lowest heat capacity

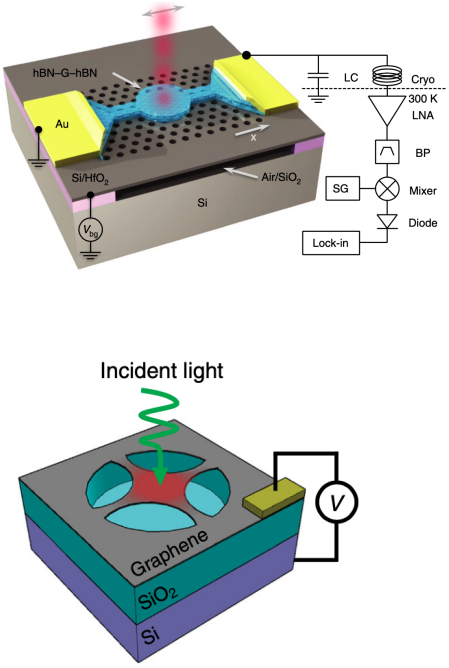


Figure 2.16: **Graphene calorimeters.** Top: cavity-coupled graphene bolometer with a Johnson noise read-out; Bottom: suspended graphene resonator (see text for details).

*This project has received funding from the European Union 's Horizon 2020 research and innovation programme under grant agreement No 800923.*

values in close vicinity to the CNP cannot be reached.

New concepts for read-out use microwave frequency Johnson noise - JN, which is emitted by thermally agitated electrons in graphene. This direct *Te* readout scheme does not require a large $\frac{\Delta R(T_e)}{\Delta T_e}$ and allows use of ultra-clean hexagonal boron nitride encapsulated graphene devices without sacrificing the detector's sensitivity(184). First prototypes of this device have reported a noise equivalent power of about 10 $pWHz^{-1/2}$, a record fast thermal relaxation time, $< 35ps$, and an improved light absorption in very broad range. While this results have been obtained at 5 K, the device can operate at 300K at the price of lower sensitivity, Even the 5K operating temperature establishes already a radical difference, in terms of complexity and cost of the related cryogenics, with respect to that required for many of superconducting technologies. These technology is nevertheless on its very early demonstration stages, and so far important challenges such as construction of arrays have not been even faced.

In a departure from conventional bolometry, very recently a new graphene nano-electro-mechanical system to detect light via resonant sensing has been proposed (135). In this approach, absorbed light heats and thermally tensions a suspended graphene resonator, thereby shifting its resonant frequency. Room-temperature noise-equivalent power ($2pWHz^{-1/2}$) and bandwidth from 10 kHz up to 1.3 MHz have been initially reported. The fabrication of the this devices should be scalable and could be used to make dense bolometer arrays. The process involves a single-step transfer of chemical vapour deposition graphene on a lithographically defined resonator support frame. The device could be fully integrated with on-chip electrical detection and actuation, allowing it to operate as a stand-alone, packaged technology.

The bottomline of graphene-based technologies is that, although very new, they offer, due to the exceptional properties of the material, a platform where very new and innovative concepts are emerging. Some of these ideas could have truly disruptive character and challenge in an unconventional way other sensing technologies.

### *2.7.4 Josephson Junction Single Photon Detector - JJSPD*

Josephson Junctions - JJ are ubiquitous superconducting devices. While their performance can be degraded by quasi particles formed from broken Cooper pairs, this phenomenon also opens opportunities to sensitively detect electromagnetic radiation. Upon being absorbed into the superconductor, a single-NIR photon will break Cooper pairs and generate QPs, which then become a noise source to switch the current-biased JJ. The probability of JJ switching can be

*This project has received funding from the European Union´s Horizon 2020 research and innovation programme under grant agreement No 800923.*

described by the resistively and capacitively shunted junction (RCSJ) model.

A single near-infrared photon detector has been already demonstrated by coupling photons to the localised surface plasmons of a graphene-based JJ (109). The role of graphene is inessential (under this hypothetical mechanism) except that it provides a shunt resistor, quasi-ballistic channel across the JJ and forms a proximity JJ that allows for the efficient coupling of photons by the dissipative surface plasmon. Since the resistance of graphene- based JJ SPD can be controlled, this feature will allow the matching of load impedance with JJ-based computer architectures to enable high-speed, low-power JJ optical interconnects.This type of devices is sensitive to polarisation: switching rate is enhanced when the polarisation is aligned perpendicular to the super current direction.

Another interesting achievement of this technology is the development of cryostat free sensor arrays for the THz range(47), which has a direct impact in cost and complexity of the systems, and opens the door for its adoption into industrial applications.

### 2.7.5 *Superheated Superconducting Granules - SSG*

This detectors consists of billions of small grains (typically 30 μm in diameter), diluted in a dielectric material (e.g. Teflon) with a volume filling factor of typically 10% (134). The detector is operated in an external magnetic field. Metastable type-1 superconductors (e.g. Sn, Zn, Al, Ta) are used, since their phase transitions from the metastable superconducting state to the normal-conducting state are sudden (in the order of 100 ns) allowing for a fast time correlation between SSG signals and those of other detectors. In order to keep the heat capacity as low as possible the SSG detector is operated at a temperature much below the critical temperature Tc at typically To $\approx$ 100 mK.

Particles interacting in a granule produce quasi-particles. While spreading over the volume of the granule the quasi-particles are losing energy via electron-phonon interactions, thereby globally heating the granule up to a point where it may undergo a sudden phase transition (granule flip). The precise temperature change experienced by the granule is known to be $\Delta T = \frac{3\Delta E}{4\pi c r^3}$ with $\Delta$E the energy loss of the particle in the grain, c the specific heat and r the radius of the grain. The phase transition of a single grain can be detected by a pickup coil which measures the magnetic flux change $\Delta\,\Phi$ due to the disappearance of the Ochsenfeld-Meissner effect. Conventional readout coils can be replaced by SQUID readout, which allows the detection of single flip signals from smaller size granules and/or the usage of larger size pickup coils.

*This project has received funding from the European Union´s Horizon 2020 research and innovation programme under grant agreement No 800923.*

One advantage of this technology relies on fabrication. Small spherical grains can be produced at low cost by industry using a fine powder gas atomisation technique, followed by sieving for selection of appropriated grain size. However, this production process affects the energy resolution of the device. SSG is a threshold detector, i.e. its resolution depends on the sharpness $\delta H/H$, respectively $\delta T/T$, of the phase transition. It was found that the phase transition smearing depends on the production process of the grains. Industrially produced grains using the atomisation technique exhibited a smearing of $\delta H/H \sim 20\%$. By using planar arrays of regularly spaced superheated superconducting microstructures which were produced by various sputtering and evaporation techniques the transition smearing could be reduced to about 2%. The improvement of the phase transition smearing is one of the most important developments for future applications of SSG detectors.

This technology, in principle, offers several unique features: (a) The large list of suitable type-1 superconductor materials allows to optimise SSG for specific applications. (b) Very low energy thresholds (eV) can be achieved. (c) The inductive readout does not dissipate any power into the grains. Therefore the sensitivity of SSG is essentially determined by the grain size and the specific heat of the grain material. (d) The sudden phase transitions are beneficial for coincident timing with other signals.

SSG detectors are among the most sensitive devices to detect very low energy transfers, i.e. nuclear recoils. They have been proposed for X-ray imaging, transition radiation, dark matter and reactor neutrino detection. It looks promising that large quantities of planar arrays can be produced industrially. Nevertheless, because of the aforementioned issues, the practical realisation of a large SSG detector is still very challenging.

*This project has received funding from the European Union´s Horizon 2020 research and innovation programme under grant agreement No 800923.*

# 3
# *Applications*

The range of applications for sensors of electromagnetic radiation is enormously wide and covers almost all domains of activity. A non exhaustive but representative first classification is provided in Figure 1. However, not all these applications are available for superconducting sensors. By all accounts, the main constrain for this family of sensors is the need of cryogenic cooling systems required for bringing the materials to their superconducting phase. In practice, the complexity, cost and logistics of the cryogenic systems are the real limiting factors, rather than the technical performance of the sensing technology itself.

We will now review the different applications in which superconducting sensors have found to be attractive solutions.

## *3.1 Nuclear Material Analysis ($X-ray$ and $\gamma-ray$ spectroscopy)*

So far, nuclear power relies on fissionable material that can sustain a chain reaction with neutrons.The nuclear fuel cycle describes how nuclear fuel is extracted, processed, used, and disposed of. The *Front End*, *Service Period* and *Back End* stages relate to the preparation, use within energy production plants and reprocess and/or disposal of this type of fuel:

- The main steps of Front End concern the exploration (search of minerals), mining, milling, conversion (uranium mineral, $U_3O_8$, for instance, is transformed into $UF_6$ or $UO_2$ ), enrichment and fabrication of the nuclear rods which are inserted in the nuclear reactor. Non destructive analysis is essential to characterise the composition, determine concentration of isotopes and control quality of fuel rods.

- During the Service Period the main activities concern transport of the fuel to the energy plants, in-core management (ordering of

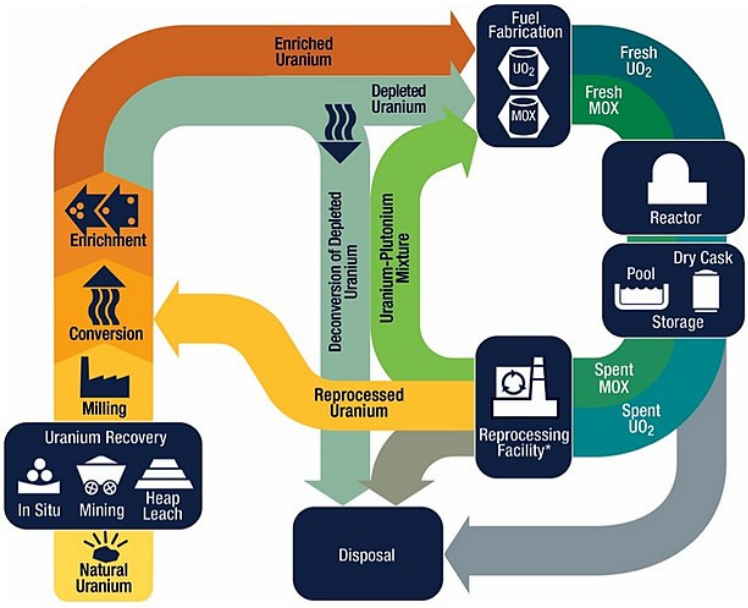


Figure 3.1: **The nuclear Fuel Cycle.**

the rods), post irradiation examination (including analysis of fuel-cladding interaction) and interim storage. Security is an essential issue during this stage, specially during transport. Examination is essential for identification of problems during the fission reaction. Interim storage is intended to provide cooling and isolation until disposal, and once more security at this stage is critical.

- The Back End period is probably the most complex, as several routes can nowadays apply, ranging from full reuse, to full disposal. At this stage used fuel is once more transported, then partitioned (for recovery of a fraction of the fuel) and transmuted (for conversion into short-lived of stable isotopes). Disposal generally involves long-term storage in specific sites.

Beyond this cycles, other aspects related with this activity are also of great importance:

- Decommissioning of a nuclear power-plant involves the stop of energy production activity, and ordered disassembly of the full power plant structure. During this approximately 40 years period, the materials of the power plant are classified according to its radioactivity levels, and then carried out of the decommissioned site for recycling or final disposal under similar conditions than nuclear fuel. Currently, more than 150 facilities are undergoing such process[1]. Because of such large volume of activity, Authorities top priority has become the monitoring of the whole process, as to avoid incorrect classification, wrong disposal or theft of nuclear fissile material.

[1] For updated information, visit the World Nuclear Association site.

*This project has received funding from the European Union´s Horizon 2020 research and innovation programme under grant agreement No 800923.*

- Nuclear accidents, despite their rareness, have proven to cause a deep negative impact in environment and human activity[2]. This type of events do not only affect energy production facilities, but also medical and military ones (Preventive action through constant analysis and early detection of abnormalities is so far the main protective measure that can be set in place. Such monitoring activity applies to all aspects of the energy cycle and the operation of the nuclear power plants.

- Terrorist activity has become a major concern since the beginning of the XXI century. While so far none of the terror acts have involved the use of nuclear material, intelligence services have detected many attempts of terrorist groups to acquire this type of materials(230). Such illicit trade often focuses on the deviation of material at vulnerable stages of fuel cycles. Given the exponential increase of global trade, the surveillance tasks for are becoming increasingly difficult.

[2] For detailed information visit United Nations Scientific Committee on the Effects of Atomic Radiation.

Finally, it is worth mentioning another field unrelated to the nuclear energy industry activity, but where nuclear material analysis is of great importance. This is the field of radiation-sensitive experiments, which comprises cosmology, particle physics and, recently, biological sciences. The search and charactersation of elementary particles (neutrinos, Higgs boson, etc) is mainly based in the study of nuclear reactions in which these particles are ventually formed and/or destroyed. Examples of this are the $2\beta$ decay (228) and dark matter detection (227) experiments. In some cases, the core of these set ups are detectors designed to identify very specific nuclear reactions. Even if this is not the case, all these experiments are very vulnerable to noise caused by unwanted nuclear reactions, occurying naturaly because of cosmic radiation and natural radioactivity present in every material.

This is the reason why these experiments are usually located in underground facilities, and their building process requires a years-long selection of low radioactivity materials which which the whole laboratory environment is constructed. All this process relies on nuclear material analisys. It is worth mentioning that there is considerable overlap between the detecting technologies which are being developed for these applications and the sensor arrays used for $X-$ray and $\gamma-$ ray spectroscopy, although the particle detectors that constitute the experiments themselves fall outside the scope of this report.

Solutions for most of these issues goes through the use of techniques that allow to indentify the nature of the radiative source, and possibly allow also to quantify the level of radioactivity.

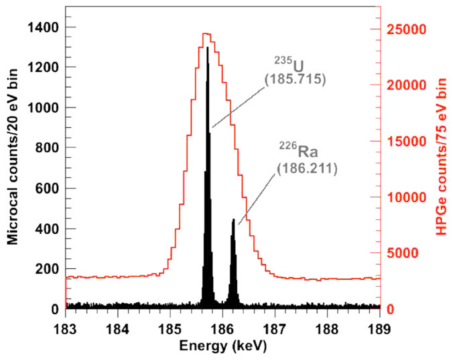


Figure 3.2: **Energy Resolution in $X-$ray and $\gamma-$ray spectroscopy.** The spectral signal obtained by the HPGe detector (in red) does not resolve neighbouring $^{235}U$ and , $^{226}Ra$ peaks. Superconductor detectors (TES in this sample, in black) do have such resolving power. Source (229).

*This project has received funding from the European Union´s Horizon 2020 research and innovation programme under grant agreement No 800923.*

$X-$ray and $\gamma-$ray spectroscopy are, for this purpose, among the best available techniques, as they allow to obtain the afforementioned information remotely, thus avoiding the destruction of the samples or the risk of exposure to radioactivity. Imaging is not essential in most of the monitoring and analytical tasks, but it still plays an important role in inspection ones, as many involve the intervention of trained technitians. Spectroscopy and imaging can be combined, either by integration (multispectral devices) or by use of advanced technologies (photon counting sensors).

Spectroscopic analisys aims to resolve the emission peaks which are fingreprints of each radioactive isotope. The brightest spectral lines of interest fall between about 40 and 200 keV, which is a complex spectral region with many closely spaced lines.

Currently, the battlehorse for $X-$ray and $\gamma-$ray is the high-purity germanium (HPGe) sensor, as it offers very good ratio between cost and energy resolution, and requires cooled operation but not deep cryogenics. The spectral resolution of HPGe sensors is determined by the statistics of charge creation and collection and is limited to about 400 eV FWHM at 100 keV. This performance is outstanding for this type of technology (semiconducting sensors), but it is not sufficient to resolve a number of overlapping spectral lines from elements relevant to the nuclear fuel cycle. This has motivated the development and application of superconducting sensors to nuclear materials analysis.

Implementation of superconducting technologies for these applications has required adaptation of the original designs. The high energy of the photons in this observation range makes it challenging to absorb photons in the thin film structure which typically forms superconducting sensors. This has motivated the development of two-body sensors in which a bulk absorber is attached to a much smaller thermometer. For gamma-ray detection, early success was achieved with semiconducting thermistors and superconducting tin absorbers (226). This type of absorbers have been also combined with TES thermometers (225).

The effective area of this type of sensors is in practice limited because of the degradation of calorimeter energy resolution with increased heat capacity(218). As a consequence, individual calorimeters designed for the 40-200 keV range to a few $mm^2$. In order to be able to compete with the collecting area of a HPGe sensor (at least several $cm^2$), superconducting technologies have been forced to adopt the use of arrays of sensors, and thus required to focus on efficient read-ou strategies. Frequency-domain multiplexing (224), time-domain(223) and microwave SQUID multiplexing(222) have been demonstrated.

A good example of state of the art set up is the one installed at Los

*This project has received funding from the European Union´s Horizon 2020 research and innovation programme under grant agreement No 800923.*

Alamos National Laboratory (LANL)(221). This spectrometer consist on a 256 unit array of TES, implementing time-domain multiplexing with 32 pixels per readout column. Because of the compromise between pixel size and energy resolution the later is 53 eV FWHM at 97 keV, although spectrometers with as much as 22 eV FWHM at 97 keV resolution have been demonstrated(220).

The resolution values achievable with superconducting sensors are sufficient to resolve almost all spectral line overlaps of interest. For example, as shown in Figure 3.2, the gamma-ray emission from fissile $^{235}U$ can readily be distinguished from that of $^{226}Ra$ (a fare less dangerous isotope found in common commercial products including cat litter and roofing tiles). This is of practical importance because confusion between these two isotopes is a source of false alarms at U.S. border crossings (219).

While this technical demonstration has managed to prove that superconducting sensors provide a effective solutions for important application needs, so far there has been no efficient transfer of this type of technology towards commercial solutions for inspection tasks. This is to be blamed on the cost and complexity of superconducting spectrometers, which remain as main obstacles to their penetration into challenging field environments.

In the near term, a more accessible but also more complex application is the quantitative measurement of isotopic fractions in complex actinide measurements. Measurements of this type are routinely performed for materials accounting purposes in large facilities related to the nuclear fuel cycle. Here, a small number of spectrometers operating in analytical laboratories could have a significant practical impact.

When characterised using with HPGe sensors, isotopic mass ratios with relative errors as good as 1% can be obtained. However, this is insufficient, as in nuclear facilities with large mass throughput (such as fuel reprocessing centres), 1% errors produce substantial uncertainties in the total mass budget of material handled at the facility. Destructive analysis techniques based on mass spectrometry can determine isotopic fractions to much better levels than the aforementioned, but these techniques are more challenging, require extensive sample handling, consume the sample under study, and generate radioactive waste.

There is, therefore, a window of opportunity for superconducting detectors if they allow to reduce errors below 1% and towards the levels possible with destructive techniques. In addition, more precise knowledge of isotopic fractions can help constrain the age, origin, and intended purpose of material. For example, the ratio of Pu isotopes in a sample depend on the type of reactor where the sample

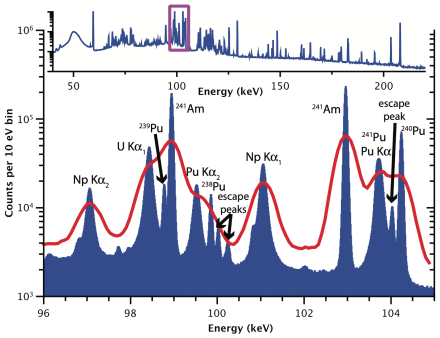


Figure 3.3: **TES vs HPGe $X-$ray and $\gamma-$ray spectrum** from a mixture of PuPu ( 85% $^{239}Pu$ and 14% $^{240}Pu$) . Quantitive determination of isotopic ratios from such spectra is a cornerstone of non-destructive nuclear materials analysis. The spectrum spans the energy range 40–220 keV and contains both bright spectral lines and a broad continuum. Zoomed view of the 96–105 keV region. Results from a HPGe sensor are shown in red and those from a TES array in blue. Source: (221).

*This project has received funding from the European Union´s Horizon 2020 research and innovation programme under grant agreement No 800923.*

was manufactured and on whether the reactor was operated for electricity or weapons production.

There are several aspects to this complicated problem. The first is the need for high statistics. For 1% relative errors, individual $X-$ray and $\gamma-$ray lines of interest must contain at least $10^4$ counts[3]. As shown in Figure 3.3, useful spectra will contain $10^7$–$10^8$ or more counts distributed among many bright spectral lines as well as an unavoidable continuum (due mainly Compton scattering in the source and in the detectors). For a 256 sensor array counting at 10 cps per sensor, a $10^8$count spectrum requires close to 11 hours of integration time (in practice, duty cycle of the adiabatic demagnetisation refrigerator must also be taken into account, as concerns several hours). Whether integration times of this length are acceptable depends on the measurement scenario, but in comparison HPGe sensors can count at up to 40 kcps without significant energy resolution degradation (188). Therefore, faster superconducting spectrometers remain desirable for the measurement of intense sources and more efficient superconducting spectrometers remain desirable for situations with small number of photons.

[3] This statistical threshold was proposed in (189) and has since become a standard.

An important functionality for non destructive analysis is the automated identification of isotopic fractions from a complex spectrum with many entangled peaks. This conversion depends on parameters of nature such as branching ratios, half-lives, line energies, and mass attenuation coefficients, as well as details of the experiment such as the effective efficiency curve from self-absorption in the source and absorption by the detector. There are software tools for HPGe to extract the effective efficiency curve from a spectrum under analysis without the need of additional information (see, for instance (187)). Then the effective efficiency curve allows isotopic activity ratios to be deduced from spectral peaks at different energies and, on turn, activity ratios can be converted to mass ratios using tabulated half-life and branching fraction data.

Versions of this type of software has been developed for superconducting sensors and applied in a series of measurements on different actinide mixtures. The measurements have shown that the statistical errors in microcalorimeter measurements of isotopic ratios are reduced compared to HPGe results for comparable numbers of counts. If the freedom afforded to individual gamma-ray energies during HPGe spectral fitting is increased, the reported uncertainties of isotopic ratios determined by HPGe become larger and the improvement provided by the microcalorimeter becomes greater, showing up to a factor of 5 improvement in some cases. For HPGe analyses, uncertainties in gamma-ray branching fractions and gamma-ray energies are the largest and limiting factors. The microcalorimeter

*This project has received funding from the European Union ´s Horizon 2020 research and innovation programme under grant agreement No 800923.*

analysis is much less sensitive to gamma-ray energy uncertainties, and is presently limited by uncertainties in gamma-ray branching fractions(183). Because spectral peaks are so well resolved in microcalorimeter data, line centroids can be treated as free parameters without introducing large statistical errors in peak intensities. In contrast, line overlaps in HPGe data make it desirable to fix certain peak centroids at their expected energies to limit statistical error at the expense of increased systematic error. For HPGe, uncertainties in line energies can introduce relative errors in isotopic ratios as large as 6.9% depending on the sample, the isotopes, and certain analysis assumptions. In contrast, the error contributed to microcalorimeter results from line energy uncertainties is almost negligible.

While these early results are promising, more data on more samples and also improved data are needed to fully understand and demonstrate the capabilities of superconducting spectrometers for nuclear materials analysis. For example, the shape of well-isolated spectral lines in microcalorimeter data conforms less well to simple spectral models than does data from HPGe, presumably due to temporal gain variation. This effect is magnified if the spectra from many individual pixels with different resolution values are co-added prior to the calculation of isotopic ratios. While not fundamental, such effects presently complicate spectral analysis of microcalorimeter data.

At this time, it is unclear whether superconducting sensors will enable a large improvement in non destructive analysis capabilities. The 40 year development history of HPGe has afforded ample opportunity to refine analysis techniques with this type of devices, using measurements of large sample sets whose composition was known from destructive analysis. Similar work remains to be attempted for superconducting sensors.

Direct improvements in tabulated branching fraction data could further enhance the value of microcalorimeter measurements. The current situation should be taken as strong motivation for further work in this very important application area. While the chief obstacles to demonstrating the analytical value of superconducting sensors for gamma-ray non destructive analysis are presently related to spectral interpretation, improvements in spectrometer performance will also be valuable.

As noted above, higher system count rates are needed to match HPGe measurements. In addition, the absorption efficiency of superconducting sensors lags HPGe. While active areas of HPGe and superconducting sensors maybe similar, a typical Ge crystal is at least 10mm thick, in contrast to the few hundreds of μm thick absorbers typically integrated into superconducting devices. Absorbers with higher Z and lower specific heat than Sn are desirable.

*This project has received funding from the European Union ´s Horizon 2020 research and innovation programme under grant agreement No 800923.*

Nuclear materials decay via paths in addition to $\gamma-$ray emission. These paths include neutron, $\alpha$, and $\beta$ decay. Cryogenic sensors can perform high resolution spectroscopy of neutrons (using current biased KID (178), and superconducting strips, with similar working principle as SNSPD (177)), $\alpha$ (using TES) and $\beta$ particles (using magnetic calorimeters(179)) as well as of total reaction energies (using TES (176)). The case of $\alpha$ particles has been interestingly developed for nuclear nonproliferation applications (180).

Finally, it is worth mentioning that these technologies are also relevant for characterisation of low-radioactivity material used for the construction of several fundamental physics experiments[4].

In a more fundamental level, these experiments also use superconducting sensors as essential part of their setups. This is the case of neutrino-less $2\beta$ decay (182) and direct measurements of the neutrino mass (181).

[4] An example of the radiopurity characterisation service in the LSC (Canfranc, Spain) can be seen here. Currently, HPGe cooled sensors are used for carrying on this measurements.

## 3.2 *Astrophysics*

Gathering and analysis of electromagnetic radiation is (with the only exception of very few return trips of spaceships) the only direct way of studying the Universe beyond Earth´s atmoshpere. After an initial, few centuries long, period where imaging in the visible spectra (using telescopes) has been the main tool, the development of sensors adapted to other wavelength rages has allowed to explore and understand the nature of many essential objects and their evolution. The wavelength range in which they are apparent is mainly related to the energy released which, in turn, relates to their temperature. A simple orientative classification can be the following:

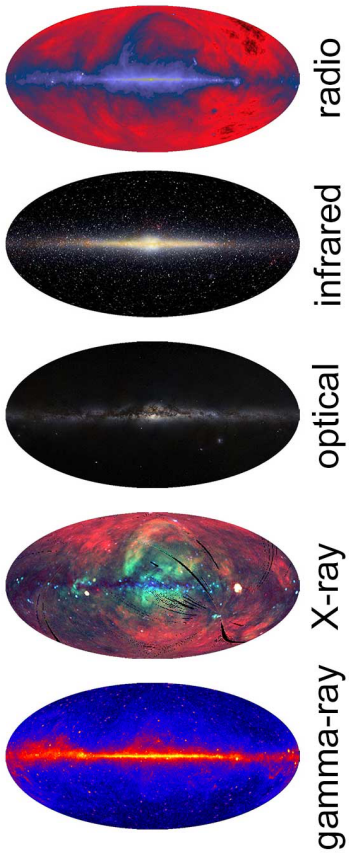


Figure 3.4: **Our Universe seen at different wavelenth ranges.**

Currently, most accurate observation is attempted from outer space, as this allows to get rid of the different negative effects that the Earth´s atmosphere has on the data acquisition (absortion windows, turbulence, scattering, etc). However, because of the cost and technical risk of this type of missions, all detecting technologies are first tested in ground based (telescopes) or balloon borne experiments. This strategy allows to service, repair and upgrade the detectors, while the technology has not yet reached and optimal grade of performance and reliability, as to allow its implementation into a spaceborne system. It must be outlined that ground based and balloon-borne experiments are also capable of producing high quality useful data.

*This project has received funding from the European Union´s Horizon 2020 research and innovation programme under grant agreement No 800923.*

| Range | T(K) | Typical Sources |
|---|---|---|
| **Gamma-rays** | $> 10^8 K$ | Accretion disks around black holes |
| **X-rays** | $10^6 - 10^8 K$ | Gas in clusters of galaxies; Supernova remnants; Stellar corona |
| **Ultraviolet** | $10^4 - 10^6 K$ | Supernova remnants; Very hot stars |
| **Visible** | $10^3 - 10^4 K$ | Planets, Stars, Some satellites |
| **Infrared** | $10 - 10^3 K$ | Cool clouds of dust and gas; Planets |
| **Microwave** | $1 - 10K$ | Cool clouds of gas, including those around newly formed stars; the Cosmic Microwave Background |
| **Radio** | $< 1$ K | Radio emission produced by electrons moving in magnetic fields |

Table 3.1: **Usual Wavelength Range Division.** For having maximum emission peaks within a given range, objects must be at the temperatures indicated. A non exhaustive listing of such objects is provided on the right column.

For the purpose of estimating the market size, it is interesting to count the number of experiments of each type:

- **Ground based experiments:** ([5]) There are more than 625 observatory locations across the Globe. Among these, 39 observe the radio range, 7 the microwave range, 11 study cosmic rays, 8 study neutrinos and 11 study solar activity. Most of the remaining experiments are focused in the visible and IR ranges.

[5] Source and updated informationhere.

- **Balloon-borne experiments:** ([6]) a total of 13 ballon-borne telescopes have been built and commissioned. 6 of them are still in operation.

[6] Source and updated information here.

- **Space-borne experiments:** ([7]) Because a single mission can carry different instruments, it is worth attending at a classification of the detectors. A total of 16 instruments have been devoted to $\gamma-$ray, 5 of which remain operational, 36 have been devoted to $X-$ray, 9 of which are operational, 22 to the UV range, 7 of which are operational, 11 to the visible, 2 of which are operational, 4 to the microwave range, 1 of which remains operational, 2 to the radio range (none currently operational) and 9 devoted to high energy particles, 3 of which reman operational. 14 more missions are already scheduled for launching.

[7] Source and updated information here.

In practice, only a few of these experiments are world-class set ups, who benefit from large budget allocation. Despite the remote location of most relevant astronomical experiments (in order to avoid

*This project has received funding from the European Union´s Horizon 2020 research and innovation programme under grant agreement No 800923.*

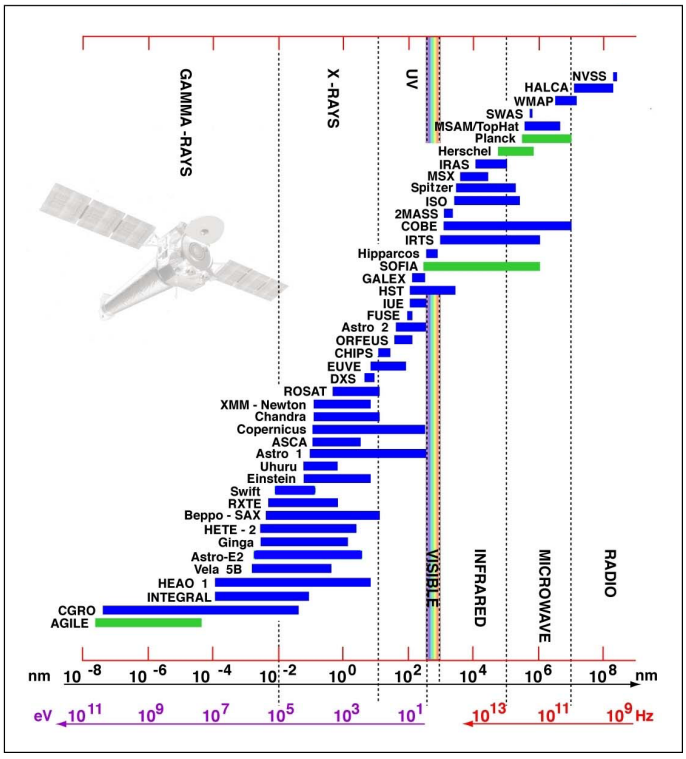


Figure 3.5: **NASA Space missions.** Blue bar indicates a past/current mission, while green bar indicates a mission in development. NASA being a leading player in space science, this gives a representative picture of the types of experiments and wavelength ranges covered by each one of them.

light pollution caused by human activity), their size and importance makes it still feasible and relatively affordable to implement expensive sensing technologies. Technical performance has therefore been the main priority, in contrast with other applications where usability and cost have a bigger weight in the decision making mechanisms. Of course, the whole of ballon-borne and space-borne classes also run on large budgets and performance is the top priority as well.

In order to structure the analysis of the type of sensing technologies used, we will focus in the different wavelength ranges of interest for the TED technology.

### *3.2.1 X-ray Astrophysics:*

X-rays are emitted by ionised atoms and energetic electrons found near active objects such as black holes, supernovae remnants, and neutron stars. Both x-ray emission and absorption are interesting; the absorption of x-rays emitted from hot objects by intervening dust and gas is a useful probe of tenuous material that is difficult to detect by other means. The energies of discrete x-ray lines reveal the constituent elements, and x-ray line energies and shapes can reveal kinematic conditions through Doppler effects. Highly ionised atomic species are common, resulting in great spectral complexity.

*This project has received funding from the European Union´s Horizon 2020 research and innovation programme under grant agreement No 800923.*

The binding energies of electronic orbitals are altered by the degree of ionisation so families of x-ray lines will be present for different ionisation states of the same element (for a detailed introduction to the subject, see (215)). While there are multiple ways to populate the orbitals of an atom with a particular degree of ionisation. the density and temperature of astrophysical plasmas can be determined from line ratios within these complex spectra (see, for instance (216)).

Astrophysical x-rays are not accessible from the surface of the earth because of atmospheric attenuation. While high altitude balloons allow access to X-rays with energies in excess of 20 keV, the rest of the X-ray band (0.1–10 keV) is completely inaccessible below about 100 km altitude. The lower energy band below 10 keV contains all the emission lines from the abundant astrophysical elements, and thus many of the diagnostic spectral features that motivate X-ray observations.

X-ray observatories must therefore operate in space. The ground rules for making detectors usable for X-ray astronomy constrain how the instrument must be packaged for an orbiting observatory or suborbital rocket. This generally means that the instruments need to be compact, low-power and stable against launch vibration. The instrument must also be robust for long term operation in a space environment. The spaceflight requirements for payload instruments affect everything from the cryogenic cooling to the room temperature electronics.

The resolving powers of the instruments limit which spectral diagnostics are accessible:

- At the most basic level, resolving the charge states of an element in order to measure the ionization balance requires separating the strongest lines, typically those of the H-like and He-like ions. The spacing between these lines scales with the atomic number roughly as $\triangle E \sim 10Z$ and the line energies scale as $E \sim 10Z^2$, so a resolving power of $R = \frac{E}{\triangle E} \geq Z$ is required to separate these features.

- Measuring the plasma density requires separating the intercombination lines from the forbidden line in the He-like ions. The energy separation between these lines scales as $\Delta E \sim 0.3Z^{\frac{4}{3}}$ so resolving powers of $R \geq 14(Z-1)$ are required.

- Measuring the width of an RRC in order to determine the temperature of a photoionized plasma requires a resolving power of $R \geq \frac{\chi}{kBT}$.

- Measuring Doppler shifts requires resolving powers of $R \geq \frac{c}{v}$ while measuring velocity widths requires resolving powers of

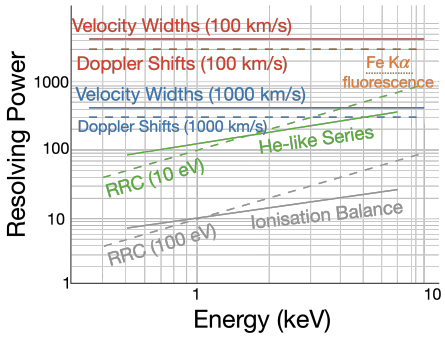


Figure 3.6: **Resolving power as a function of energy** for the spectroscopic characterisation of X-ray events.

*This project has received funding from the European Union´s Horizon 2020 research and innovation programme under grant agreement No 800923.*

$R \geq \sqrt{2}\frac{c}{v}$.

- The resolving powers required for these spectroscopic diagnos-tics are summarized in Fig. 5. An excellent review of spectroscopic diagnostics, and the required instrumental resolving powers is given in Paerels [10].

In designing new spectrometers, or evaluating the usefulness of possible instrumentation, these resolution requirements must be taken into account. The required spectral detail described above can only be achieved with sensors with excellent resolving power. This is the reason why development of superconducting sensors has been profoundly backed by this branch of science since the early days of X-ray astrophysics (217).

An array is intrinsically an imaging device, since the location of the X-ray in the focal plane is uniquely determined. A spatial-spectral imaging detector where every pixel in the focal plane array gives a complete high-resolution spectrum of the source. In principle all the superconducting technologies have the potential to provide both highresolution spectroscopy and imaging capabilities in the same instrument, although not all the sensing technologies can be scaled up easily to the required pixel numbers and densities.

Resolving powers of $R \sim 500$ to 2000 have been demonstrated over a broad energy band of 1 to 10 keV. Superconducting sensors are, in general, instruments are non-dispersive. As such they provide resolving powers that are independent of the angular extent of the source. LTDs can therefore observe spatially extended objects with the same spectral resolution as point sources.

Superconducting sensors have additional benefits:

- Since they are not integrating detectors, they convey precise timing information for each photon, with high "pile-up" limits. They can therefore be used for precision spectroscopy of rapidly varying sources such as X-ray binaries.

- They are also broad-band spectrometers. They can be tuned to cover almost any spectral range from optical to gamma- ray energies with some tradeoff in the resolving power as the energy band is expanded. Most X-ray LTDs easily cover the full band from 0.1 to 10 keV with a single instrument.

- They are very efficient photon detectors. The quantum efficiency is limited at energies below 1keV by the infra-red blocking filters, and at the high energy end by the absorption cross sections of the absorbing material. However, across most of the 0.1 to 10 keV band the quantum efficiency is near unity.

*This project has received funding from the European Union´s Horizon 2020 research and innovation programme under grant agreement No 800923.*

The recent satellites Chandra[8] and XMM-Newton[9] use gratings to perform high-resolution x-ray spectroscopy. For this type of setups, cryogenic micro calorimeters offer higher efficiency, higher resolving power (at energies near 6 keV) and better performance for spatially extended sources.

Small arrays of X-ray micro calorimeters based on semiconductor thermistors have been used on a sounding rocket and a series of satellites (214).

The European ATHENA satellite mission will carry an array of several thousand x-ray TES offering 2.5 eV spectral resolution, with 5" pixels, over a field of view of 5 arc minutes in equivalent diameter sensors[10]. TES sensors have also been implemented a sounding rocket mission that collected 27,000 counts in 300 seconds at 2 eV resolution across the 0.3-2.5 keV band(213).

Plasmas which are relevant for astrophysics science are produced in terrestrial facilities, where is much easier to integrate cryogenic detectors for studying them. Electron-Beam Ion Traps (EBITs) are used to produce plasmas with considerable elemental and charge-state selectivity[11]. X-ray spectrometers based on small arrays of cryogenic semiconductor thermistors have been commissioned in several EBIT facilities. For instance, the XRS/EBIT instrument, installed at EBIT I and SuperEBIT facility at the Lawrence Livermore National Laboratory, has 32 pixels in a square geometry and achieves an energy resolution of 6 eV at 6 keV, with a bandpass from 0.1 to 12 keV, or more at higher operating temperature(211). A larger array of TES x-ray sensors has been commissioned for EBIT at the National Institute of Standards and Technology (NIST). This instrument utilises 192 individual TES x-ray microcalorimeters (166/192 yield) to improve upon the collection area by a factor of $\sim$30 over the 4-pixel neutron transmutation doped germanium-based microcalorimeter spectrometer previously used at the NIST EBIT. The NETS microcalorimeters are optimised for the x-ray energies from roughly 500 eV to 8000 eV and achieve an energy resolution of 3.7 eV–5.0 eV over this range, a more modest (<2×) improvement over the previous microcalorimeters(212).

The instrument scientist must face the very real problems of scaling up to the megapixel arrays needed for future instruments. This is a non-trivial task, and each order of magnitude expansion in the number of pixels brings daunting challenges to the detector design and instrument implementation.

Lastly we discuss some of the practical rather than technical constraints of using cryogenic detectors in space. Cryogenic detectors and their infrastructure are new and largely untested on space platforms. This is changing, especially with the launch of the missions along the last two decades. However, one must justify the risk[12] of

[8] Updated info on Chandra mission can be found here.
[9] Updated information on XMN-Newton mission can be found here.

[10] A detailed description of the X-IFU instrument of ATHENA mission can be found here.

[11] A detailed description of EBIT can be found here.

[12] Risk, in the management definition, includes anything that can interfere with the success of the mission from an outright failure of the observatory, launch vehicle, or ground support equipment, to delayed development cycles, and overspent budgets.

*This project has received funding from the European Union´s Horizon 2020 research and innovation programme under grant agreement No 800923.*

using unproven technology and the expense of its full development cost to traditionally conservative technical review panels in order to win approval for new missions. In today's risk averse environment proposing new technology can be difficult. Demonstrating low risk must involve full system modelling for both short term instrument survivability as well as the long term viability in space, including effects such as radiation damage. Winning approval for new space instruments requires that these systems issues are addressed up-front, with viable full instrument designs, analysis, and demonstrations. This is at least as important as demonstrating the ultimate performance of the detector system itself. In a head-to-head competition, a low-risk proposal will almost always win over an instrument with slightly higher performance but also higher perceived risk.

### 3.2.2 *Optical/IR range:*

By obvious reasons, as optical range is the only which can be perceived by human eye, the origin of observational astrophysics can be traced down to direct observation (both with naked eye and using telescopes). The development of photographic emulsion allowed recording of images for later and more detailed analysis. But it is the development of electronic sensors the milestone that has transformed astrophysics. These devices allow not only recording, but also transmitting in real time, thus enabling remote control of instruments (both ground based and air or space borne) and much more powerful data processing. Observational astronomy expanded rapidly towards the IR range, as both photographic plates and electronic sensors could be straightforwardly adapted to these wavelengths.

The Charge Coupled Device (CCD) was invented by Bell Telephone Laboratories in late 1969 and first described in 1970 (210). This detector was recognised almost immediately after its invention for its scientific imaging potential. The UCL Image Photon Counting System (IPCS)(209) and the CCD for ground-based observing at the University of Arizona (208) were among first practical high-performance implementations. "Solid State Imaging" developed rapidly in the 1970s and beyond as a replacement for photographic techniques. Further developments of the CCD would lead to increased quantum efficiency and image format (size and pixel count) and reduced noise. By the 1980s, it was clear that CCDs would be the sensor of choice for future astronomical imaging. Continued developments from the 1980s to the present have led to devices with over 100 million pixels and QE values of greater than 80% (which is 8 times more efficient than the human eye and almost 30 times more efficient than photographic plates), although integration of antireflective coatings has

*This project has received funding from the European Union´s Horizon 2020 research and innovation programme under grant agreement No 800923.*

allowed quantum efficiency near 100% for some wavelengths(207).

While CCDs are losing favour to Complementary Metal-Oxide-Semiconductor (CMOS) imagers for commercial imaging applications, they are still state-of-the-art sensors for astronomical imaging due to their size, efficiency, and low noise. It is likely that CMOS imagers will continue to improve and eventually replace CCDs in astronomy, especially as the number of fabrication facilities in which CCDs can be manufactured decreases worldwide. However, there are still significant advances in CCD technology every year as scientists and engineers develop ever more demanding applications for sensors in the instrumentation needed for the next generation of very large telescopes.

Since CCD and CMOS technologies are largely baser in Silicon as core material, they can rely in the mature and optimised micro-electronic industry for production. This makes these technologies extremely cost competitive, and the ultimate reason why they are the detectors of choice for the vast majority of observatories.

Even within such competitive landscape superconducting sensors have established themselves as devices with very high quantum efficiency, fast timing capability and ability to resolve the energy of incident photons (in principle, they have are able to detect all aspects of the incoming radiation apart from the polarisation state). Many world-class experiments are currently being equipped with these technologies.

The first TES-based sensor application in astronomy was in 1999 with the use of a tungsten TES to perform spectrophotometric measurements of the Crab pulsar (PSR B0531 + 21)(206). The choice of tungsten as the superconducting material for the TES sensor was useful as it offers $\gtrsim$ 50% in the UV/Optical region of the spectrum to ~ 10% in the IR region.

A second test of a 6 × 6 pixel Stanford TES was undertaken in early 2000 using the McDonald 2.7m telescope. The Crab pulsar was observed and the mode space of the instrument was expand to carry out spectro-photopolarimetric observations using a simple polaroid filter placed before the focal plane and observations were carried out with the polaroid at; 0◦, 45◦, 90◦ and 135◦ enabling the linear polarisation of the flux to determined (205).

Apart from these developments, very little further use of TES sensors in the optical/IR region of spectrum has been carried out since these early tests and it seems that further development of optical TES- based detectors is no longer ongoing.

STJ instrumentation for astronomy has been limited by development issues mainly due to scalability of the single junctions to larger arrays. The very first optical/IR photon detection by a cryogenic de-

*This project has received funding from the European Union ´s Horizon 2020 research and innovation programme under grant agreement No 800923.*

tector was performed by a prototype STJ in 1996(198). Prior to this the only extensive use of STJs was in the X-ray region of the EM spectrum, as the photogenerated free charge carrier density is 3 orders of magnitude larger when compared to optical/IR.

In 1999 the European Space Agency (ESA) initiated the Superconducting Camera Programme (SCAM) with the aim of developing cryogenic STJ-based detectors for astronomy. The S-Cam 1 instrument was the first prototype for testing realised by this project and was developed for use on the William Herschel Telescope (WHT). This prototype instrument consisted of a 6 × 6 array of 25 μm square tantalum pixels, which gave a plate scale at the WHT of 0.6″ per pixel (i.e. a FOV of 3.6″) which gave enough spatial resolution to study single point objects assuming atmospheric seeing of 2″. The S-Cam programme continued over four iterations of a planned development path of six detectors, though only S-Cam 1–4 were developed to the instrument stage (1).

S-Cam 2 was the development of the prototype detector into a fully usable instrument, which offered the same array size as the S-Cam 1 prototype. The resolving power of the array almost doubled from R ~ 5 to R ~ 9 at a detection wavelength of 500 nm.

The S-Cam 3 programme was based on a new sensor design of a 10 × 12 array of 33 μm square tantalum pixels, giving a FOV for this sensor on the WHT of 10″ × 12″. IR rejection for the instrument was improved over the previous designs and the detector quantum efficiency showed an improvement of the order 50% at 500 nm. The energy resolution of the S-Cam 3 detector is R ~ 13 at a wavelength of 500 nm. The red response of the S-Cam 3 detector was also improved extending the usable spectral range to approximately 750 nm.

Further development of the S-Cam programme led to the development of an STJ array as a Distributed Readout Optical Imaging Detector (DROID), as there were fundamental problems with detector scalability to larger arrays using smaller square pixels(197). The DROID approach was a fundamental change as the photons are not absorbed by the junction, rather a tantalum superconductor absorber strip. This allowed the use of larger pixels, without a degradation in performance, to increase the coverage of the sensor to larger FOVs ( ~ 1 × 1 arcmin). This upgrade was performed and the sensor was used in the existing S-Cam 3 instrument. Though the image quality of this array was good, it was found that the uniformity of the pixel response was quite low and further development of the S-Cam instrument has stopped, due to the low bandgap energy of the Ta/Al STJs used in S-Cam they are very sensitive to wavelengths to ~ 1 mm. This resulted in very tight requirements for IR blocking and filters, resulting in a relatively narrow passband of ~ 300 nm.


Figure 3.7: **Planar Array sensitive to millimetre and sub-millimetre radiation for space-borne mission.** On top, array layout. Each colour represents sets of detectors engineered for detection of a single frequency (between 60 and 600 GHz). On middle, integration of the array in the focal plane, showing the cryogenic stages. At the Bottom, schematics of the spaceship. Position of focal plane unit is indicated by the black arrow.

*This project has received funding from the European Union´s Horizon 2020 research and innovation programme under grant agreement No 800923.*

STJ-based detectors are limited in the future scalability of these detectors to larger arrays. STJ-based arrays have inherent issues with respect to Josephson current suppression across large arrays of individual pixels. Discrete feedback methods to enable the current suppression to occur on each pixel individually may be the only possible approach to allow scalability without the need for biasing wires across the arrays, which have the potential to limit the fill factor of large arrays to the point of being unusable. DROIDs as a superconducting absorbing layer have been proposed as a solution to the issue of increasing the fill factor of STJ-based arrays, but they lead to issues that are intrinsic to using larger superconducting layers; a reduced spectroscopic resolution and a resulting lower sustained count rate.

The first optical/IR astronomical instrument developed using MKID technology was the Array Camera for Optical to Near-IR Spectrophotometry (ARCONS). ARCONS is an integral field spectrograph consisting of a 2024 pixel array (44 x 46 pixel) which has been deployed on the Palomar 200 in. Telescope and the Lick 120 in. Telescope. ARCONS was the first MKID-based instrument to produce published results at any region of the EM spectrum(203).

The DARK-speckle Near-Infrared Energy-resolved Super- conducting Spectrophotometer (DARKNESS) integral field spectrograph uses MKIDs with a similar lumped element design as that found in the ARCONS detector and the initial array designs used titanium nitride (TiN) on an silicon (Si) substrate and followed a similar design and fabrication process as the ARCONS sensor (202). The array was redesigned to use platinum silicide as the superconductor material, resulting in a much more uniform sheet resistivity. This uniformity offers a much greater precision when tuning the resonant circuits and offers improved Q values for resonant circuit arrays. Using PTSi as the superconducting material offers better optical transmittance, reflectance and absorption properties than TiN across the 700nm - 1500 nm region of the EM spectrum.

A current development project is the Microwave kinetic inductance detector Exoplanet Camera (MEC) which uses a 20 kpix MKID sensor (201). The aim of the project is to enable the reduction of speckles by post processing data using Dark Speckle and Chromatic Differential Imaging techniques. The use of a MKID sensor is critical to the operation of the adaptive optics suite, with its inherently fast and noise-free readout allowing for controlling speckles with lifetimes of the order ~ 1 s. The MEC instrument is currently in commissioning at the Subaru telescope in Hawaii as a component of the Subaru Coronagraphic Extreme Adaptive Optics (SCExAO) instrument and the aim of this instrument is to allow for direct exoplanet imaging by enabling real-time speckle-nulling.

*This project has received funding from the European Union ´s Horizon 2020 research and innovation programme under grant agreement No 800923.*

Another proposed instrument in development is the Keck Radiometer Array using KID ENergy Sensors (KRAKENS) which is aiming to produce an MKID-based, low resolution, high sensitivity integral field unit (IFU) for the Keck I Telescope(199). KRAKENS is a distinct design, but follows from the work undertaken to develop the ARCONS sensor and it is an enlargement and optimisation of the arrays used. It will be a 30 kpix integral field spectrograph (IFS) with a 42.5" x 45" field of view, wide wavelength coverage from 380-1350 nm, and a spectral resolution R=$\lambda/\triangle\lambda$ > 20 at 400 nm. (ARCONS array offered a spectral resolution of R ~ 10 at 400 nm), although final spectral resolution of the KRAKENS array is expected to be R ~ 100 at a critical temperature, $T_c$, of 100 mK. This is approaching the fundamental spectral resolution limit of MKID technology, although, this is a material dependent feature. Future add on modules could enable polarimetry and higher spectral resolution. KRAKENS will be built using the same style MKID arrays, cryostat, and similar readout electronics to those used in the DARKNESS instrument.

KIDSPEC (Kinetic Inductance Detector Spectrograph) is a current development project using MKIDs as a replacement for the cross-disperser which will act as an order sorter in a two-arm spectrograph. It would provide an R=4000-10,000 spectrum covering the entire optical and near-IR spectral range(200).

The DROID design paradigm for STJs has been realised in MKID strip detectors. Strip detectors use a rectangular absorbing strip (typically made of Tantalum) which is 30 μm wide and several hundred μm long and uses MKIDs on both ends of the absorber strip to detect the quasi-particle current(196). These devices improve the spatial resolution of detectors, but currently suffer from poor coupling between the strip and the MKIDs, resulting in poor quasiparticle transmission.

The only devices for which large scale arrays are currently and cost-effectively realisable are MKIDs and array scalability has been demonstrated, with current MKID arrays projects already surpassing TES and STJ-based arrays in the UVOIR region of the spectrum. The MEC instrument already surpasses any STJ or TES array developed for astronomy research across every figure of merit and the continued development will lead to even further performance gains. The array sizes of MKID instruments in the UVOIR are already two orders of magnitude larger than those using STJ or TES sensors.

### 3.2.3 *Submilimeter, THz and GHz*

Astrophysics studies in this range of wavelengths involve different disciplines such as cosmology, astrophysics, and particle physics. The most relevant example could be the study of Cosmic Microwave

*This project has received funding from the European Union´s Horizon 2020 research and innovation programme under grant agreement No 800923.*

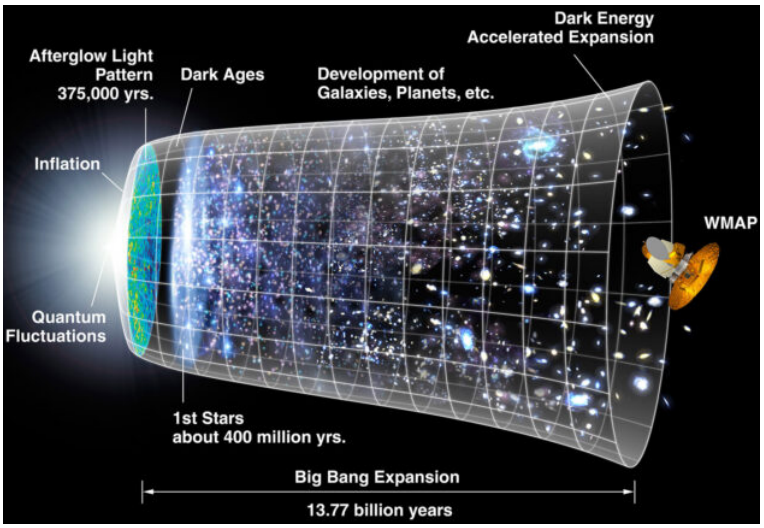


Figure 3.8: **Representation of the evolution of the universe since the Big Bang.** General Relativity starts to be valid after quantum fluctuations, early before the CMB was emitted. Source: NASA

Background (CMB), which is indeed the oldest electromagnetic radiation in the universe, produced approximately $10^{-6}$ seconds after the Big Bang.

The energy density of the CMB is 0.3825 $eV/cm^3$ $(4.0204 \times 10 - 14J/m^3)$ which yields about 400 $photons/cm^3$.The CMB glow is very nearly uniform in all directions, but the tiny residual variations show a very specific pattern, the same as that expected of a fairly uniformly distributed hot gas that has expanded to the current size of the universe. In particular, the spectral radiance at different angles of observation in the sky contains small anisotropies, or irregularities, which vary with the size of the region examined. They are being measured in detail, for verifying if they could correspond to small thermal variations, generated by quantum fluctuations of matter in a very tiny space, and later expanded to the size of the observable universe we see today.

Measurements explore the physics of the extremely early universe, constrain the properties of neutrinos, and enable multiple probes of the growth rate of structure. Detection of the gravitational wave signature as a curl component in CMB polarisation on degree angular scales, referred to as primordial B-mode polarisation, is the most promising technique to determine what produced the initial conditions of standard big bang cosmology.

Precision measurements of CMB polarisation are challenging for several reasons:

- Foremost, the signal-to-noise ratio is extremely low. Even in the most favourable scenario, the detection of primordial B-modes requires the measurement of $\sim$ 80 nK fluctuations on top of the 2.73 K uniform background. Consequently, instruments must not

*This project has received funding from the European Union´s Horizon 2020 research and innovation programme under grant agreement No 800923.*

only have extremely high sensitivity, which has motivated the use of large arrays of sensors, but must also mitigate sources of systematic error.

- Instrumental polarisation, which undesirably converts power from the unpolarised CMB temperature anisotropy into polarisation, is of particular concern because the temperature anisotropy is > 1500× stronger than the most stringent upper limit on the amplitude of primordial B-modes at l = 80. Thus, 0.1% temperature-to-polarisation leakage manifests a false signal that is larger than the expected cosmological signal.
- The 2.73 K CMB blackbody spectrum dictates measurement at millimetre (mm) wave- lengths, which presents unique challenges. In mm-wave optical systems, diffraction is very significant and requires the use of quasi-optical methods. Signal attenuation arises due to beam divergence and loss both in on-wafer transmission lines and in camera optical elements. This in synth of the difficulty of finding materials with low loss tangent in the mm regime.
- Astrophysical foregrounds (synchrotron emission, galactic dust, anomalous microwave emission (AME), free-free, etc.) also emit at mm- wavelengths. To separate these sources from the CMB, we rely on the fact that the frequency spectrum of foreground sources differs from a thermal source. Broad frequency coverage (∼30-300 GHz) is therefore necessary for component separation.
- In addition, many science drivers require ∼ arc-minute resolution, necessitating a >5 m class telescope. Such large telescopes with high throughput create large focal plane areas that require many detector wafers. This increases wafer volume, which is a significant challenge. Second, the elevated running cost of the telescope motivates the collection of as many photons as possible. Broad bandwidth detection is advantageous for this purpose and has driven the development of multichroic detector architectures.

Taking all of this into account, ideal CMB imaging arrays should take fast scans of the sky using polarisation sensitive detectors in multiple frequency bands over a 10:1 bandwidth ratio (∼30-300 GHz). Despite diffraction, this array should couple efficiently to receiver optics over the entire bandwidth. This task is most efficient carried out with photon-noise-limited detectors, that is detectors for which the dominant noise source arises from the incident photons and not from the detector or other sources. This is one of the aspects in which superconducting sensors display a competitive advantage.

Besides superconducting technologies most employed sensing technologies used for this application depend on the wavelength.

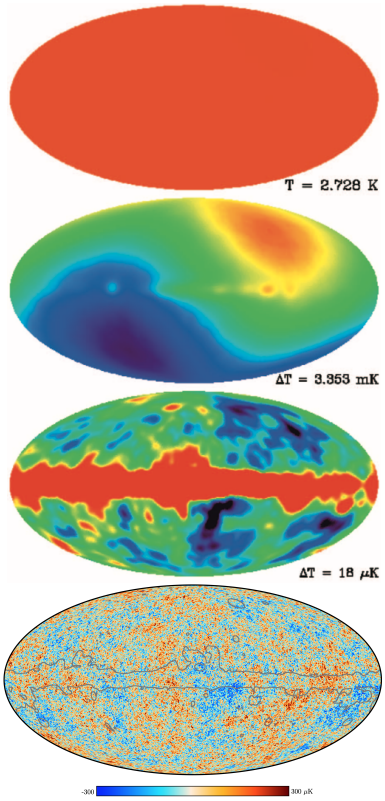


Figure 3.9: **Full map of the CMB.** The breakdown of the CMB sky map: starting from top, monopole, dipole, and multipole. At T= 3 K radiation is uniform in any direction. With sensitivity in mK level, the dipole pattern shows up (due to motion of our solar system relative to the CMB rest frame). If sensitivity is 10 $\mu$K, the multipole features of anisotropy become apparent. They give information about the early universe(175). At bottom, the most detailed, so far, CMB map obtained by Planck mission. The image reveals 13.77 billion year old temperature fluctuations that correspond to the seeds that grew to become the galaxies.

*This project has received funding from the European Union´s Horizon 2020 research and innovation programme under grant agreement No 800923.*

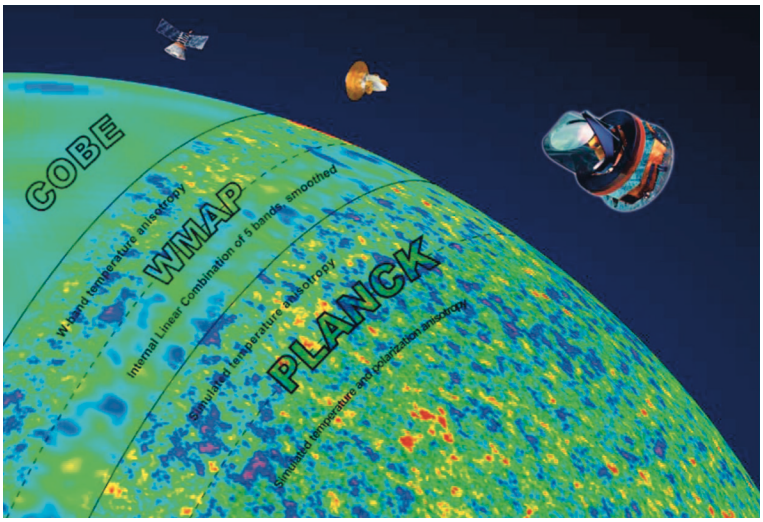


Figure 3.10: **Impact of sensor sensitivity on CMB measurement accuracy.** The space borne missions COBE (commissioned 1989), WMAP (commissioned 2001) and PLANK (commissioned 2009) carried on a full scan of CMB. Each generation significantly improved the resolution of the map.

Cooled high electron mobility transistor - HEMT amplifiers, followed by diode detectors, are often used for $\lambda \geqslant 3$ mm (76). Thermal direct detectors, especially semiconducting bolometers have been used for $3 \geqslant \lambda \geqslant 0.2$ mm (75). Semiconducting photon detectors are generally used for wavelengths $\lambda \leqslant 0.2$ mm (74).

In what concerns superconducting technologies, two generations of detectors have progressively reached important milestones. First generation of devices, basically operating in a single frequency, were used for state-of-the-art mapping of the CMB angular power spectrum. Second generation devices expanded pixel bandwidth and several frequency bands per spatial pixel. These multichroic arrays have been deployed in multiple instruments:

- The Sub-millimetre Common-User Bolometer Array 2 (SCUBA-2) is the most mature and largest TES-based detector currently in operation(8), covering the 450 $\mu$m - 850 $\mu$m range. The SCUBA-2 detector is a 10,000 pixel device consisting of four 32 × 40 pixel sub-arrays on a ceramic PCB. Each pixel is fabricated from a molybdenum/copper bilayer with the relative thickness of the bilayers determining the transition temperature of the pixel. This fabrication techniques allows for the operation of the SCUBA2 detectors in both of the pass bands with arrayed 5120 pixel detectors at both of the passband focal planes . The pixel yield for the SCUBA-2 detector array is approximately 70%.
- The very first instrument using MKIDs was a technology demonstrator DemoCam which operated in millimetre/submillimetre bands at the Caltech Submillimeter Observatory (Mauna Kea, Hawaii, US) (204). This detector showed to have large sensitivity to the orientation of the array with respect to the Earth's magnetic

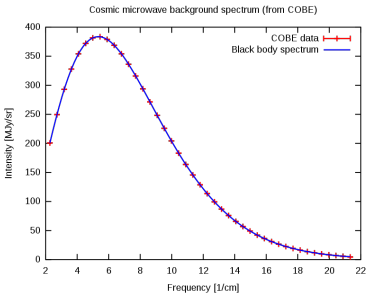


Figure 3.11: **Graph of cosmic microwave background spectrum** measured by the FIRAS instrument on the COBE, It is the most precisely measured black body spectrum in nature(195).

*This project has received funding from the European Union´s Horizon 2020 research and innovation programme under grant agreement No 800923.*

field. This effect was minimised using correction factors based on the telescope position relative to the external magnetic field. Instrument NIKA2, already commissioned and operating in the IRAM 30 m telescope (Pico Veleta, Spanish), represents the first demonstration of competitive performance using large-format (i.e. thousands of pixels) KID (9). Dual imaging is obtained with simultaneous readout of a 1000 pixels array at $\lambda = 2mm$ and two 2000 pixels arrays at $\lambda = 1.2mm$. The two arrays at 1.2 mm allow the measurement of the linear polarization in this band. Sensitivity to external magnetic fields is prevented by integrating magnetic shielding on each cryogenic stage. The pixel yield for the NIKA2 detector is also around 70%. The integration of KID technology will allow to upgrade the instrument during its lifetime (upgrades currently being evaluated are widening the 260 GHz channels band in order to match the "1 mm atmospheric window", adding a third band, reducing the pixel size, adding a polarised channel at 150 GHz or increasing the illumination of the primary mirror)(**?** ).

An in-depth comparative, mainly between TES and MKID technologies applied to the measurement of CMB can be found in ref (7). An interesting point rose by these study is that upcoming third generation will most likely focus on the technical challenge of scaling up the size of arrays in order to meet the order of $10^6$ detectors. NIST (US), for instance, has demonstrated the streamlined fabrication of deployment quality arrays for CMB measurement made in 150mm wafers, in single fabrication runs (6).

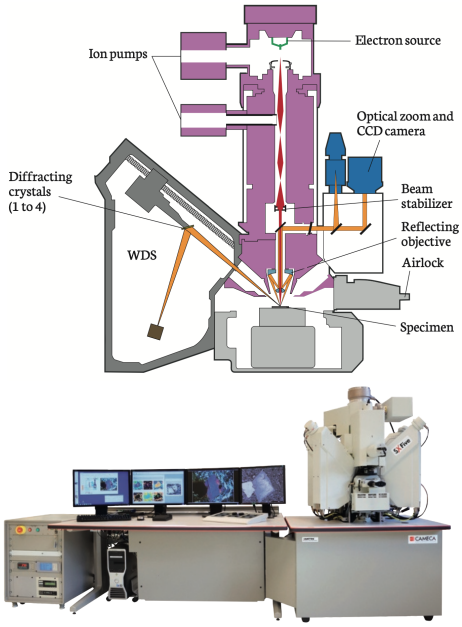


Figure 3.12: **EPMA setup.** On top, schematic structure. Main parts of the instrument are the electron source and focussing (purple), sample holder and scanning (light grey), wavelength-dispersive spectrometer (dark grey), and imaging (blue). On bottom, picture of a commercial system,

## 3.3 *Microbeam analysis*

Electron probe X-ray microanalysis (EPMA) for characterising the chemical (elemental) composition of matter on micrometer to nanometer lateral and depth scales. EPMA is widely applied in those scientific and engineering disciplines where knowledge of the chemical microstructure is critical to understanding the relationship of fine structure to macroscopic physical and chemical properties and behaviour. Fields that regularly employ EPMA include materials science (e.g., metallurgy, ceramics, composites, semiconductors, etc.), semiconductor device manufacturing, geology, mineralogy, environmental science, biology, and failure analysis in many branches of engineering.

EPMA is based upon the use of a focused, high current density electron beam (5 to 30 keV in energy) to excite characteristic X-rays from a picogram mass of a solid target. At the specimen surface the atom density changes abruptly to the very high density of the

*This project has received funding from the European Union´s Horizon 2020 research and innovation programme under grant agreement No 800923.*

solid. The beam electrons interact with the specimen atoms through a variety of physical processes collectively referred to as "scattering events." The overall effects of these scattering events are to transfer energy to the specimen atoms from the beam electrons, thus setting a limit on their travel within the solid, and to alter the direction of travel of the beam electrons away from the well-defined incident beam trajectory. These beam electron–specimen interactions produce the backscattered electrons, secondary electrons, and X-rays that convey information about the specimen, such as coarse- and fine-scale topographic features, composition, crystal structure, and local electrical and magnetic fields. EPMA technique focuses in the analysis of the X-ray emission, although the information can later be combined with SEM and BSE imaging, plus sophisticated visible light optics. Determination of thickness and elemental composition from nm to mm thick layers in stratified materials is possible.

Because the wavelengths of these X-rays are characteristic of the emitting species, the sample composition can be easily identified by recording WDS spectra (Wavelength Dispersive Spectroscopy). WDS spectrometers operate based on Bragg's law and use various moveable, shaped monocrystals as monochromators. EPMA is a fully qualitative and quantitative method of non-destructive elemental analysis of micron-sized volumes at the surface of materials, with sensitivity at the level of ppm. Routine quantification to 1% reproducibility is obRtained over several days. It is the most precise and accurate micro-analysis technique available and all elements from B to U and above can be analysed.

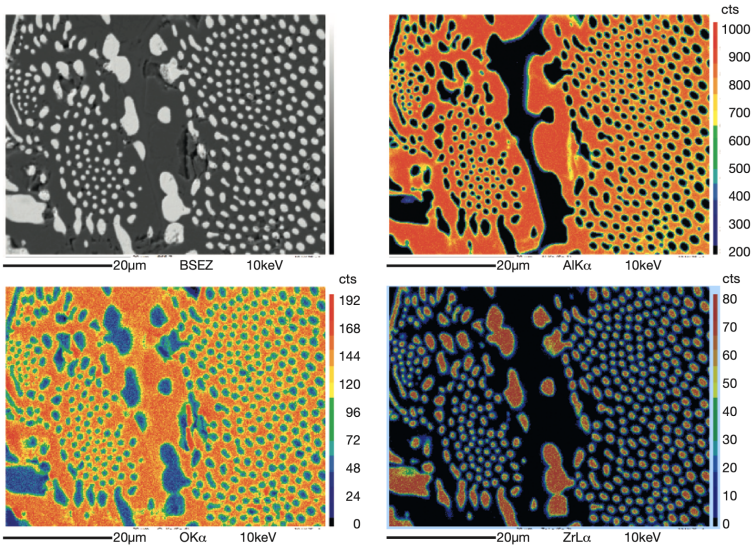


Figure 3.13: **High-magnification X-ray maps acquired on a ceramic specimen.** They illustrate the ability of EPMA to detect even light elements (oxygen in this case) in a complex ceramic matrix also containing zirconium and aluminium.

Despite the fact that Solid State Detectors - SDD (lithium-drifted

*This project has received funding from the European Union´s Horizon 2020 research and innovation programme under grant agreement No 800923.*

silicon, Si(Li) or high purity germanium, HPGe, cooled with liquid N) are presently the most common x-ray detector on SEMs, superconductor detectors were quickly adopted for high performance studies(174).

While superconducting sensors and SDDs have similar broadband response and simple efficiency curves, the energy resolution of superconducting detectors is significantly better; SDDs achieve about 125 eV FWHM resolution at 6 keV and about 50 eV FWHM at 677 eV (fluorine $K\alpha$). Better energy resolution is helpful to resolve overlaps between fluorescence lines, particularly at energies below 2 keV. Small features and thin films must be analysed at low beam voltages in order to localise the electrons to the material of interest as opposed to the substrate below. Low energy electrons can only excite low energy $X-$rays, so analysis of sub$-\mu m$ structures often relies on features with $X-$ray energies below 2 keV. An energy resolution near 10 eV is sufficient to resolve most line overlaps.

Technologically relevant examples of line overlaps include:

- the detection of hafnium against background x-rays from Si. Hafnium oxides are used as high-k dielectrics in transistor gates. The M $X-$rays of Hf fall between 1.645 and 1.698 keV whereas the Si $K\alpha$complex is centred on 1.740 keV.
- Tungsten is used in integrated circuits in a variety of interconnection roles. The M lines of W fall between 1.775 and 1.835 keV and are also challenging to detect against a Si background using conventional sensors. Other overlaps include Ti/N and Ta/Si.

Fluorescence detection is not limited to qualitative analysis; quantitative composition measurements are possible in combination with either reference samples or models of $X-$ray generation and propagation. Even better resolution, near 2 eV or below, enables the detection of slight changes in $X-$ray line shapes and positions due to the bonding state of the target element. These spectral features are sometimes but not universally called chemical shifts. For example, the Al$K\alpha_{1,2}$ and $K\alpha_{3,4}$ peak energies are slightly increased in $Al_2O_3$ compared to metallic Al.

While a significant challenge, the ability to routinely detect these small spectral changes would extend SEM $X-$ray analysis to chemical analysis which would be a dramatic increase in measurement scope. Presently, this level of chemical detail can be obtained using $X-$ray photoelectron spectroscopy (XPS) but XPS requires excellent vacuum conditions and is limited to surface analysis.

Coupling superconducting detectors to a SEM is a significant technical challenge. The safety and ease-of-use issues from liquid helium are nearly insurmountable outside of a cryogenic research laboratory

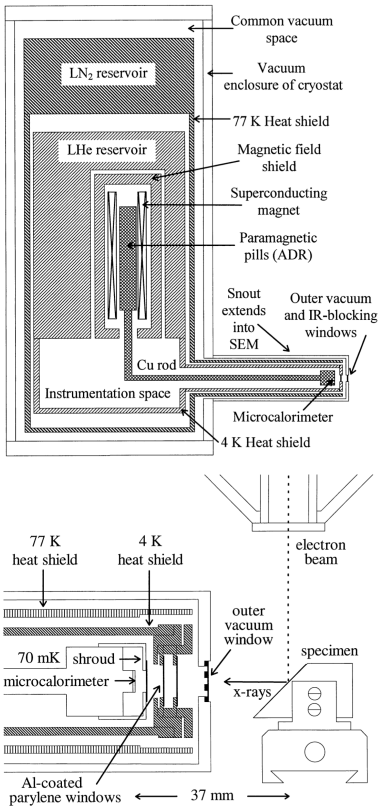


Figure 3.14: **Integration of superconducting sensor in an EPMA system.** On Top, example of cryostat system (ADR in this case). On Bottom, detail of the coupling to the sample holder and electron optics. Source: (174).

*This project has received funding from the European Union´s Horizon 2020 research and innovation programme under grant agreement No 800923.*

while vibration levels from mechanical cryocoolers must be compatible with imaging at high magnifications. The superconducting spectrometer must closely approach the specimen beneath the pole piece of the microscope with little or no modifications to the specimen chamber. Sensor resolution and gain stability must be preserved during operation of the SEM which includes the use of large magnetic fields in the electron optics. Pulse data must be processed in real time with little user intervention and the spectrometer must be easily operated by non-experts.

Up to a degree most of these technical challenges to the use of superconducting sensors, have been overcome, as it proves the emergence of commercial systems:

- An instrument called POLARIS from Vericold appeared in 2002 (173). This instrument contained one TES x-ray sensor and a polycapillary optic to increase the effective solid angle of the sensor. Vericold was purchased by Oxford Instruments in 2007 and the POLARIS was discontinued.
- Star Cryoelectronics has brought the MICA-1600 system to market (172). This instrument contains an array of TES $X-$ray sensors for increased collection area and count rate.

Whether use of the technology becomes widespread will depend heavily on the cost of the systems. On the technical side, important remaining challenge is the routine detection of chemical shifts. If this level of performance can be achieved in commercial spectrometers, the attractiveness of these instruments will be significantly increased.

## 3.4 *Beamline Science*

Large facilities such as synchrotrons and free electron lasers produce beams of electromagnetic radiation and/or particles, with very interesting characteristics:

- Broad spectrum (from microwaves to hard$X-$rays): the users can select the wavelength required for their experiment.
- High flux: high-intensity photon beam allows rapid experiments or use of weakly scattering crystals.
- High brilliance: highly collimated photon beam generated by a small divergence and small-size source (spatial coherence).
- High stability: sub-$\mu m$ source stability.
- Polarization: both linear and circular.

*This project has received funding from the European Union´s Horizon 2020 research and innovation programme under grant agreement No 800923.*

- Pulsed time structure: pulsed duration down to tens of picoseconds allows the resolution of process on the same time scale.

This has lead to the concept of beamlines, which are points at which the radiation is extracted from the sources for being used in experiments in particle physics, materials science, chemistry, and molecular biology (but can also be used for irradiation tests or to produce isotopes). The rapidity of the data acquisition, due the high flux of the radiation, has proved to be a very attractive factor for industrial research.

While superconducting sensors can (correctly) be seen as high performance detectors, ideal for such high-performance experiments, their integration within the beamline environment poses many challenges.

The extreme fluxes at large facilities will overwhelm the count rate capability of present and probably future superconducting detectors of any kind in applications that require measurement of the primary beam.

The situation is much more promising for so-called photon-in, photon-out measurements in which sensors are used to detect radiation scattered from the main beam or produced by the sample when exposed to it. This is the case, for instance, of fluorescence detection (similar to on a SEM instrument) and fluorescence-detected absorption spectroscopy.

In the latter example, and in particular in the $X-$ray range, fluorescence yield is measured as a monochromatic excitation beam is scanned in energy. Scanning over an elemental absorption edge provides a measurement of the unoccupied density of states of the element in question. Here, the energy resolution of the density of states measurements is provided by the high quality, monochromatised exciting beam. However, the energy resolution of cryogenic sensors allows elemental $X-$rays excited by the primary beam to be unambiguously counted in the presence of $X-$rays from other elements and from the scattered excitation beam. Measurements of this type have been successfully performed with both STJ(151) and TES (150). An efficient TES spectrometer can provide an emission spectroscopy capability at beamlines traditionally considered too dim for such measurements, at beamlines with limited space for a traditional emission spectrometer, for very radiation-sensitive samples, in the 2–3 keV energy range that is traditionally difficult to measure, or in photon-starved sce- narios such as time-resolved measurements. TES X-ray spectrometers already provide resolving powers E/DE greater than 103, and performance metrics such as collecting area, count rate, and resolving power are steadily improving. Existing SQUID multiplexing techniques are compatible with kilopixel arrays.

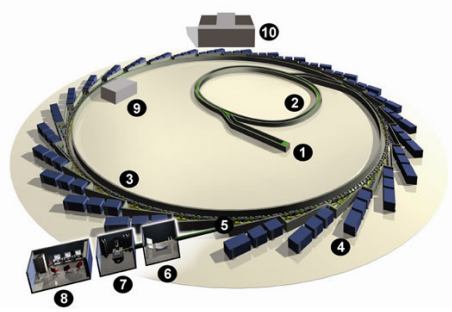


Table 3.2: **A synchrotron will ultimately many beamlines,** supporting the life, physical and environmental sciences. Each individual beamline is specifically designed to support a particular research community or technique. A beamline has four major sections: a) Front end where light is extracted from the storage ring b) Optics hutch where certain wavelengths of light are selected and focussed c) Experimental hutch housing the experimental equipment. d) Control cabin where the scientific team monitors and controls every aspect of the experiment and takes data.

*This project has received funding from the European Union ´s Horizon 2020 research and innovation programme under grant agreement No 800923.*

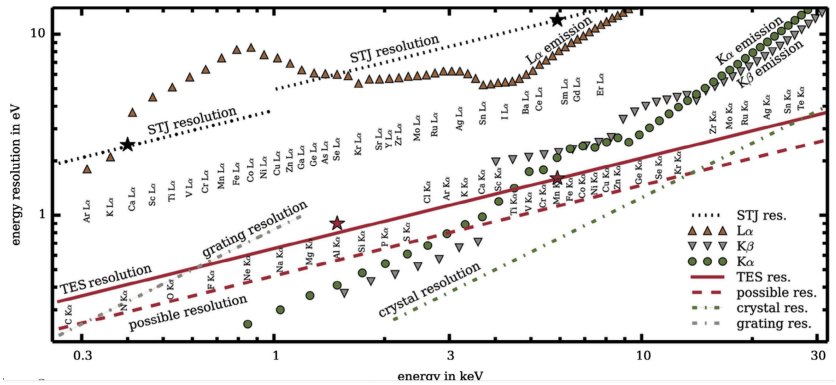


Figure 3.15: **Resolution of microcalorimeter detectors** compared with natural line widths of K$\alpha$-, K$\beta$- and L$\alpha$-lines of a number of elements. Resolving powers of 8000 (green dash-dot) and 1200 (grey dash-dot) are shown which are realistic for a high-efficiency crystal analyzer and grating, respectively. Source: .(149)

Another measurement of interest is emission spectroscopy which is a close cousin to fluorescence detection but that differs by requiring much higher resolving powers in order to extract more subtle information from the detected $X-$ray energies. In emission spectroscopy, the energy distribution of the detected $X-$rays from a single element at a single excitation energy is used to deduce the occupied density of states of that element which, in turn, is indicative of its chemical environment (note that emission spectroscopy at a large $X-$ray facility and chemical shift detection on a SEM differ primarily in the excitation mechanism).

A mainstream technology for this type of measurements are Wavelength Dispersive - WD spectrometers which use optical elements and position sensitive or spatially scanned detectors to achieve energy resolution. The relevant technologies for soft X-rays and hard X-rays differ significantly. Soft X-rays of a few 100 eV (XUV) up to ~1.5 keV are dispersed by use of gratings in large vacuum chambers. These are based on grazing-angle reflections and thus require long path lengths. Surface imperfections do not allow the same approach for hard X-ray radiation, which instead utilises Bragg diffraction. High efficiency requires a curved scatterer so that the Bragg condition can be met for one energy at a range of positions on the optical component. The size of crystalline optics is limited by, for example, the bending radius of single-crystal materials, the quality of the bent-crystalline media and the spatial and financial resources available. Several large research facilities have developed specialised beamlines with spectrometers that combine multiple crystals. Crystal $d-$spacing and elemental absorption edges further complicate the design of a WD analyser in the energy region close to 2keV. The resolution of WD analysers depends on the geometry of the setup, typically allowing a maximum spot size of the exciting beam at the sample position of several tens of micrometers in the dispersive direction.

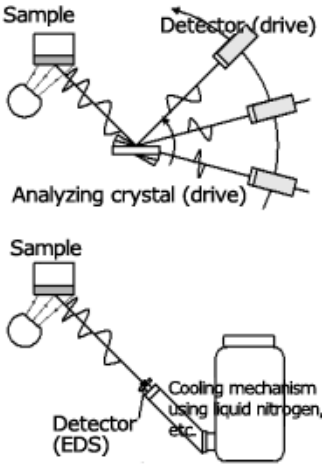


Figure 3.16: **Wave Dispersive vs Energy Dispersive spectrometers.** In WD setups (top) scattered radiation is directed towards a grating or crystal, which reflects each wavelength along a different direction in space. Movement of either the grating or the detector is then used to allow the detector to record intensity at each position/wavelength. In ED set up, scattered radiation hits directly the detector, whose signal is then processed through a pulse detector.

*This project has received funding from the European Union´s Horizon 2020 research and innovation programme under grant agreement No 800923.*

As an alternative, Energy Dispersive - ED spectrometers . An ED spectrometer is able to observe a highly diffuse (many millimetres) beam spot on a sample with no loss in performance, which has profound consequences both for synchrotron-based XES of radiation-sensitive samples and for XES performed with unfocused laboratory-scale X-ray sources. In many scenarios the X-ray flux available to excite a sample is limited by source characteristics, e.g. small laboratory sources, bending-magnet beamlines, sources with special temporal characteristics, or very high energy beamlines. Radiation-sensitive samples including biological materials can also effectively limit the permissible X-ray flux. High detection efficiency is needed for the outgoing secondary X-rays in these scenarios. The detection efficiency of ED devices can be much higher than those of WD approaches because ED detectors do not suffer placement constraints or the Bragg–Darwin losses typical for narrow-band spectral designs.

Most energy-dispersive detectors rely on charge generation in a semiconductor such as silicon or germanium. Stochastic processes during the creation of the charge cloud from an initial interaction (usually photoelectric or Compton) limit the energy resolution possible with this approach to levels inadequate for many X-ray spectroscopies including XES and X-ray absorption spectroscopy (XAS). In spectrometers equipped with superconducting sensors, the energy resolution of a properly designed microcalorimeter is limited by power fluctuations between the sensor and thermal bath and by broad-band noise contribu-tions from Johnson fluctuations or the read-out amplifier.

Emission spectroscopy at a synchrotron using TES arrays was first demonstrated to distinguish between two nitrogen-bearing explosive compounds. These data and a detailed analysis of the potential of TES arrays for emission spectroscopy at large facilities has been demonstrated(149). While the energy resolution of cryogenic sensors is unlikely to be as good as competing gratings and crystals, the resolution of cryogenic sensors can be comparable to the natural lifetime broadening that sets the energy-scale of many spectral features of interest (see Figure 3.15). On the other hand collection efficiency of arrays of superconducting $X-$ray sensors is potentially several orders of magnitude larger than competing gratings and crystals. Increased collection efficiency is desirable for a range of photon-starved experiments including measurements of dilute samples, radiation-sensitive samples, and time-resolved measurements.

A few examples of other opportunities for superconducting spectrometers include Compton scattering, energy-resolved diffraction, and resonant inelastic $X-$ray scattering where an emission spectrum is generated for each setting in an energy sweep of the exciting beam.

*This project has received funding from the European Union ´s Horizon 2020 research and innovation programme under grant agreement No 800923.*

Overall, it seems that large facilities will provide interesting opportunities for superconducting. Perhaps the largest outstanding challenge is to streamline and automate the pulse processing from the arrays of hundreds to thousands of sensors that are needed to obtain interesting collection areas and count rates. This issue does not fall directly onto the area of sensor development, but rather on that of processing technologies (hardware and software).

## 3.5 *Quantum Information Technologies:*

The promise of quantum information is high, including quantum computers and unbreakable cryptography.

The basic concept underpinning all these expectations is that information can be stored in a quantum system (normally defined by a two-dimensional Hilbert space). Because the general state of the system is defined by a linear superposition of all possible eigenstates, they have amplitudes for and thus carry information about all these eigenstates at the same time. Similarly, a collection, or register, of $N$ of these systems can have exponentially many $(2^N)$amplitudes, whereas the analogous conventional binary data register can only hold one of these states at any given time. Clearly, if it is possible to operate, or compute, simultaneously with all the amplitudes of a quantum register, there is the possibility of massively parallel computation based on quantum superpositions. Also, since the interaction with the system (measurement) will irreversibly collapse its state into one of the eigenstates, it is impossible to read, copy or clone this type of systems. This unavoidable disturbance through quantum measurement can be used to detect eavesdropping on quantum communications and provides the basis for guaranteed security.

This type of encoding system is known as qubit. On the technological plane, efforts are now focused on the search of technologies that could allow to build qubits (i.e. systems where two orthogonal quantum states are or can be separated from the rest of the space). Examples of this, or in some cases reasonable approximations, include: two adjacent energy eigenstates of atoms or ions (separated by a microwave or an optical transition); the vacuum or single photon state of a mode in a small optical or superconducting microwave cavity; two orthogonal linear or circular polarisations of a traveling photon or weak light pulse; the 'which path' label of a photon or atom in an interferometer; the energy eigenstates (up or down) of a spin -1/2 in a magnetic field; two adjacent energy eigenstates of an electron or exciton in a quantum dot; two charge states of a tiny superconducting island or flux states of a superconducting ring; and so on. This list is not at all exhaustive, and many more candidate qubits

*This project has received funding from the European Union 's Horizon 2020 research and innovation programme under grant agreement No 800923.*

have been proposed and are under investigation.

So far, all the foreseen applications remain at a conceptual level, and their practical use is not even within a mid term horizon. However, as demonstrations of qubits based in any of the aforementioned systems continue to emerge, the landscape is evolving into a middle stage where the goal is the controlled evolution. This is the aim in systems with several interacting qubits according to some prescribed quantum algorithm to effect a computation, or in systems where there is propagation of qubits from Alice to Bob for communication (perhaps also with processing at A or B). The implementations must fulfil a minimum of the following requirements.

a) A collection of well-characterised qubits is needed. One at a time will do for cryptography; interactions and scalability in number are necessary for computing.

a) Preparation of known initial states for the qubits must be possible.

a) The quantum coherence of the system(s) must be maintained to a high degree during the evolution stage.

a) The unitary quantum evolution required by the algorithm or protocol must be realisable. As with conventional computing, the minimum of a universal set of elementary gates must be possible.

a) Quantum measurements on specific qubits must be possible.

a) The capability to interconvert stationary (processing or memory) qubits and flying (communication) qubits must exist.

a) It must be possible to transmit flying qubits coherently between specified locations (note that point 3 is effectively implicit in 7).

Quantum computing requires *a-e*, although distributing it between processors would add f and *g*. Elementary quantum cryptography requires *a*, *b*, *e*, and *g*; Usable teleportation essentially requires the lot, although *f* can be dropped for demonstrations and it should be noted that the processing demands *d* are very simple compared with all-purpose computing. Qubit storage as needed in *d* is implicit, although stable long term storage would also be desirable for teleportation and other communication applications.

The demands outlined above are very tough indeed, and require quires many experimental breakthroughs[13]. The construction of useful system will not be easy and the issue of quantum coherence (point *c*) is always lurking. With the additional freedom of Hilbert space, which gives quantum systems their potential advantage, comes the penalty that quantum states are very delicate. Qubits can entangle with environmental elements over which there is no

[13] An updated overview on the challenges regarding current quantum computing systems can be found in ref (106).

*This project has received funding from the European Union´s Horizon 2020 research and innovation programme under grant agreement No 800923.*

control. This decoherence is easier to tame for the case of individual photons propagating down standard optical fibers or even through free space, so usable quantum cryptosystems have already made it out of the laboratory. However, decoherence was thought to be a terminal problem for many interacting qubits, which is essential for practical quantum computation. The bottomline of all this is that optical/photonic technologies have made very significant progress and present some of the most mature alternatives, at least for quantum cryptography and communications.

Quantum information protocols require single-photon states, which are difficult to prepare in practice because attenuated laser pulses obey Poissonian statistics: the probability of producing a photon state $|n\rangle$ is $P(n) = (\frac{\mu n}{n!})e^{-\mu}$ where $\mu = \langle n \rangle$ is the mean number of photons per pulse.

On-demand single-photon sources for quantum information applications are a highly active research field. Despite significant progress, current single-photon sources are imperfect because the second-order correlation function $g(2)(0)$ is non-zero, implying residual multiphoton emission, and also because source emission rates are low (that is, $\mu << 1$).

In quantum key distribution, multiphoton states represent a security 'loophole' that can be exploited by eavesdroppers. In linear optical quantum computing, efficient detection of different photon number states is crucial for many protocols. For these applications, a detector able to measure the number of photons (in the range 1-10) is highly needed.

There are two classes of photon number resolving detectors. One class has intrinsic photon number resolving - PNR capability producing an output which is inherently proportional to the number of photons, i.e. like in TES. A second approach multiplexes conventional detectors. This can be achieved either by combining the output signals of an array of detectors (spatial multiplexing) or by splitting the multiphoton pulse via a cascade of beamsplitters and then delaying the signals so that they can be detected sequentially by a single detector (time multiplexing). The fidelity with which an n-photon state can be recorded scales as $\eta$n thus, high-efficiency detectors are desirable for these applications. In a multiplexed photon-number-resolving scheme, it is necessary to have a large number of pixels (or time bins) N, such that $N >> n$, to reduce the possibility that two or more photons were absorbed at any one pixel.

Commonly an ideal single-photon detector - SPD should satisfy several requirements like:

- the probability that a photon incident upon the detector is successfully detected (the detection efficiency, $\eta$) must be 100%;

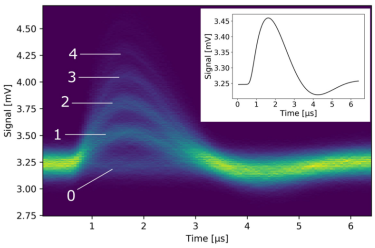


Figure 3.17: **Photon Number Resolving using TES.** Heatmap of measured photon traces with different peak heights corresponding to different photon numbers per pulse, pointed out by the displayed numbers, for an on-chip TES. The inset shows the average TES response.(171)

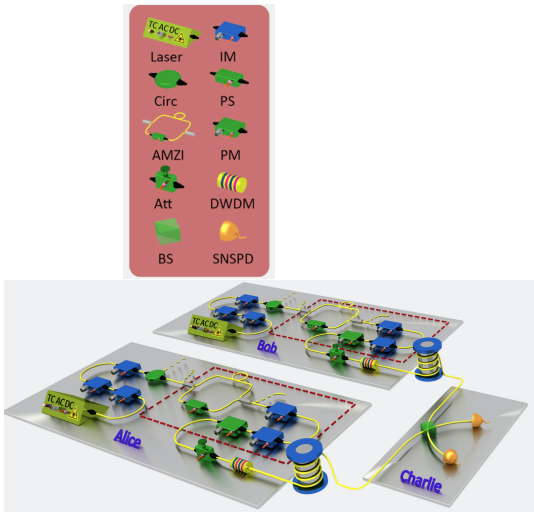


Figure 3.18: **Example of Quantum key distribution set up.** TC, temperature controller; AC, alternating current; DC, direct current; Att., attenuator; DWDM, dense wavelength division multiplexer; BS, beam splitter; SNSPD, superconducting nanowire single-photon (SP) detector.Source: (111)

*This project has received funding from the European Union´s Horizon 2020 research and innovation programme under grant agreement No 800923.*

- the rate of detector output pulses in the absence of any incident photon (the dark-count rate , DCR) must be 0 Hz;
- the time after a photon-detection event during which the detector is incapable of detecting a photon (dead time or recovery time, $t_d$) must be 0 s. This is related to the maximum count rate of the detector, $R = 1/t_d$;
- the variation from event to event in the delay between the input of the optical signal and the output of the electrical signal (timing jitter, $\Delta t$) should be 0 s;
- the device must have photon number resolving capability. Many SPDs cannot discriminate between one or more incident photons, while in many quantum optics applications it is important to be able to resolve the number of absorbed photons.

There are a number of well established SPD technologies (which are, up to a degree, competitors of superconducting ones):

- **Photomultiplier Tubes - PMT** consists of a vacuum tube with a photocathode for light absorption from which electrons are ejected through the photoelectric effect (the energy of the incident photon must be higher than the work function of the photocathode material). This single- or few-electron photocurrent is then multiplied by a series of electrodes (dynodes) each one biased at a greater, positive, voltage than the one before producing a macroscopic current pulse of $>10^6$ electrons.
- **Single-photon avalanche photodiodes - SPAD** uses a similar process to the PMT, but the initial photon absorption creates an electron-hole pair and the charge multiplication is continuous, with a voltage applied across a thin semiconductor layer rather than between discrete dynodes suspended in vacuum. SPADs are typically operated in what is referred to as "Geiger-mode," where a bias voltage greater than the diode's breakdown voltage is applied. Thus when a charge is generated by an incoming photon, the charge multiplication (or avalanche) proceeds until it saturates at a current typically limited by an external circuit, and that current is self-sustaining. The saturated avalanche current must be terminated by lowering the bias voltage below the breakdown voltage before the SPAD can respond to a subsequent incoming optical pulse.
- **Frequency up-conversion devices:** the goal of frequency up-conversion single-photon detection schemes is to convert a telecommunications wavelength photon to a shorter wavelength that

*This project has received funding from the European Union´s Horizon 2020 research and innovation programme under grant agreement No 800923.*

can be more efficiently detected by a commercial single-photon detector. The mechanism used is sum-frequency generation in a nonlinear optical crystal: a weak signal at frequency $\omega_{in}$ is combined with a strong pump signal at frequency $\omega_{pump}$ to yield an output signal at the summation frequency of $\omega_{out} = \omega_{in} + \omega_{pump}$. If sufficient pump power is available, this frequency up-conversion can occur with near-unity efficiency.

- **Visible-light photon counter - VLPC** is a low-temperature semiconductor-based photon counting technology. The device offers high-efficiency detection of single photons up to wavelengths of 1 $\mu m$, the ability to resolve photon number, good timing resolution and moderate dark counts. The VLPC is based on an earlier concept called the solid state photomultiplier, a blocked-impurity-band device based on As-doped silicon, which gives single-photon sensitivity from visible wavelengths up to $30\mu m$. Solid-state photomultiplier and VLPC devices operate at low voltage through a controlled single-carrier multiplication process, giving rise to a signal that is proportional to the photon number. In a VLPC the gain region and absorber are separate, maximising the sensitivity in the wavelength range of 400–1000$nm$.

In what concerns superconducting technologies, mainly two of them (TES and SNSPD) have been employed in this type of applications. TES have been applied in quantum information processing and quantum photonic systems (65), quantum key distribution (**?** ) and quantum steering (64) and quantum computing(65). SNSPD have been used for quantum key distribution up to 250 km away, as well as for demonstrating long distance(62), entanglement based quantum key distribution(61), and high key transmission rates (60). In the field of quantum optical computing, key demonstrations employing SNSPDs include the demonstration of the first telecom wavelength controlled-NOT gate(63).

The combination of single-photon sources, passive optical circuits, and single-photon detectors enables important functionalities in quantum communications, such as quantum repeaters and qubit amplifiers, and also forms the basis of all-optical quantum gates and of linear-optics quantum computing. However, present implementations are limited to few qubits, due to the large number of optical components required and the corresponding complexity and cost of experimental set-ups.

The monolithic integration of quantum photonic components and circuits on a chip is absolutely required to scale implementations of optical quantum information processing to meaningful numbers of qubits. The integration of passive circuits has been demonstrated in

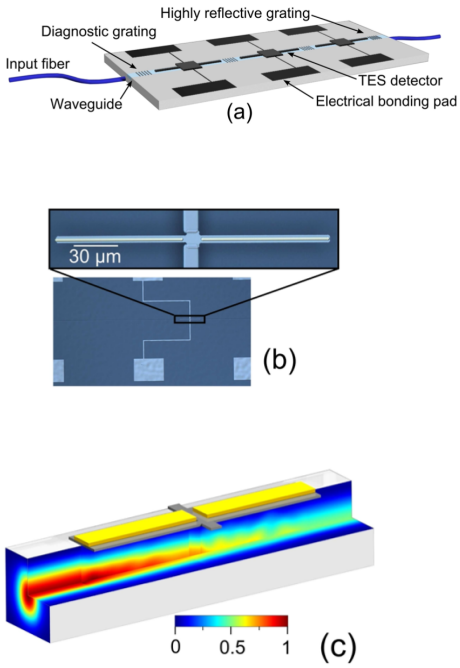


Figure 3.19: **On-chip photon detection scheme.** (a) Three TES detectors with extended absorbers are operated in series on a single waveguide. Integrated Bragg gratings and two-way fibre coupling allows for the precise determination of each device efficiency without additional assumptions. (b) The extended-absorber detector utilises a gold spine to increase thermal conduction and allow absorbed energy (from photons) to be detected by the TES (square device, centre). (c) Simulated mode profile as light propagating in the waveguide is absorbed by the detector due to evanescent coupling.(153)

*This project has received funding from the European Union´s Horizon 2020 research and innovation programme under grant agreement No 800923.*

waveguides based on silica-on-silicon and on laser-micromachined glass, but a platform for the simultaneous integration of sources, detectors, and passive circuitry is still missing.

The integration of detectors is particularly challenging, as the complex device structures associated to avalanche photodiodes are not easily compatible with the integration with low-loss waveguides and even less with sources.

Lithium niobate is an established platform in the field of classical integrated optics because of its high second-order susceptibility and electro-optic properties. Until now, detection from lithium niobate waveguides has been restricted to fiber-coupled detectors, which adds an extra interface and associated losses. Of the various types of fiber-coupled detectors, those based on the breakdown of superconductivity offer the highest efficiency at telecom wavelengths and can be tailored for low timing jitter, different photon numbers, or even photon-number resolution. However, the positioning of fiber-coupled detectors with respect to an integrated optical circuit is limited, and their scaling towards complex circuitry is challenging. Integrated detectors, using the coupling from an evanescent field of a waveguide into an on-chip detector, enable more complex circuitry, as they can be deposited at different positions inside the optical circuit.

On platforms such as silicon or III-V semiconductor waveguides, both integration of SNSPDs (154) and TESs(153) has been realised. Proof-of-principle detection of single photons using TESs on lithium niobate waveguide has been provided recently (171).

Although it is often considered a secondary application (because sensors are not part of the qubit system) mitigation of decoherence, particularly in quantum computing, is quickly becoming an important issue. In superconducting qubits (so far one the leading platforms for quantum computing applications[14]) coherence of the system is affected by the breaking of Cooper pairs of electrons. The experimentally observed density of the broken Cooper pairs, or quasiparticles, is orders of magnitude higher than the value predicted at equilibrium by the Bardeen–Cooper– Schrieffer theory of superconductivity. It has been shown that infrared photons considerably increase the quasiparticle density, yet even in the best-isolated systems, it remains much higher than expected. Evidence that ionising radiation from environmental radioactive materials and cosmic rays contributes to this observed difference has been provided recently (110). The effect of ionising radiation is to elevate quasiparticle density, which would ultimately limit the coherence times of superconducting qubits of the type to milliseconds. While this effect is small for today's (rather primitive) qubits, reducing or mitigating the impact of ionising radiation will be critical for realising fault-tolerant superconducting

[14] IBM Quantum Experience is currently one of projects allowing public and premium access to cloud-based quantum computing services.

*This project has received funding from the European Union 's Horizon 2020 research and innovation programme under grant agreement No 800923.*

quantum computers (110). Concepts integrating TES nearby qubits have been proposed recently (108). The neighbouring sensor provides the potential to detect environmental disturbances causing errors in a quantum computation. In the simplest form, such co-located sensors provide a means to selectively reject just those calculations where an environmental disturbance is likely to result in an incorrect calculation result. Independently of whether superconducting sensors will be integrated or not into a qubit system, these technologies offer an important scientific platform for understanding the physical mechanisms underpinning quantum decoherence. Some proposed solutions derive directly from this kind of scientific approach (107).

In summary, quantum information applications constitute an area where superconducting technologies could have an important opportunity. The reason for this are:

- many of the technological platforms intrinsically need to operate at very low temperatures in order to mitigate effects which are detrimental for the quantum encoding mechanisms. The need for costly and complex cryogenics is therefore not a limiting factor necessarily imposed by the sensing technology itself.
- very high performance of the sensors, which can be summarised in the requirements for single photon detection, is needed in many cases.

in order to remain competitive, the focus must be placed in the integration of the sensors.

## 3.6 *Terahertz spectroscopy and imaging*

Terahertz - THz range usually relates to frequencies ranging from $10^{11}$ to $10^{13} Hz$. This region of spectrum provides information about absorption and the complex dielectric constants of materials[15]. This, on turn, relates to the investigation of the rotation of molecules in the gas phase, molecular interactions such as van der Waals forces and hydrogen bonds in the liquid phase or the solid phase, and ferroelectricity of solid materials.

From the point of view of applications, the main advantages of THz spectroscopy and imaging are:

- **good transparency for optically opaque materials** (mainly because at THz wavelengths, longer than visible ones, light scattering in materials is reduced),
- **sub-mm spatial resolution** for imaging (the diffraction limit $\lambda/2$ is $\sim 150 \mu m$ @ 1 THz, thus allowing for spatially resolved spectral mapping) and

[15] In molecular vibrations, the basic theory of THz spectroscopy is similar to that of infrared spectroscopy. For example, the harmonic vibration of a two-atom molecule is

$$\nu = \frac{1}{2\pi}\sqrt{\frac{\kappa}{\mu}}$$

where $\nu$ is the frequency, $\mu = \frac{m_1 \times m_2}{m_1 + m_2}$ is reduced mass (where $m_1$ and $m_2$ are the masses of two atoms), and $\kappa$ is the spring constant. THz spectroscopy generally detects very slow vibration of molecules, which typically means weak molecular interactions when k is very small, or large molecule interactions when m is very large.

*This project has received funding from the European Union´s Horizon 2020 research and innovation programme under grant agreement No 800923.*

- **significant information regarding intermolecular interactions** (in particular, about hydrogen bonds between molecules).

The development of systems adapted for applications has required a prior stage of development of components, among which sources of radiation and detectors are certainly essential.

In what concerns sources, a first classification can be:

- **Broadband:** Thermal emitters, such as glow-bars and mercury lamps, and liquid-helium cooled bolometers are conventionally used in Fourier transform far-infrared spectroscopy systems. However, they are limited within laboratory investigations due to low output powers and liquid-helium cooling.

  Free electron lasers are the most powerful sources of THz radiation available, producing either CW or pulsed beams of coherent THz waves with an efficiency potentially close to unity. Their bulky size and high cost prevent their use in non laboratory applications.

  Near-infrared femtosecond lasers can be used for generation of picosecond THz pulses by a coherent and time-gated method. The generated THz power is not high, typically with an average power from nW to hundreds of $\mu W$. One common way to generate THz emission is by up scaling a fundamental frequency via frequency multiplication, although down-conversion is also possible coming from the photonics side.

  Biased photoconductive antennas, which are made of semi- insulating GaAs or low-temperature-grown GaAs (LT-GaAs) have been used both as sources and detectors.

  Unbiased bulk semiconductors and other crystals, such as InAs, InSb, ZnTe, InP, GaP, GaAs, GaSe, $LiNbO_3$, $LiTaO_3$, and polymer films are also widely used as THz emitters, based upon the mechanism of either the ultrafast transport of charged carriers or the optical rectification.

  The bandwidth of the radiated THz spectrum depends on the laser bandwidth, the emitter and the detector. Using short laser pulses with a pulse duration of $\sim$ 10 fs along with specific emitters and detectors, the achieved bandwidth can reach up to 60–100 THz, by trading off SNR. Usually a system with a narrower bandwidth has a higher SNR. For instance, using LT-GaAs antennas as the emitter and detector, a THz spectrum with a smooth spectral distribution between 0.3 and 7.5 THz, and a dynamic range of $\sim$ 60 dB (for THz power) can be obtained, which is ideal for THz spectroscopic sensing.

- **Narrowband Continuous-Wave:** Electronic sources include frequency-multiplied Gunn diode oscillators and backward wave oscillators

*This project has received funding from the European Union´s Horizon 2020 research and innovation programme under grant agreement No 800923.*

- BWOs. Gunn diode oscillators can provide power ranging from $\sim$ 200mW near 0.1 THz to $\sim$ $\mu$W near 1.7 THz. The BWO's power varies from $\sim$ 100mW at 0.1 THz to $\sim$ 1mW at 1.25 THz.

  Nonlinear optical sources include THz-wave parametric oscillators - TPOs and photocurrent-based photo-mixers. TPOs provide ns THz pulses with the maximum THz peak power of above 100 mW, and a range of 0.7–3.8 THz. CW coherent THz radiation can be generated by photo-mixing, where two lasers with slightly different frequencies are overlapped on an fast semiconductor such as LT-GaAs. This material will generate a THz wave with a frequency equal to the difference of the laser frequencies, and changing the laser frequencies will change the difference and, thus, change the frequency of the THz wave. This mechanism allows photo-mixing to sweep a broad range of frequencies and use it as an spectroscopic tool, although the time to acquire a spectrum is typically much longer than with other available techniques. Photocurrent-based photo-mixers using biased semiconductors with ultrafast carrier recombination time have a tuning range from 0.1 to above 3 THz in a single device, with power levels typically below 1 $\mu$W beyond 1 THz.

  There are also three types of THz lasers available for CW generation: gas lasers, quantum cascade lasers - QCLs, and free-electron lasers - FELs. THz gas lasers are not continuously tuneable, but have been shown to operate at over 2000 frequencies from 0.9 to 6.86 THz, with power levels ranging from 1 to $\sim$ 180 mW. The QCL is a major step toward a compact and practical electrically pumped THz emitter. It features high output powers (above 100 mW) and a control of layer thickness which allows the emission wavelength to be designed in (the lowest frequency reaches $\sim$ 2.1 THz). However, it works at liquid-helium or liquid-nitrogen temperature. FELs are very powerful pulsed or CW sources for widely tuneable and coherent radiation. But their large sizes limit their applications.

In what concerns detectors, several physic phenomena have been exploited, where THz radiation interacts with:

- **the electron gas contributing to its kinetic energy**, in heating it and producing a change in a physical property of the material. This can be:

  a) thermal expansion as in Golay cells, nano-cantilevers and liquid-in-gas-thermometers;

  a) surface charge as in Triglycine sulfate, Deuterated triglycine sulfate, Lead (Pb) zirconate titanate, Barium strontium titanate

*This project has received funding from the European Union´s Horizon 2020 research and innovation programme under grant agreement No 800923.*

and Lithium tantalate;

a) electrical potential as in thermocouples, thermopiles;

a) ionisation (of a gas) as in Neon tube/glow discharge detectors;

a) electrical resistance, as in metal bolometers, carbon resistor bolometers, graphene bolometers, Si or Ge hot electron bolometers, microbolometers and TED.

a) electrical inductance as in KID.

- **the electron gas creating plasmon oscillations.** This can take place:

  a) in a narrow channel, as in GaN and graphene field effect transistors;

  a) at a surface, as in sensors based in surface plasmons and surface plasmon polaritons.

- **individual electrons within the electron gas,** inducing a transition across:

  a) a metal-semiconductor barrier, as in Schottky barrier diodes;

  a) a barrier within a semi-conductor, as in a tunnelling junction backward diode;

  a) a superconductor-insulator-superconductor junction (typically via photon assisted resonant tunnelling);

  a) from bound state to bound state, as in quantum dots;

  a) from bound state to continuum, as from a quantum well, or intrinsic semiconductors (Ge:Ga, Ge:B, Ge:Zn)

- **electrons under the influence of a secondary (reference) radiation field** in a nonlinear medium. This can be:

  a) other radiation (heterodyne detection), using hot electron bolometers bolometers, Schottky barrier diodes, field effect transistors or superconductor-insulator-superconductor junctions

  a) with itself, as in the cavity of a quantum cascade laser.

- **probing pulsed radiation.** This can lead to:

  a) rotation of polarisation state, as in electro-optic detection, optical rectification techniques;

  a) producing harmonics as in air biased coherent detection

  a) inducing a current floe, as in photoconductive receivers and rectification techniques.

*This project has received funding from the European Union´s Horizon 2020 research and innovation programme under grant agreement No 800923.*

Such a wide choice of possibilities has led to a large amount of knowledge and technological development[16]. Obviously not all the detectors compete in the same level, but the choice of the optimal ones, as we will discuss in the following subsections, ultimately depends on the requirements of the applications.

At system level, the most important techniques are:

- **CW systems** operate at a single frequency and emission is continuous or modulated, so they are narrowband in nature and may have a limited tuneability, but are capable of high spectral resolution (~100 MHz). CW sources typically allow to reach output powers above 10 mW, which is higher than average power of pulsed sources ($\sim \mu W$). Because of their high spectral resolution, they are useful for gas phase spectroscopy but not for solid or liquid phases.

  CW systems can be set both in active or passive configurations. A passive system detects the radiation emitted by the sample, whereas an active system illuminates the sample and detects the reflected or transmitted radiation.

  Both narrowband or broadband detectors can be integrated in CW setups. Narrowband detectors are only sensitive to a specific frequency and, often, they pick up less noise and do not require modulation to reach high sensitivities. Broadband detectors are sensitive to a broader range of frequencies and modulation or filtering is necessary to reduce the effects of the background noise in order to achieve good sensitivities. In some cases cryogenic conditions are required for operating the detectors (like in the case of superconducting sensors).

- **Time-domain systems** are based on the generation and detection of an electromagnetic transient (or pulse) that has a duration of few picoseconds[17].

  THz Time Domain Spectroscopy - TDS measures two electromagnetic pulse shapes: a reference signal and a sample signal. The later is used for generating a THz pulse, which is then sent towards the sample. Then THz radiation is collected, reconverted into the original radiation wavelength, and recombined with the reference signal. Due to interaction with the sample, the sample beam will have a modified shape. These modifications to the pulse shape are related to the optical properties of the sample. Fourier transformation of the detected pulses allow to extract dielectric properties (absorption coefficient and refractive index), given than certain parameters (thickness of the sample, if working in transmission mode, for instance) are know. Since THz-TDS uses time

[16] A rather comprehensive comparative, attending precisely to this classification, can be found in ref (78). Another detailed description of many of the technologies can be found in ref (77).

[17] An introduction to the technique can be found in ref: (66).

*This project has received funding from the European Union´s Horizon 2020 research and innovation programme under grant agreement No 800923.*

gating in sampling the THz pulse, it reduces background noise and has a high signal-to-noise ratio. THz-TDS measures transient electric fields (amplitude and phase), and this gives THz- TDS superior sensitivity and better dynamic range compared to Fourier transform infrared - FTIR spectroscopy, which only measures intensity.

THz time-domain is the "de facto" standard technology for spectroscopic and ultrafast dynamics studies of matter in the THz range. The time-resolved nature of most THz systems offers the possibility to probe dynamic processes in the sub-picosecond range. The short pulse acquired in the time-domain (or waveform) contains many frequencies that can be accessed with a Fourier transform. Therefore, time-domain systems are broadband in nature and they are ideal for spectroscopic applications and the study of ultrafast phenomena.

Major application for THz time-domain spectroscopy (TDS) has been in spectroscopic studies to analyse the spectral features of organic molecules mostly in solid phase but also gaseous and liquid forms.

Time-domain systems have traditionally evolved from the photonics side using femto-second lasers to pump a PCA or EO crystal to generate the THz pulse. A typical THz TDS system implements an emitter based on PCA and a detector based on EO sampling or PCA as well. However, surface emission, EO rectification, and tilt-front generation in $LiNbO_3$ are also commonly used as emitters in research setups. Typical bandwidth ranges from 2 to 5 THz with signal-to-noise (SNR) between 50 to 60 dB at 1 second integration time.

It has been demonstrated that air plasma can be used to generate and detect THz waves. This method, called THz Air- Biased-Coherent-Detection, is capable to provide a bandwidth in excess of 10 THz with intense electric fields (>100 kV/cm), which allows covering the entire THz range and conduct non-linear spectroscopy. This technique requires a powerful and short pulse amplifier laser, which limits its application outside research environment.

In what concerns applications, the THz technologies have triggered an, almost surprising, enormous amount of expectation and related research activity. In a nutshell, the hype is mainly due to the possibility, deduced from the intrinsic properties of THz radiation, of having fast, non-invasive technologies for inspection/diagnose which are safer alternative than ionising radiation (X-ray and $\gamma$-ray) technologies.

*This project has received funding from the European Union´s Horizon 2020 research and innovation programme under grant agreement No 800923.*

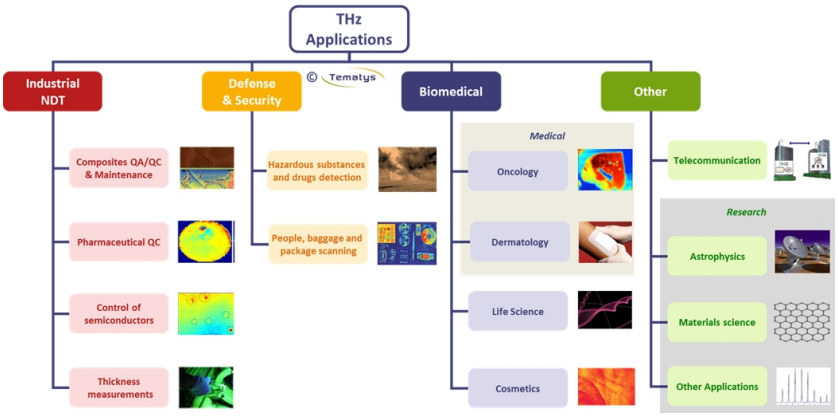


Figure 3.20: **Terahertz application families,** as proposed by market analyst Tematys.

There has been much discussion[18] about the reasons why, despite the large amount of research effort, this has not yet translated into consolidated value chains and markets beyond small niches.

One of the reasons is certainly maturity. Many technological challenges need to be solved in order to have access to very complex applications, and particular those where end-users do not have a technical background, so they need very automated systems, and to have information processed up to a level which is comprehensible for them. Examples of this are both medical and security applications. In any case, the history of the development of THz applications is still relatively short, as compared with that of other, now mainstream technologies, which they are trying to displace.

[18] See, for instance, this presentation by Dr. Patrick Leisching in Teraflag (EU funded) project.

> We will now provide a fast overview over the different sectors. As the number of applications very large, so is the amount of published material. An interesting recent review, indicating main current challenges and guidelines for short-term research for each type of application can be found in ref. (56). The information provided here is complementary to this updated work.

### 3.6.1 *Polymer Industry*

Polymers are transparent or semi-transparent for terahertz waves and thus among the most important materials for implementations of THz technology. One of the most important industry market drivers for THz technology is currently the field of non-destructive testing of plastics and plastic products. There is an very significant demand for test equipment, both to ensure acceptable product quality and to reduce material usage and wastage[19].

[19] With material savings in production of approx. 1%, even a test instrument of about €100 k will amortise itself within 2 years. See, for instance, the value proposition of INOEX.

Currently, established and cost-effective nondestructive testing technologies include X-ray scanners, ultrasonic sensors and microwave transceivers, but the integration of these technologies in industrial environments rise some issues. X-rays are ionising radi-

*This project has received funding from the European Union´s Horizon 2020 research and innovation programme under grant agreement No 800923.*

ation and thus extra-ordinary safety measures have to be set in place. Ultrasound inspection requires a contact medium, which on turn brings the need for cleaning and add-on cost of consumables. Compared to microwaves, THz waves achieve higher spatial resolution. Non static properties such as crystallisation and polymerisation, can also be observed and tracked.

Among the extended range of polymers handled by industry, it is worth mentioning:

- **Extrusion manufacturing:** Due to their good optical penetration through most polymers, THz systems are particularly suitable for the inspection of plastic components and the detection of defects, like air bubbles where THz waves are strongly scattered at the air-polymer interfaces, reducing transmission. THz techniques can reveal not only voids but also thermal or mechanical stress, deformations and ageing processes in polymer materials. The effects of these processes can be seen, for example by observing changes in the degree of crystallinity or changes in the glass transition temperature.

- **Composites:** In these type of materials polymers are integrated with some other elements with the purpose of engineering and optimising properties (mechanical, optical, electrical, etc). For the plastics industry, it is important to verify the additive content , homogeneity of the distribution of the added components (degree of dispersion, orientation of the particles, molecular chains and/or fibres) and moisture content. All these can be deduced from measurements of the THz refractive index and absorption coefficients.

- **Foams:** have increasing demand in construction, automotive, aerospace and rotor blade industries. The cellular structure and the effective density of the foam are decisive quality parameters that have to be controlled during the production process. Refractive index in the Thz range increases linearly with the effective density of the material, and thus can be used for this monitoring tasks. Presence of defects with potentially detrimental effects (mainly in mechanical properties) can be also detected through imaging in the THz range as mentioned before. .

- **Adhesives**: are essential parts in several construction and manufacturing processes in which several elements must be assembled together, generally with the aim of achieving same mechanical integrity as if the whole assembly was built from a single piece of material. THz spectroscopy can be used for: 1) determining thickness and distribution of adhesive joints, 2) detecting presence of moisture that could degrade material properties, 3) monitor-

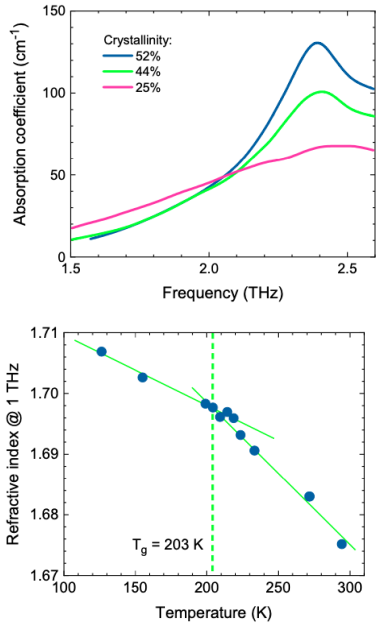


Figure 3.21: **THz absorption spectrum of polymer** (polybuthylene terephathalate) with different degrees of crystallinity. The glass transition temperature can be determined from the intersection of the two linear slopes. Source: (104).

*This project has received funding from the European Union´s Horizon 2020 research and innovation programme under grant agreement No 800923.*

ing of polymerisation process in UV-cured and two-component adhesives.

- **Paints and Coatings:** High-tech and/or heavy duty surfaces make intensive use of surface coatings for increasing protection against harsh environmental conditions or decorative purposes. These application has been widely used in the manufacturing industry of virtually any type of vehicle, from space-ships and aeronautics down to automotive, but it has also gained importance in mass-consumer electronics (decorative and protective coatings for mobile phones, laptops and tablets) and construction. Monitoring of thickness and homogeneity is essential for optimising lifetime of coated objects and cost of the coating process[20]. Complex multi-layer coatings push established measurement technologies to their limits, and indeed many of the conventional techniques, such as magnetic gauges or eddy-current fail in the case of non-metallic substrates (such as glass-fibre reinforced plastics). Until recently it has only been possible to test the paint on these substrates using destructive methods in which the surfaces are destroyed with a wedge cut. Time of flight measurements allow to deduce the thickness of consecutive layers through detection of the fraction of THz radiation reflected at each interface. Due to the complexity of the signal, advanced processing algorithms (like frequency domain analysis) may be required. The main advantage of THz in this case is the possibility to apply non-contact acquisition, which allows monitoring even when layers are still not completely solid. Improvement of signal-to-noise ration seems to be a current need in this application (103).

### 3.6.2 *Pharmaceutical Industry*

High-precision quality monitoring is of paramount importance in pharmaceutical production, because the efficacy and safety of a medicinal product deeply on accurate control of both its chemical composition and its microstructure and mechanical properties. From the point of view of business operations, pharmaceuticals are high-value products where increased product consistency and reduced wastage bring significant cost benefits, therefore justifying investment in relatively expensive technologies that improve the effectiveness of quality monitoring.

Pharmaceutical materials are (semi-) transparent at THz frequencies and often possess characteristic spectral signatures, whereas they are opaque in the visible and near-infrared. Because of this, use of THz spectroscopy have been continuously growing in pharmaceutical and biochemical R&D. In general, detailed spectroscopic measure-

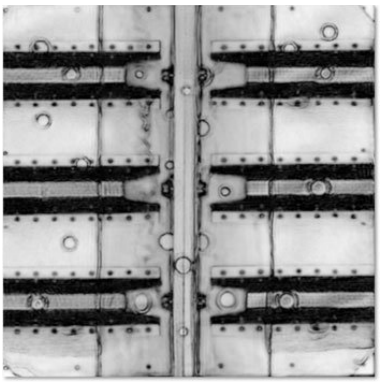

Figure 3.22: **Inspection of Polymers:** An emblematic example is the inspection of the insulating elements made of foam which caused catastrophic accident of the Space Shuttle. The defects become evident as round features in the THz image. Source: (105)

[20] See, for instance, value proposition at IGOS.

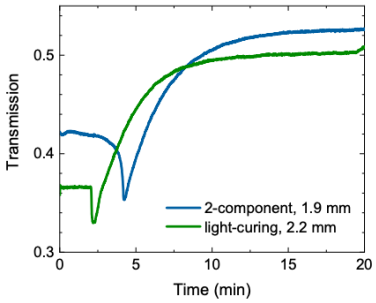


Figure 3.23: **Monitoring of adhesive polymerisation process.** The drop in the transmission of THZ radiation indicates beginning of polymerisation. The refractive index increases (and absorption decreases) as the exothermal reaction causes heating and softening of the material. Example of application developed at Toptica Photonics AG.

*This project has received funding from the European Union´s Horizon 2020 research and innovation programme under grant agreement No 800923.*

ments require precise control of experimental conditions and specific forms of sample preparation, and are neither suitable nor desirable for direct industrial applications such as in-line production monitoring or near-line quality inspection of finished products. However, these techniques play and undeniably significant role in the study and development of new drugs as it is detailed in section 3.6.3.

Industrial applications of THz sensing in the pharmaceutical industry have focused on two main areas: inspection of tablet and capsule coatings; and monitoring of tablet porosity and pore size[21].

[21] An updated review of this applications can be found in ref (98).

Tablets are compacted into a solid pellet, and often coated with a specialised protective layer. In contrast, capsules consist of uncompacted power which is encased in a specialised shell. The functional performance of tablets and capsules is strongly dependent on the physical and structural properties of both the coating and the internal blend.

The most important functions of tablet and capsule coatings are: a) to preserve drug functionality while in storage, and b) to facilitate timely drug dissolution (which may involve rapid or timed-release or release at the correct location in the gastrointestinal tract). The performance of coatings can be affected by their thickness, structural uniformity, and defects. Inspection of such coatings is very challenging, especially with respect to coating thickness. Reflection THz time domain spectroscopy - TDS offers an obviously suitable tool for monitoring coating thickness because the time delay between the two reflection signals from the surface and from the coating-core interface provides a direct measure of the coating layer thickness. This allows monitoring tablet dissolution performance by confirming the dependence of mean dissolution time of tablets on their coating thickness[22]. However, this approach presents important challenges: 1) the spatial resolution is limited by the wavelength of THz radiation (to about 100 μm), and 2), reflection measurements are made difficult by the curved surfaces of tablets and capsules, whose curvature is of the same order as the THz wavelength.

[22] This is the standard reference technique used by the pharmaceutical industry to test the dissolution performance of solid dosage medicines.

In what concerns tablets, these are typically manufactured by uniaxial compaction of powder confined radially in a rigid die. This directional compaction results in anisotropic mechanical properties and pore structure, where pores are elongated and predominantly aligned in the plane of the tablet. The distribution of pores in a tablet directly affects the rate at which the physiological fluids enter the tablet, leading to swelling of the particles and eventually causing the break-up of the compact into smaller agglomerates. The size of the disintegrated particles then drives the dissolution rate of the drug. Despite the widely recognised importance of monitoring the tablet porosity during the manufacturing process, currently there are no

*This project has received funding from the European Union´s Horizon 2020 research and innovation programme under grant agreement No 800923.*

there are no continuous in-line non-destructive techniques available, although the application of THz sensing is promising. Porosity has a dual effect on THz transmission properties of a material. The effective refractive index decreases roughly linearly with porosity because the effective interaction length with the material shortens (there is less substance in the beam path). In contrast to refractive index, loss tends to rise with porosity (the effective absorption of porous material declines with shorter interaction length, while scattering rises strongly due to higher pore density and/or larger size of pores).

### *3.6.3 Biomedical Sciences*

The development of biomedical sciences has experienced a quantum leap in the last two decades, mainly due to the development of many characterisation and processing technologies which have very significantly increased the capacity of addressing the study of biological systems at molecular level.

Vibration spectroscopy has played an important role in studying the composition, structure and properties of proteins, nucleic acids and other biomolecules. The vibration frequencies of the biomolecules in THz are related to collective vibrations, distorted vibrations and structural deformation of them. From an energy point of view, weak interactions between molecules (such as hydrogen bonds, van der Waals forces), macromolecular skeleton vibration bending (such as configuration bending), and low frequency vibration absorption in the lattice correspond to frequencies in the THz range. THz spectra can show three-dimensional arrangement of molecules and their characteristic absorption in low frequency. Biological molecular skeleton bending vibrations and configuration of collective vibrational modes are highly correlated with their structures and conformation. Thus, more accurate understanding can be obtained in biomolecules with THz detection.

THz spectroscopy has its several advantages: 1) the spectral characteristics of absorption (weak interactions between macromolecular skeleton, crystal lattice in the low frequency and the vibrations among biomolecules are all located in the THz frequency range); 2) the low energy of the photons involved (THz electromagnetic radiation is within the millivolt range, which is a safe and effective non-destructive testing method) and 3) and the suppression of low noise interference[23] (the THz spectroscopic techniques use pulse widths in picosecond level, which can not only study the time-resolved biological samples, but suppress the interference of far-infrared background noise effectively).

[23] Time domain spectroscopy in the THz range shows a much higher signal-to-noise ratio than Fourier transform infrared spectra.

It is interesting to observe how THz -based techniques (mainly

*This project has received funding from the European Union´s Horizon 2020 research and innovation programme under grant agreement No 800923.*

spectroscopy) have contributed to the study of several main types of biomolecules[24].

- **Amino acids and peptides:** There is a clear difference between the amino acids and the polypeptides in THz frequency dynamic range. The naturally occurring amino acids have dense absorption characteristics in the 1–15 THz range. Also, because of the sensitivity to THz radiation, it is possible to distinguish chiral amino acids and the isotopologues[25].

  The use of THz pulse spectroscopy can be an off-line tool for assessing crystallinity in co-lyophilized amino acid/gelatine mixtures and for the development of freeze-drying processes. Experimentally, there is a correlation between the THz absorption change of solvated water and the specific properties of solution such as polarity and hydrophobicity.

  Peptide is a compound formed by the combination of a-amino acid with peptide bond, which is also the intermediate product of protein hydrolysis. The THz spectral characteristics of the peptide are closely related to their amino acid composition, permutation sequence, intermolecular hydrogen bond and crystal structure.

- **Nucleic acids:** Nucleic acids are crucial biological macromolecules, which are composed of nucleotide linear polymers linked by phospholipid bonds. In recent years, there have been many applications of THz spectrum in the identification and quantitative analysis of nucleic acids, nucleic acid molecular conformation and label-free detection[26].

  The vibrational spectroscopy in the THz range is sensitive to the DNA sequence, geometry, and hybridisation, and can be used as a tool for monitoring DNA junction structures from their components. Absorption peaks are directly related to the base of mutations, and hybridised DNA membranes have a higher refractive index than denatured DNA membranes do. This can be a basis for detecting the mutation of gene points.

  THz spectroscopy has also been used for qualitative and quantitative analysis of various nucleic acids by elucidating the mechanisms of biomolecules THz fingerprints. The absorption coefficient of the DNA sample in aqueous solution decreases as its concentration increases because the super-absorbent water molecules are replaced by less DNA molecules.

  THz spectroscopy can also detect the binding state of DNA and ligands (DNA molecules promotes the formation of more complex hydrogen bond networks in the surrounding solution than bulk

[24] This subject is reviewed in depth in (144) and references therein. We provide here a brief summary of this work.

[25] Isotopologues are molecules that differ only in their isotopic composition. They have the same chemical formula and bonding arrangement of atoms, but at least one atom has a different number of neutrons than the parent.

[26] There have been many label-free methods to detect nucleic acid molecules, such as colorimetric method, microwave resonance absorption method, optical biosensor and electrochemical method. So far, the development of the label-free technology is not good enough to replace the fluorescence labelling method.

*This project has received funding from the European Union´s Horizon 2020 research and innovation programme under grant agreement No 800923.*

water). This can be used as a basis for DNA biosensors based in THz technology.

THz radiation can also induce a significant change in the expression of numerous mRNAs and microRNAs. THz radiation can affect several gene expression pathways and, consequently, can alter various biochemical and physiological processes in cells. This may be a useful as a THz-based non-contact tool for the selective control of specific genes and cellular processes.

- **Proteins:** These are essential constituents of all cell and tissues of complex organisms. THz spectroscopy applied to proteins can provide information related to the molecular conformations, molecular interactions and quantitative analysis.

  Conformational changes, which are essential for protein function, directly affect the dielectric response in the THz range. Absorbance and refractive index increase after oxidation of proteins. This can be the basis for detecting the flexibility of protein structures (the large dielectric increase at THz frequencies with oxidation suggests either a significant global softening of the potential and/or a significant increase in polarisability after oxidation).

  THz spectroscopy can monitor the binding process of protein–ligand quickly, as refractive index and absorption coefficient of a whole solution become smaller after the combination. THz timescale fluctuations identified in the protein–ligand system may also reveal the molecular mechanism of substrate recognition.

  Studies on immune-detection showed that when antigen combined to antibodies specifically, the hydrogen bond between the polar liquid molecules and the protein is affected. Indeed, the dielectric properties and protein concentration in the THz frequency are non-linear and the thickness of the water layer surrounding the protein can be measured. Compared with the standard ELISA method[27], THz dielectric technology can detect the combination of specific antigen and antibody at a lower concentration level.

  Various kinds of proteins can be distinguished through the refractive index of the THz transmission spectra. The intensity of THz spectroscopy can help to detect proteins quantitatively, and the refractive index can be used to distinguish between various proteins. The image constructed by THz can resaolve the amount of protein with a resolution better than $0.5\mu g$.

  Because hydrogen bonds have distinctive spectral responses to THz radiation, measurements within this wavelength range can serve as an initial estimate of the protein hydrophobicity.

[27] The enzyme-linked immunosorbent assay - ELISA is a commonly used analytical biochemistry assay, which uses a solid-phase type of enzyme immunoassay to detect the presence of a ligand (commonly a protein) in a liquid sample using antibodies directed against the protein to be measured.

*This project has received funding from the European Union´s Horizon 2020 research and innovation programme under grant agreement No 800923.*

Protein-induced solvation kinetics can be accurately determined through THz spectroscopy. This information, on turn, can be used to characterise the hydrated shell of a protein. Solvent kinetics on the picosecond time scale can help both to characterise protein flexibility, and the types of fluctuations that may take place in protein structures.

Protein denaturation refers to the change of the specific spatial conformation of protein in certain physical or chemical factors, resulting in the change of physical and chemical properties and loss of biological activity. This will induce changes in the low-frequency vibration modes, thus enabling the possibility of applying THz spectroscopy to the study of this type of processes.

### 3.6.4 *Electronics and Solar Cell Industry*

Modern electronics and, in particular, integrated microelectronics, relies heavily in the use of semiconductor materials as the basis of many components. Electronic properties of semiconductor materials such as carrier concentration and mobility determine their dielectric properties at THz frequencies, allowing non-destructive, non-contact measurements. Wafer inspection, and quality control of circuits and devices (specially in the cases where opacity of the substrates and/or packaging makes other inspection techniques unsuitable) are among some of the first real applications of THz technologies, soon followed by inspection of solar cells; and conductivity measurements/mapping of thin films, particularly as applied to graphene.

In what concerns inspections of electronic circuits, the intrinsically limited resolution of THz far-field ($\sim 1mm$)has limited the potential of the technique until the development of microscopy techniques, such as:

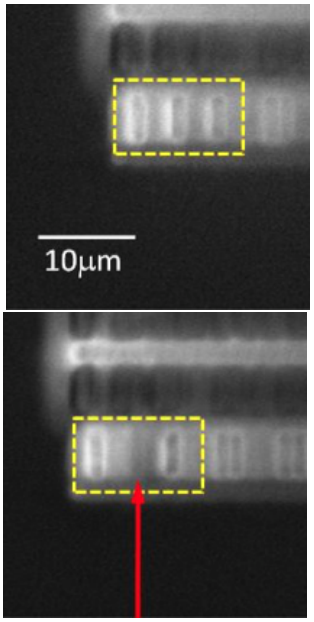


Figure 3.24: **LTEM imaging** of a functioning circuit (top) and a defective one (bottom). The arrow shows the location of the broken contact. Brighter areas indicate stronger THz emission. Source: (101).

- **Laser Terahertz Emission Microscope - LTEM,** in which femtosecond laser is used to excite structures within the material, so that they emit a response in the THz range (THz field amplitude is proportional to the local electric field). These structures can be photoconductive switches with an external bias voltage (i.e., Auston-type switches), unbiased interfaces carrying electric fields (e.g., p-n junctions, Schottky contacts), and some semiconductor surfaces. Resolutions can reach few $\mu m$, and $0.1\mu m$ if near-field techniques are applied. Further evolutions of the technique allow time-resolved transmission imaging, demonstrating measurements of carrier lifetimes and mobilities with a spatial resolution of tenths of μm.
- **Scattering Near Field Optical Microscopy - SNOM,** using light

*This project has received funding from the European Union´s Horizon 2020 research and innovation programme under grant agreement No 800923.*

sources with the THz range has demonstrated resolutions of tenths of nm. This is enough to resolve individual transistors, identify the materials in a device, and measure carrier concentrations. Although such systems are still too complex for industrial deployments, they can provide insights into device structure and performance.

- **Time-domain reflectometry - TDR:** is a widely used non-destructive technique for detecting faults and discontinuities in electronic circuits. Non-contact sampling can be done by employing a TDS system and a tip radius of few less than $1\mu m$ thus allowing for detection of discontinuities in electronic structures with a spatial resolution of 0.55 μm. Commercial THz-TDR instruments are currently deployed in the semiconductor industry.

Inspection of already packaged devices is another important field of application. The concept is based in the detection of fractions of light reflected at the interfaces of the device, and allows for resolutions below 1 mm. Apart from quality control tasks, this technique is also important for detection of counterfeit circuits (which usually have unexpected materials, blacktopping layers, hidden structures, sanded and contaminated components and other differences with respect to original components).

In this type of inspection tasks, there is still a need for methods that could allow hardware testing for performance, authentication and security in a non-destructive, rapid technique that could be applied in enough large scale. Some interesting concepts study the electrical response generated at the circuit pins when the component was illuminated by THz or sub-THz radiation.

Characterisation of the solar cell material involves determining its electrical properties in order to predict its performance and efficiency. The parameters measured are typically complex conductivity, charge carrier density and mobility, and their dependence on solar-type illumination. Inspection, on the other hand, involves detecting a variety of flaws and irregularities. The situation is similar to that of electronic circuits: straightforward imaging in the THz range lacks enough spatial resolution, while LTEM is a useful complementary technique (usually combined with conventional analysis methods like electroluminescence, photoluminescence, and laser beam induced current), that has advantages in spatial resolution and in its ability to observe electric fields, surface defects, grain boundaries, and photocarrier dynamics in the vicinity of the depletion layer. Time domain spectroscopy and frequency domain spectroscopy can be employed in reflection mode for inspection of commercial solar cells, successfully detecting manufacturing faults such as defects in tab wires

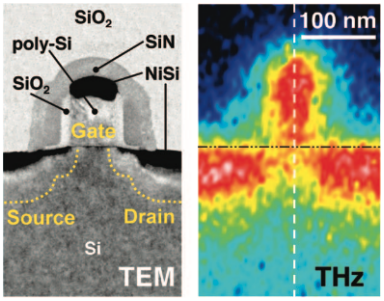


Figure 3.25: **SNOM imaging** showing the cross section of a transistor. While Transmission Electron Microscope image (left) provides high resolution detail of the structure of the device, SNOM image (right) allows for probing of mobile carriers. Source:(100).

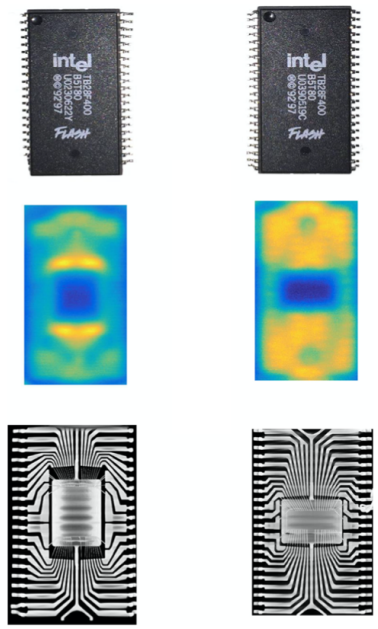


Figure 3.26: **Counterfeit detection:** imaging in the THz range (in transmission mode, in this case) allows to detect differences in the inner structure between two apparently identical microchips. Source: **(102)**.

*This project has received funding from the European Union´s Horizon 2020 research and innovation programme under grant agreement No 800923.*

and soldering, cracks, and variations in doping. Tip-based near-field transmission measurements improved the spatial resolution of the image down to 10 $\mu m$, producing maps of sheet resistance capable of revealing faults in individual devices.

Applications on inspection of thin films have gained importance as bi-dimensional materials, and in particular graphene, have entered the market. Industrial-scale manufacturing of high-quality graphene sheets is challenging, and the quality of the product depends critically on its conductivity and carrier mobility. Quality and uniformity of graphene sheets are essential for its commercialisation, requiring large-scale inspection techniques that are non-conduct and rapid. THz transmission and reflection measurements can provide solutions where optical techniques cannot(99).

### *3.6.5 Oil, Petrol and Gas Industry*

Although petrochemical products may be classed as low value commodities, their quality control, and condition monitoring can deliver large benefits in cost savings, improved safety, and reduced wastage:

- **In fuels,** important tasks are identification and grade, detection and quantification of contaminants and product optimisation (to improve engine performance and reduce wear).
- **Lubricating and insulating oils** differ from fuels in that their performance depends critically on specific viscoelastic or dielectric properties, and to achieve this they tend to be highly purified and their compositions tightly specified. Moreover, both lubricating and insulating oils degrade in the process of normal operation, therefore, continued performance requires periodic monitoring and replacement. For these reasons, most work in this area has focused on detecting contamination or degradation of oils.
- **Gas sensing** for environmental monitoring requires detection of pollutants and contaminants to meet the requirements of health and safety and monitoring of atmospheric components for weather and climate observation. Typically, detection of pollutants demands high sensitivity, selectivity and specificity; whereas atmospheric monitoring may have less stringent requirements.

Petrochemicals consist primarily of hydrocarbon chains of various lengths, mixed with other types of hydrocarbons such as aromatics. They may also contain other flammable components, such as alcohols, as well as non-flammable impurities and contaminants. They are refined from crude oil using distillation processes that separate crude petroleum into grades according to the number of carbons in the molecular chain[28].

[28] Gaseous fuels (1–4 carbons), gasoline (5–12 carbons), jet fuel, diesel, heating oil (12–20 carbons), lubricating oils (20–30 carbons), fuel oil (30–40 carbons), and paraffin wax or petroleum jelly (40–50 carbons).

*This project has received funding from the European Union´s Horizon 2020 research and innovation programme under grant agreement No 800923.*

Pure hydrocarbons are non-polar substances, which makes them low-loss in the THz range[29]. On the other hand, their THz refractive indices increase monotonically with the number of carbons, making it possible to use THz sensing for qualitative and quantitative identification or grading of petrochemicals (this is particularly useful for heavier grades which are opaque in the visible). Moreover, additives or contaminants in petrochemicals (e.g., bioethanol, water, oxidation products) tend to be polar substances that have strong THz absorption, enabling easy detection at low levels of contamination.

In crude oil, THz spectroscopy can be used for identifying the composition of crude petroleum, thus allowing to determine its source. For production purposes, it is important to quantify the fractions of oil, wax, asphaltene and tar and the presence of water and sand (main contaminants in raw material).

In refined fuel, THz spectrum allows to quantify octane number[30], as fuels with higher octane numbers have shorter carbon chain lengths, so THz refractive indices and absorption coefficients are lower than those of low-octane (longer carbon chains) fuels. Similar principle can be used to for identification of additives such as used to augment fuel and to improve its performance (ethanol, toluene, ethylbenzene, and xylene, methyl methacrylate). All these are polar liquids which strongly increases both the refractive index and the absorption coefficient of the mixture compared with those of pure fuels. Finally, some contaminants like sulphur can also be identified through the increase in THz absorption.

In lubricant oil there is a linear relationship between oil viscosity and its THz refractive index, since both viscosity and refractive index increase with the number of carbons in the chain. In general, both lubricant and transformer oils degrade through oxidation. THz spectroscopy allows to identify carbonyl and hydroxyl compounds (resultant of the oxidation process) even at very low concentrations (because they are polar and therefore cause strong increase of absorption). In what concerns contaminants, water can also be a cause of oil degradation, especially in engine oils where water is a product of fuel burning. In this context (lubrication of mechanical parts) gasoline is also a contaminant which can be cause of accidents through detonation. Both types of contaminants can easily be detected in the THz range ( in the case of gasoline the refractive index of oil decreases and its absorption coefficient increases in the presence of this substance).

In what concerns gas sensing, THz spectroscopic information is complementary to spectroscopic information in other ranges, with the added value of providing spectral fingerprint of gas molecules. At THz frequencies, gases have relatively few lines, facilitating spe-

[29] A review about this application can be found in ref (97).

[30] Octane number, is a standard measure of an engine or aviation gasoline capability against compression. The higher the octane number, the more compression the fuel can withstand before detonating.

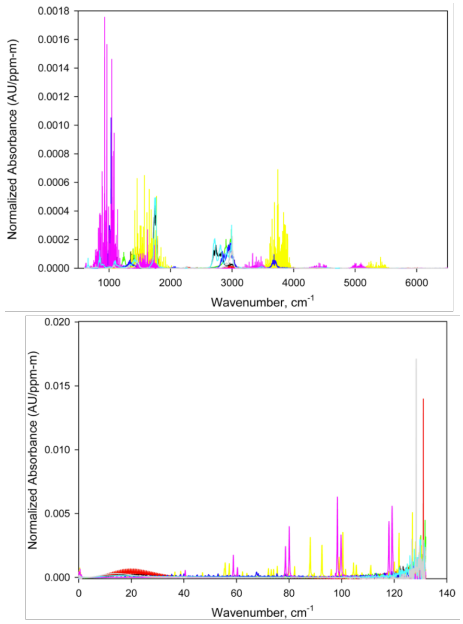


Figure 3.27: **IR (top) and THz (bottom) spectral signature of several gases:** acetaldehyde (black), acetonitrile (red), ethanol (green), water (yellow), methanol (blue), ammonia (magenta), propionaldehyde (cyan), and propioni- trile (gray). The THz range is less crowded and allows for more reliable identification. Source: (96).

*This project has received funding from the European Union´s Horizon 2020 research and innovation programme under grant agreement No 800923.*

cificity and selectivity[31]. An additional advantage is the vast amount of knowledge generated in scientific studies (in astrophysics, planetary and atmospheric disciplines) which is well structured and can be used for training of advanced processing algorithms(95). Since gas absorption lines are commonly very narrow[32]and their central frequencies have been previously established or can be calculated, many of these studies used narrow-band high-resolution techniques, often employing electronic devices, in contrast to the broadband photonic techniques typically employed in other THz applications. Although electronic systems are incapable of delivering frequencies and bandwidths as high as photonic systems, target gas species have sufficient lines at lower frequencies and in narrow bands to permit detection and identification.

When applied to environmental monitoring (for detection of detection of pollutants and contaminants) systems must have high sensitivity, selectivity and specificity whereas atmospheric monitoring (for weather and climate observation) may have less stringent requirements. A large effort has been devoted to developing dedicated electronic systems for gas sensing (integrating source and detector). As it has been mentioned before, the narrow frequency range typical of this technologies can be engineered to detect specific gases, while they offer a clear advantage in compactness, robustness and low power consumption. This said, there is a clear market space for systems capable of scanning a wide range of the THz spectrum without being bound to detect a specific compound. The challenge here falls also on the side of data processing, as cleaver algorithms are needed to interpret very complex spectra. It is worth mentioning that, since THz radiation can penetrate optically opaque environments (such as black smoke) it can be successfully deployed in challenging environments like disaster sites (industrial fires, battlefields, etc).

When applied to extractive gas industry, THz tools can be of use for quality monitoring of natural gas. In this case the requirements in terms of sensitivity, selectivity and specificity are pronounced than in previously mentioned applications. Natural gas is a mixture hydrocarbons (methane, ethane, and propane), the ratio of which determines its calorific content. It is also important to detect and quantify monoxide and carbon dioxide ($CO_2$), which are contaminants. In principle, the refractive index provides a good indicator of the mix, due to the differences in the indices of individual gases(94).

In natural gas pipelines, water vapour can induce the formation of ice particles, reducing or even blocking gas flow and it can also accelerate corrosion on the internal pipe surface. Conventional methods of monitoring water vapour include the use of chilled mirrors, impedance hygrometers, and IR and microwave spectroscopic hydrometers.

[31] Many of the gases of interest do not have lines in the near-IR. In contrast, in the mid-IR where the great majority of gases have their main absorption bands, spectroscopy is challenging as polyatomic gases have dense and complex absorption bands with a high multiplicity of lines. This makes it difficult to achieve sufficient specificity and to identify gas mixtures.

[32] Typically a gas absorption band in the THz range has a few GHz at atmospheric pressure. Lines width is linearly proportional to pressure.

*This project has received funding from the European Union´s Horizon 2020 research and innovation programme under grant agreement No 800923.*

Except for microwave hydrometers, these methods lack selectivity for water, such that other gases may interfere and produce incorrect readings. Microwave hydrometers have good selectivity for water, but their sensitivity is low. Time domain spectroscopy in THz range can be used to monitor water vapour in a pressurised gas pipeline (93). The relative humidity can be determined from the intensity of the absorption peaks (see Figure 7), which is increasingly sensitive as the humidity increases.

### *3.6.6 Other Industries*

The fact that THz offers capacity for fast and safe, non-contact and non-invasive inspection makes it very tempting for many industries to explore the possibility of using these type of technology for quality control tasks.

Both automotive and aeronautic industries manufacture high added value products, and have a reasonably high capacity for investing in high performance quality control tools. Up to a certain degree, they have adopted several THz sensing based techniques(3), mainly for inspection of electronic components, isolation layers (foam) and coatings/painting (all the related techniques have already been described in subsections 3.6.1 and 3.6.4). An important constraint comes from portability and form factors, as the inspection tools must be integrated in production lines and handled efficiently by operators (in other words, quality control techniques based on extraction of samples for further analysis at laboratory are of very limited application and almost useless in the context of these industries).

Food industry keeps an interest on the detection of contaminants and pesticides, foreign objects, and the presence of antibiotics[33]. The reasonable penetrating capability through plastic layers of THz radiation is attractive because allows inspection of already packaged products. Demonstration of set ups for detection of glass, ceramic, and metal insertions in food samples have been already demonstrated more than a decade ago(85). With regard to detection of contaminants, the challenge is to achieve the minimum detection levels required by various government regulations.

[33] An updated review can be found in ref (59).

In textile industry, there is a need for fast quality inspection of tissues where some defects cannot be detected through inspection in the visible range. Time domain spectroscopy has shown to provide such capacity.

Neither wood nor paper are specially cooperative in the THz range, since many elements in the structure of these materials contribute to strong absorption (manly due to the presence of moisture) and scattering (due to their anisotropic structure consisting of aligned

*This project has received funding from the European Union´s Horizon 2020 research and innovation programme under grant agreement No 800923.*

fibres). This, however, has been remarkably turned into an advantage, as characterisation of THz transmission allows to determine thickness, composition, moisture content and texture. In the case of wood, reflective measurements also allow to detect damage underneath the bark caused by insects.

While all these applications have even been demonstrated even with industrial prototypes, the low value of the products of this industries also limits its capacity to invest in high performance systems. The strategy in these fields has been to use this type of high-end equipment for calibration of lower cost compact systems. It is nevertheless unlikely that these activities will justify the development of systems based in costly technology such as superconducting sensors.

### *3.6.7 Medical Applications.*

The use of THz radiation as a basis for fast, non invasive diagnose has generated large expectations. The main reason for this is that photons in the THz range have very low energy, and therefore, and unlike X-rays[34], do not rise any health issues and can be used safely and intensively. In principle, spectral fingerprint of key substances in the THz range allow for r their qualitative and quantitative identification. This has potential application in early diagnosis of cancer, accurate boundary determination of pathological tissue and non-destructive detection of superficial tissue.

It is worth listing (even if non exhaustively) the many concepts which have being proposed and are being, up to a degree, developed:

- **Breath Analysis,** providing qualitative and quantitative information (through THz spectroscopy) about gases exhaled in human breath is a highly promising application could allow for early detection of disease biomarkers related to lung cancer, diabetes, some neurological disorders, and smoking and alcohol consumption. Systems capable of discriminating up to 21 different substances (water, hydrogen cyanide, carbon monoxide, nitrogen oxide, formaldehyde, methanol, hydrogen sulfide, acetonitrile, methyl isocyanide, acetaldehyde, ethanol, vynil isocyanide, acrolein, acetone, carbonyl sulfide, dimethyl sulfide, isoprene, butyraldehyde, methyl nitrite, pyruvic acid, butyric acid) have been demonstrated (92).

- **Skin Cancer diagnose**: THz radiation has been successfully used for imaging the human skin where a few millimeters of penetration depth are sufficient for gathering all relevant information. The technique is based in detection of the spectral fingerprints of sur-

[34] Radiation in the X-ray range carries enough energy to break chemical bonds within biomolecules. This may cause interference with normal biomolecules functioning and, in particular, generate mutations in genetic material (DNA, RNA).

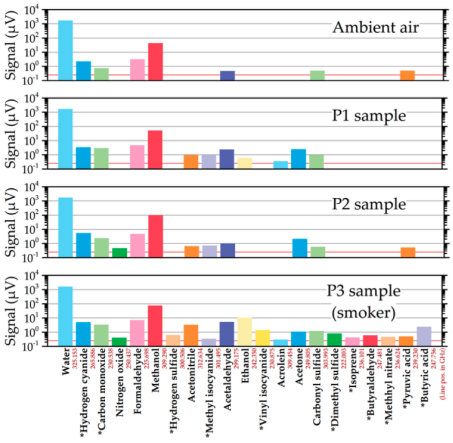


Figure 3.28: **Breath analysis** showing composition of samples from air and three patients (last one of them being smoker). Source :(92).

*This project has received funding from the European Union´s Horizon 2020 research and innovation programme under grant agreement No 800923.*

face proteins that are markers for certain cancers. This technology is envisioned to reduce or probably eliminate the need for the ex-vivo biopsies of anomalous skin tissues, and enables early stage recognition, which drastically reduces the risk of these cancers (as well as the treatment costs).

- **Wound and Burn**: burned and unburned areas show a distinct difference in THz reflectivity. Tomographic inspection (raster scanning through the area of interest while sending pulses of THz radiation and measuring the shape and size of each reflected pulse, allows to obtain a reconstruction of the area, which an accurate delimitation of the damaged tissue(91). Such imaging is possible even under layers of medical cotton (gauze) and bandage.

- **Endoscopic diagnose (Colon Cancer):** technical progress in the development of endoscopes (flexible probe set used to provide a visual from inside the body) has allowed to obtain high signal-to-noise ratio and a wide frequency spectrum similar to the conventional THz time-domain spectroscopic systems(90). In a recently proposed method, cancerous tissue is identified because it contains more water than healthy tissue, the reflection of the cancerous colon tissue is less than normal colon tissue sample(89).

- **Dental Imaging:** the development of this application is driven by the will of displacing X-ray imaging as a widespread diagnose tool, which poses certain health risks. Also, X-rays do not provide an accurate tool for detecting tooth decay in early stages when tissue damage can be effectively remedied. THz radiation has higher attenuation in decayed enamel relative to healthy enamel, providing a distinctive contrast in the image. Caries are a result of mineral loss from enamel, causing a change in the refractive index within the enamel. There is also change in the refractive index between dental enamel and dentine tissues, so that a detailed structural mapping of the teeth can be obtained even at early stages(88). Despite all this potential uses, it is worth mentioning that, given the structure of the dental care value chain (with end-users running small business, and having limited investment capacity) it is unlikely that this segment could accept the entrance of costly and complex systems.

- **In-vivo examination of tissue:** Surgical procedures for removal of cancerous tissue often contemplate extraction of a fraction of healthy tissue surrounding the tumour, with the aim of avoiding risk of its regeneration. Compromise must be made, as excess removal of healthy tissue lengthens recovery and affects patient overall clinical condition. The same technologies proposed for

*This project has received funding from the European Union´s Horizon 2020 research and innovation programme under grant agreement No 800923.*

detection of skin cancer or colon cancer can be applied to this case, in order to precisely map the zone containing tumour cells. Such proposal has, so far and due to the many technical difficulties involved, remain just at concept stage(87).

Despite all these attention the penetration into the medical market of THz technologies remains very limited so far (at least as compared with the size of the opportunities). Some of the reasons for this are technical. In contrast with many other applications, biological systems present an impressive complexity. Just as an example, biological samples usually contain a large number of substances (such as water, proteins, fat, fibre and a mixture of organic compounds), which are in different proportions in depending of the patient histology and overall health state. This leads to very complex spectra where it is very challenging to resolve and identify the different contributions, and where signal-to-noise ratio for the absorption peaks of target substances are very small(86).

There are, however, other reasons which are not technological. Solutions for the medical market are constrained to undergo through very lengthy validation and homologation processes (designed to ensure that all medical tools work as intended and do not produce dangerous side effects). From the point of view of business, this translates into very heavy mid- and long-term investments, which severely influence the development of successful entrepreneurial projects. Paradoxically, and precisely because of these difficulties, the medical industry has developed business models which open an opportunity for costly technologies. While some type of end-users (dentist, practitioners, etc) may not have the financial capacity to adopt very expensive equipment, others (hospitals) do have such capacity and often invest giving priority to performance over cost. The applications which will be developed by this type of end users (large diagnostic systems, assistance for large surgery procedures, etc) could then be an interesting field for superconducting sensing technologies.

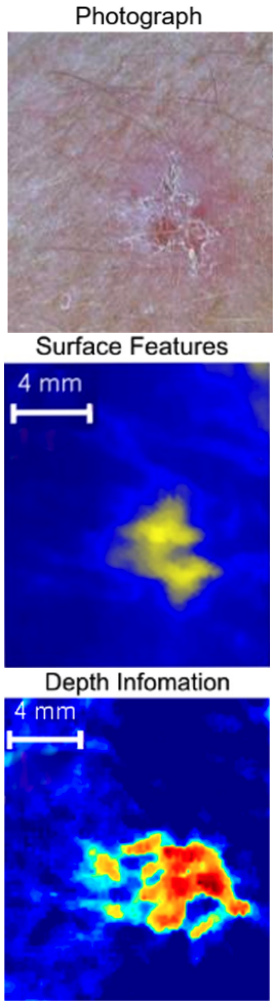


Figure 3.29: **In vivo cancer imaging.** The clinical photo (top) show only surface feature, similar to the terahertz image (centre). The depth image (bottom), where THz pulse penetrates below the surface, reveals feature not visible to the naked eye, and guides surgical removal of tumour. Source:(57).

### *3.6.8 Security*

Monitoring of both individuals and goods is at the core of security applications. Different police, custom and private security organisations share the task of identifying, as much in advance as possible, breaches of trade and security regulations and/or threads:

- **To enforce trade laws effectively,** customs authorities carry on inspections of the goods in transit. Maritime shipping is the backbone of world trade; it is estimated that some 80 percent of all

*This project has received funding from the European Union´s Horizon 2020 research and innovation programme under grant agreement No 800923.*

goods are carried by sea. The number of goods carried by containers increased from around 102 million metric tons in 1980 to about 1.83 billion metric tons in 2017, with the global fleet currently having more than 5300 cargo ships, and a capacity of 25 millions containers[35], most of which are channeled towards destination through train or road transport. From all these, it is estimated that inspection involving all means of transport remains at levels in the order of 10% of overall traffic (82). The main reason for such low level of inspection is the slowing of trade caused by screening tasks, which constrains authorities to select even only a fraction containers which raised doubts regarding the customs declaration or suspicion of smuggling or trademark violations.√

[35] Updated statistics can be found here.

Screening of pedestrians at ports of entry has often been a lower priority, in large part due to the lack of viable solutions. As a result, pedestrian-based smuggling of items such as currency, opioids, narcotics and other illicit items is a point of vulnerability for border security and customs enforcement. International tourist and business travel arrivals increased from approximately 800 million to 1.4 billion[36]. Permanent cross-border migration has also risen, from 107 million persons in 2010 to 130 million persons in 2019.

[36] Detailed data can be found in United Nations Migration Report (80).

Inspection techniques vary from visual inspection (where seals and packaging are broken), to imaging in a range of wavelengths (gamma/X-ray for exploring inside, IR for detecting heat sources, etc.). The later type is preferred because it is non-invasive, faster and safer for the staff in charge of screening tasks. Sizes of inspected elements range from few cm (postal shipments) up to several meters (cargo containers). The cost of inspections ranges from tenths to thousands of euros, and is usually transferred to the responsible of the merchant.

Because of the need to improve the ratio of inspected goods and to avoid intrusive and/or expensive methodologies, there is a constant demand of new inspection technologies.

- **To avoid terrorism threads and violent attacks,** and in particular those at small scale arising from low-profile agents, whose actions are difficult to be foreseen by law enforcement authorities.

  Three dominant trends shape terrorism in the 21st century[37]:

  [37] Updated information can be found in this report by EUROPOL (81). Some of the statistics have been gathered here.

  a) First is the overrepresentation of the Middle East, North Africa, and South Asia in the number of terrorist attacks by region. Together, these regions account for over 74,700 of the 98,328 terrorist attacks worldwide between 2002 and 2019;

*This project has received funding from the European Union´s Horizon 2020 research and innovation programme under grant agreement No 800923.*

a) Second is the high high number of attacks by terrorist groups that are both ideologically religious, and aiming for political control of territories in the aforementioned regions. Perhaps the two most infamous such organisations are Islamic State and the Taliban, who were responsible for a combined 1,836 terrorist attacks in 2019 alone. Despite these high numbers, such organisations have a relatively small presence in Western Countries. Seven jihadist terrorist attacks were carried out (completed or failed) in the EU in 2019. Twice this number of terrorist plots were thwarted by law enforcement, continuing a trend from 2018;

a) Third is the violence promoted by politically extremist groups, which is rapidly increasing after the financial crisis started in 2010 and the COVID-19 pandemics. In 2019 three EU Member States reported a total of six right-wing terrorist attacks (one completed, one failed, four foiled), compared to only one in 2018. Additionally, two attacks not classified as terrorism under national law but committed by right-wing extremists were reported by Germany and claimed the lives of three people.The number of left-wing and anarchist terrorist attacks in 2019 (26) reached the level of 2016 and 2017 after a decrease in 2018.

Within this context, law enforcement authorities are in need of tools that could allow to detect presence of security threads. This can be mainly of two types:

a) Concealed weapons or explosives, generally carried by individuals underneath clothing or transported in vehicles as part of luggage or goods.

a) Biological or nuclear substances employed with the aim of spreading contamination over a perimeter (dirty bomb) or a strategic good (in particular drinking water).

Tactically, the unsophisticated nature of these threats poses significantly greater technical challenges in both point and stand-off detection. This threat is growing due to increased globalisation and mobility within society, the explosion in chemical and biotech expertise (and its accessibility through the internet) and the relative ease with which chemical weapons can be prepared at off-sites.

Once more, priority must be given to avoid bottlenecks caused by control points, and exposure of individuals to dangerous radiation sources. Another important factor concerns processing of the information. The sophisticated screening technologies (scanners, etc) must be handled by end-users with little or no technological background. The systems must therefore integrate means of identifying

*This project has received funding from the European Union´s Horizon 2020 research and innovation programme under grant agreement No 800923.*

and outlining the relevant information (nature of the substances, shapes in images indicating potential threads, etc).

In general, security applications are characterised by the need of displacing the detection system towards the check points where security inspections or surveillance tasks are carried on. Portability may or may not be required (scanning systems in airports, for instance, remain installed on site, while detectors for military need to be displaced as battleground evolves). Given the current increase of security activities the need for multiplying the number of systems is also growing rapidly. Because of this, there is a tendency to weight the cost of the systems (provided that they meet a minimum of functionality requirements).

Electromagnetic waves at terahertz frequencies (0.1–3.0 THz) have been considered a promising candidate for security applications mainly because of the following reasons:

- Many explosives and illicit substances have characteristic transmission and reflection features in the THz range that could help to distinguish them from other common materials in an automated way(83).
- THz radiation has some penetrating character because it is not absorbed by certain common materials, and can, for instance, be transmitted through clothes with small attenuation.
- On the other hand, it is strongly reflected by metallic materials, usually employed in the construction of weapons. The use of THz illumination of sufficient power levels and fast image detection and processing, has shown that non-metallic weaponry can also be detected.
- THz waves pose minimal health risk to human beings and they do not affect the operation of various systems because photon energy is very small (4.4 meV @ 1 THz). THz radiation is rapidly absorbed by the water contained in human body, thus penetrating only to a skin depth. Potential adverse health impacts are therefore significantly less than those from the competitive imaging technologies using x-rays.

When compared to other spectroscopic techniques available, THz spectroscopy offers an interesting balance, with fast acquisition time (essential for stand-off surveillance and avoidance of bottleneck situations in screening) and good molecular sensitivity.

Due to advantages described above, and the exponential growth of the security applications, the development activity is intense,

*This project has received funding from the European Union´s Horizon 2020 research and innovation programme under grant agreement No 800923.*

| Method | Sample Type | Sensitivity | Molecular Sensitivity | Acquisition Time | In Situ Monitoring |
|---|---|---|---|---|---|
| **TS** | condensed | medium | good | fast | yes |
| **LIBS** | condensed | low | medium | fast | yes |
| **RS** | condensed | medium | good | slow | yes |
| **IMS** | gas | high | medium | medium | yes |

Table 3.3: **Performance of different spectroscopic technologies when applied to drug and explosive detection.** TS - THz Spectroscopy, LIBS - Laser Induced Breakdown Spectroscopy, RS - Raman Spectroscopy, IMS - Ion Mobility Spectrometry. A detailed analysis can be found in ref: (67).

and several products are already commercially available. Many approaches are pursued and can be divided in the following categories:

a) Spectroscopy allows detecting and identifying different chemicals, thanks to their characteristic spectral signatures, even when hidden inside dress clothing(79), or mail(68).

a) 2D Terahertz imaging capable of making visible metals and even plastics and ceramic, materials that are hard to be detected using backscatter X-ray (84; 45).

a) 3D imaging through tomographic reconstruction allows reconstruction of the target structure while simultaneously gathering information about its composition. In this approach high power laser sources are used in setups designed to collect radiation reflected in the target. This is, however, technology at early stages of development(46).

However, so far these attempts have only been partially successful. In the case of spectroscopic detection of substances, the main reason is that current technologies allow the collection in a narrow terahertz window (3–6 THz). This is not sufficient to differentiate, for instance, many explosives and their matrix separately, as many compounds may appear similar. A wider terahertz bandwidth is expected to identify the salient features in the acquired spectrum unique to each molecule. Since the reflection of hazardous materials is weak and the dependence on the surface quality is strong, this measurement requires a more sensitive arrangement and careful signal processing to achieve reliable results(67).

In what concerns superconducting technologies, several proposal have been made. An array of 64 TES has been applied in the construction of a security camera, capable of recording videos with 256 × 128 pixels at 25 Hz frame rate and a working distance of up to 20 meters(58). Antenna-coupled superconducting micro-bolometers (a variant of HEB) has been the basis for the commercial products by Finnish company Asqella (55). The same team has opened a route towards high-definition imaging based in KID technology with a pro-

*This project has received funding from the European Union´s Horizon 2020 research and innovation programme under grant agreement No 800923.*

totype array of 2500 sensors capable of operating at 5-10K(44). The cryostat-free imaging array, based in High Temperature Superconductor Josephson Junction technology has established an important milestone, as a significant reduction in cost, complexity of the system and logistics and maintenance tasks can be achieved(47). While the system has demonstrated operation at 77K, best results have been obtained with a working temperature of 50K, where sensitivity of $\sim 7000VW^{-1}$, SNR $\sim 1 \times 10^5$ and a NEP $\approx 3 \times 10^{-13}W/\sqrt{Hz}$ were obtained.

In summary, security applications offer markets in growing dynamics, where THz technologies can displace mainstream inspection technologies as they are intrinsically and fundamentally safer alternatives. Superconducting technologies have demonstrated impressive progress and some of them are still competitive solutions that could soon be transferred to commercial products. The combination of both high integration (focal plane arrays) and simple cryogenics/cryocooling, not yet demonstrated, could definitely open a very significant market opportunity.

## 3.7 *Ranging Applications*

A wide spectrum of very different applications is based upon the non-contact determination of the distance between the observer and an object/target. This is determined by recording the time between transmitted and backscattered pulses and by using the speed of light to calculate the distance traveled. This concept derives directly from radar (radio detection and ranging), which uses radiation in the radio wavelengths, and quickly evolved from its original military applications (for location and ranging of enemy units) into important civil applications such as maritime and airborne traffic control, and weather monitoring and forecast.

In LIDAR (light detection and ranging) the radio waves are replaced by radiation in the visible or infrared range. The typical Lidar setup consists of a light emitter pointed toward a target, and a receiver formed by a telescope, a stage of filters for spectral selection, optics elements to redirect the collected beam on a detector and the electronic readout. The use of laser sources (because of their low divergence and wavelength selectivity) has considerably expanded the range and accuracy of the technique.

An interesting evolution of LIDAR technology allows, on top of ranging, making further analysis of the returned radiation, thus gathering information of the interaction of radiation with the target (or the substances present along the trajectory of the beam). Doppler LIDAR and Rayleigh Doppler LIDAR are used to meas-


Figure 3.30: **Portable system for stand-off surveillance,** shown on top image, integrates cryostat with a 20 TES array (A), pulse tube cooler (B), Cassegrain main mirror (C), optomechanical scanner (D), readout electronics (E) and control electronics (F). At bottom image, example of image acquired with the system, of a person carrying concealed objects: a mock-up handgun (1), a plastic tube filled with sugar (2), and a jelly bag (3). Source: (42).

*This project has received funding from the European Union´s Horizon 2020 research and innovation programme under grant agreement No 800923.*

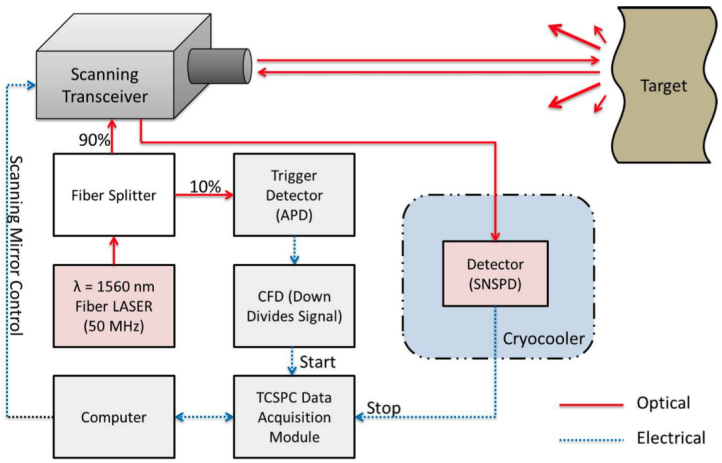


Figure 3.31: **Typical LIDAR set up** including a superconducting sensor, in this case a SNSPD. Source: (114).

ure temperature and/or wind speed along the beam by measuring the frequency of the backscattered light. The Doppler broadening of gases in motion allows the determination of properties via the resulting frequency shift. Measure of surface reflectivity (assuming the atmospheric transmittance is well known) at the LIDAR wavelength is typically used for making absorption measurements of the atmosphere. Differential Absorption LIDAR use two or more closely spaced (<1 nm) wavelengths to factor out surface reflectivity as well as other transmission losses, since these factors are relatively insensitive to wavelength. When tuned to the appropriate absorption lines of a particular gas, the measurements can be used to determine the concentration (mixing ratio) of particular gases in the atmosphere.

In a zero order approach, applications of LIDAR technology can be grouped in four main areas:

- **Applications in forest studies**, including canopy surface height modelling and mapping; metrics for vegetation modelling; individual tree isolation and mapping; area-based modelling and mapping; and estimating biomass.
- **Urban analysis:** including urban flood risk modelling, mapping power transmission lines, modelling Global Positioning System (GPS)/airport signal obstruction, solar radiation assessment, road extraction, building extraction and 3D reconstruction, population estimation, change detection, assessment of post-disaster building damage, and assessment of post-disaster road blockage.
- **Geosciences:** changes in geomorphic surfaces, surface hydrology and flood models, tectonic geomorphology, lithological mapping, rock mass structural analysis, and natural hazards, such as landslides, debris flows, and earthquake damage.

*This project has received funding from the European Union´s Horizon 2020 research and innovation programme under grant agreement No 800923.*

- **Robotics:** 3-D reconstruction of robot environment, driverless cars, industrial structure and infrastructure mapping.

In later of this areas (robotics) parameters like portability of the system, and cost are given priority over performance, and therefore superconducting technologies lose ground with respect to other technologies (mainly semiconductor based). In all other three areas accuracy is in principle the top priority, so high performance technologies gain competitive advantage. In what concerns superconducting technologies, only SNSPD have been applied integrated in LIDAR setups, demonstrating a quantum leap in overall system performance:

- LIDAR based on single photon detectors is used to detect the range and concentration of clouds, humidity, wind fields, air pollution, pollutant diffusion, and to provide weather forecasts. At present, the single photon detectors used in lidar weather prediction are mainly InGaAs/InP avalanche photodiodes operated in the Geiger mode. The infrared detection efficiency is often less than 30% and the dark counts are a few kHz. Thus, traditional Lidar for weather prediction was around 20 km. The quality of LIDAR data is currently improved by facilitating superconducting nanowire single-photon detectors (SNSPDs) as transducers. The detection efficiency is up to 93% in the near infrared band while the dark count is less than 100 Hz, which extends the ranging area to 180 km (126).

- Integration of SNSPD technology adapted to the IR wavelength range has allowed to build LIDAR systems capable acquiring depth profile images with millimetre-scale depth resolution at a distance several km away from the target (114). In comparison, set ups using Avalanche Photodiode arrays in Geiger Mode will achieve 30 cm depth-resolution at distances of 20 meters (113). The use of IR radiation enables the possibility of using many ready-made components which have beed developed for optical telecommunications, thus considerably reducing the overall system cost.

- SNSPD has been applied to distance measurements based on a satellite laser system. Satellites in orbits between 1600 km and 19500 km where ranged with an accuracy of less than 8 cm (127; 125).

- Although no practical implementations have yet been presented, theoretical models demonstrate that the high efficiency and low noise of superconducting detectors could bring an improvement of several orders of magnitude in the signal-to-noise ratio of Differential Absorption LIDAR systems (124) . This allows to push

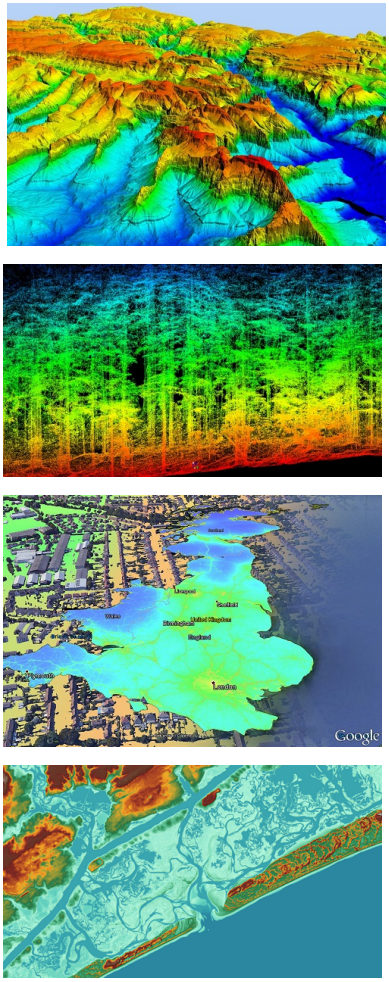


Figure 3.32: **Applications of LIDAR technology**, from top to bottom, Digital Elevation Model (used for cartography and civil engineering), Vegetation Density Mapping (used for forest management), Aerosol and Pollution Monitoring and Water Mapping (used for flood hazar assessment and cartography of the oceanic floor).

*This project has received funding from the European Union´s Horizon 2020 research and innovation programme under grant agreement No 800923.*

the system to work at higher wavelengths. This could be very advantageous for the detection of many pollutants, whose spectral fingerprints are at $\lambda > 2\mu m$. Providing high sensitivity and low dark count rate, allows to detect small concentrations of gases, and this feature can be very incisive in the scenario of environments defence protocols.

Once more, the battlefront for successful adoption of superconducting sensors is cryogenics. If the cryocooler instruments get rugged enough they will certainly be a valuable replacement of state-of-the-art technologies. Practical demonstration of LIDAR measurements using detectors integrated into miniaturised 4 K cryostats have already been presented (118).

## 3.8 *Optical Communications*

Communication with orbiting satellites and spaceships relies, by obvious reasons, on telecommunications through chosen bands of the electromagnetic spectrum. As the density of satellites and complexity of the missions increases, so does the amount of data to be exchanged between the ships and the earth-based mission controls. Such demand has been satisfied by migrating towards higher frequencies.

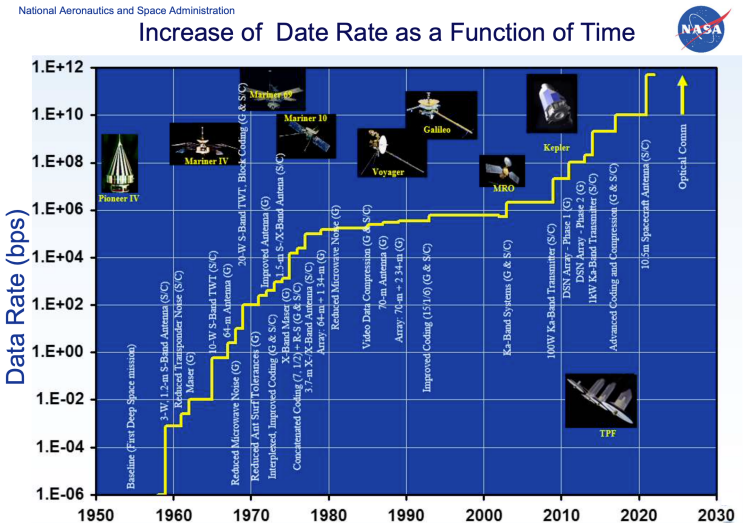


Figure 3.33: **Evolution of data rate needs for space communications** in NASA missions.

The natural progression of increasing radio-frequency - RF bands (S, X, and Ka) that can be efficiently transmitted through the Earth's atmosphere have been implemented for both near-Earth and deep space telecommunications. Inherent beam-width and spectrum allocation restrictions of these bands limit further significant expansion of

*This project has received funding from the European Union´s Horizon 2020 research and innovation programme under grant agreement No 800923.*

data return capacity. Use of significantly higher frequencies becomes thus, the most efficient way of expanding data transmission capacity:

- In 2013, NASA's Lunar Laser Communication Demonstration (LLCD) has successfully demonstrated between the Lunar Atmosphere and Dust Environment Explorer - LADEE and ground stations, the demonstration has achieved almost an order of magnitude higher data rate than the best Ka-band radio (115).
- In 2014, the European Data Relay System - EDRS was carried out the first ever use of gigabit laser-based communication. On the same year, NASA, through the OPALS experiment announced a breakthrough in space-to-ground laser communication, downloading at a speed of 400 megabits per second. The system is also able to re-acquire tracking after the signal is lost due to cloud cover.
- In 2016, and the first quantum-limited experiments from space were done by using the SOCRATES micro satellite.
- In 2020, the Small Optical Link for International Space Station - SOLISS) developed by JAXA (Japanese Space Agency) established bidirectional communication between the International Space Station and a telescope of the National Institute of Information and Communications Technology of Japan. The same country launched the LUCAS inter satellite optical data relay with high speed laser communication technology.

It is worth mentioning that this fast pace technological competition does not only aim for communication with spaceships. In 2016, the same technology has been used by (private company) Google for establishing a stable laser communication connection between two stratospheric balloons over a distance of 100 km. The connection was stable over many hours and during day and nighttime and reached a data rate of 155 Mbit/s. This proof of concept aims to offer stable access to the internet in remote locations.

For the purpose of illustrating the technological challenge we will keep the focus on optical deep-space communications. These can be implemented in two ways: 1) A direct optical link is set up between the earth station and space-craft, and 2) the optical signal is sent from a satellite outside the atmosphere. In the former case, atmosphere disperses and attenuates the transmitted and received signals, but high power transmitter and large receivers can be used. In the later case atmosphere effect is mitigated, but transmitter and receiver sizes are limited, and so does available power. Operational considerations largely dictate key requirements for designing viable, cost-effective space communication services. A detailed discussion of this topic can be found in ref (119).

Figure 3.34: **Lunar Laser Communication Demonstration - LLCD** successfully demonstrated for the first time high-rate duplex laser communications between a satellite in lunar orbit, the Lunar Atmosphere and Dust Environment Explorer (LADEE), and multiple ground stations on the Earth.

*This project has received funding from the European Union´s Horizon 2020 research and innovation programme under grant agreement No 800923.*

Space-to-ground demonstrations have included optical links to spacecraft in: geosynchronous transfer orbit -GTO, low-Earth orbit - LEO, and geostationary-orbit - GEO. Space-to-space demonstrations have included bidirectional LEO-to-GEO and link between two LEO platforms. Successful demonstrations from near-Earth distances have cleared the path toward the development of operational optical communication systems for LEO and GEO spacecraft.

Most of optical links demonstrated so far correspond to near-Earth orbit as opposed to deep space. Deep space for our present discussion is considered to be distances beyond the Moon. Relative to near-Earth, communication from deep space presents link difficulty that increases as the square of the link distance. For example, factors of 60–80-dB additional gain will be required from Mars distances relative to GEO. The distance from Earth to Neptune or Pluto can be on the order of 4,000,000,000 km. After propagating over such a distance, the communications beam from a spacecraft will spread to an area 10 billion times (100 dB) larger in area than if the beam from the same system traveled from just the GEO distance (40,000 km). A system capable of transmitting 10 Gbps from GEO to the ground would only achieve 1 bps from Pluto/Neptune distances.

A mere scaling of near-Earth communication systems to overcome the increased difficulty will prove insufficient. The optical signal from deep space terminals, which suffers the limited transmitting power and huge link loss, only contains several photons when incident on receiving surface. This poses big challenges to the modulation method and detection techniques. Instead, new technologies and strategies for increasing the bits per photon received with efficient lasers, detectors, and signalling (modulation and coding) are required.

The intrinsic properties of laser sources (very small beam divergence, monochromaticity, etc) have made them, from early stage, the natural candidates for emitting stations. Narrow laser beam divergence can provide 10–100 times higher data rates with lower size, mass, and power flight systems. Furthermore, unrestricted spectrum with a few orders of magnitude bandwidth expansion (tens of terahertz at optical versus hundreds of megahertz in the RF) becomes accessible.

In what concerns data modulation Pulse position modulation - PPM has been chosen to provide an energy-efficient means of using high peak power laser for transmitting signals from deep space to earth-based receiving stations. each channel symbol period is divided into $2^M$ equal non-overlapping time slots, and the information comprised of M bits is sent by pulsing the optical intensity in one of these slots. Each slot is very short ($\sim$ns), but the laser power that

*This project has received funding from the European Union´s Horizon 2020 research and innovation programme under grant agreement No 800923.*

the signal slot contained is very high (∼kW). Therefore, the PPM can compensate the huge link loss and suppress the background photons, and now it is the preferred technique for DSOC system. PPM can overcome the power restriction on payload and greatly reduce background photons in signal slots.

To support high data rates over such distances while keeping the mass and power on the spacecraft comparable to radio-frequency communication systems, extremely high-performance single photon detectors are required at the ground receiver. With the development of single photon detection technology, a variety of high-sensitivity single photon detectors have been developed. So far, two kinds of detectors have been well applied: 1) Geiger Mode-Avalanche Photodiode - GM-APD and 2) Superconducting Nanowire Single Photon Detector - SNSPD. The former type, due to its small size and low power consumption is so far considered as the most more suitable for satellite platforms, but the detector's performances of detection efficiency at1550 nm, dark count rate and the dead time are limited. SNSPDs, on the other hand, have a higher photon detection efficiency (50%∼93%), lower DCR (∼100Hz), low timing jitter (∼ps) and fast reset time (∼ns), but the complexity and weight of the associated cryogenics has prevented its integration as part of satellite payloads. Next generation miniaturised closed-cycle cooling platforms which are compatible with space applications are under development(118).

Just to give a better idea of the state-of-the-art regarding the use of superconducting sensors (SNSPD in this case), an specific sensor developed for this application (117) implements 64-pixel tungsten silicide superconducting nanowire single photon detector (WSi SNSPD) arrays suitable for use in the ground terminal. To efficiently couple to a 5-meter telescope aperture in the presence of atmospheric seeing, the arrays are free-space coupled and have a combined 320 $\mu m$ diameter active area. The development is targeting 70% system detection efficiency at an operating wavelength of 1550 nm, 150 ps time resolution, a maximum count rate approaching $10^9$ counts per second, a numerical aperture capable of supporting an $f/1.2$beam, a background-limited dark count rate, and an operating temperature of 1K. Other developments with similar performance, also based in SNSPD technology are already available (116).

Overall, the market for optical communications is expanding very quickly and offering opportunities for hardware suppliers. Superconducting technologies can occupy a leading position in terms of performance, but the challenge of producing reliable, cost/effective cryostats remains unsolved and constitutes the main entry barrier for this technologies.

*This project has received funding from the European Union´s Horizon 2020 research and innovation programme under grant agreement No 800923.*

## 3.9 *Particle Physics*

This scientific discipline focuses on the definition of the fundamental particles and their interactions. The pillars in this area where established during the second half of the XXth century:

- **Large High Energy Experiments,** like CERN (Switzerland) and Brookhaven and Fermi National Laboratories (both in the US) have been possible thanks to significant efforts in the financial and scientific cooperation areas. The construction of these large infrastructures and the development of many key technologies have been essential for achieving experimental confirmation of the theoretical models.
- **The Standard Model** groups the set of theories which arrange logically the smallest particles found so far. It describes the strong, weak, and electromagnetic fundamental interactions, using mediating gauge bosons (eight gluons, W− , W+ and Z bosons, and the photon). The Model also describes the 24 fundamental fermions (12 particles and their associated anti-particles), which are the constituents of all matter, plus Higgs boson.

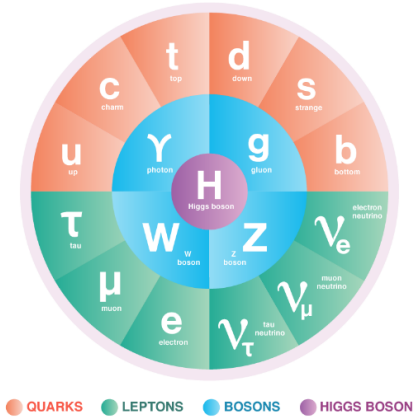


Figure 3.35: **The Standard Model** includes the matter particles (quarks and leptons), the force carrying particles (bosons), and the Higgs boson.

These are undeniably major scientific achievements, capable of justifying a very large fraction of our Universe structure and dynamics. However, they leave some phenomena unexplained and falls short of being a complete theory of fundamental interactions. Probably the two most important open questions are:

- Standard Model does not contain any viable dark matter particle that possesses all of the required properties deduced from observational cosmology.
- It also does not incorporate neutrino oscillations and their non-zero masses.

These scientific challenges are currently at the very frontier of scientific research. It is clear that their solution will require the development of new generations of detectors, whose construction pushes to the limit the capacity of current industrial and laboratory level manufacturing capabilities. The objectives are to achieve the levels of sensitivity required, and to generate a stable environment that could allow the detectors to operate without being buried in noise. In practice, the experimental strategies which are being developed overlap to a very large degree.

Some experimental routes being proposed involve superconducting sensors. These are certainly well positioned in this race, mainly because of three reasons: 1) there is a need for achieving extremely

*This project has received funding from the European Union´s Horizon 2020 research and innovation programme under grant agreement No 800923.*

high performance, 2) cryogenic conditions are in many cases needed anyway as part of the stable detection environment and 3) the cost of the experiments, ranging in the level of many millions of euros, makes this type of technologies affordable within this context.

We will now provide a very brief (and therefore inevitably shallow) introduction to the two scientific challenges, and then focus quickly into the description of the contribution of superconducting sensors in this area.

### *3.9.1 Dark Matter Detection.*

There is plenty of indirect evidence from astronomy and cosmology that a large fraction of the matter in the Universe is dark. This adjective is given because this type of matter neither interacts electromagnetically nor strongly with other types of matter and fields. Its existence, however, has been proposed as a justification for the evolution of the Universe which can be seen. For instance, the velocities of stars in the solar neighbourhood are too high to be explained by the luminous mass in the Galaxy. Further evidence comes from gravitational lensing, where invisible dark matter clumps in the foreground distort the images of luminous objects in the background. At largest scales, evidence for dark matter comes from the distribution of structure in the Universe as well as from the precision analysis of the Cosmic Microwave Background [38]. While it has been proposed that neutrinos could be responsible for the missing fraction, the sensitivity reached by present searches excludes that neutrinos can play this role and experimental evidence tends to suggest that contribution of neutrinos could be at most a few percent to the missing mass.

[38] An introduction to the subject and further references can be found in (41).

Determining the precise nature of Dark Matter is one of the main open questions of contemporary physics. Hypothetical (so far) particles, named Weakly Interacting Massive Particles (WIMPs) are presently considered as the best motivated candidate to solve the missing matter enigma. The nature of such elementary particles is still rather undefined. In zero order approach, they can be described as particles who interact through gravity and another force which is not yet part of the Standard Model. From observations, it is possible to guess that such force must be as weak as or weaker than the weak nuclear force, but also non-vanishing in its strength. The theoretical framework that supersedes the Standard Model and accommodates these concepts is Supersymmetry[39].

[39] For an introduction to the subject can be found in ref: (40).

WIMPs must in principle have been produced thermally in the early Universe, similarly to the particles of the Standard Model. Experimental efforts to detect WIMPs include the search for products of WIMP annihilation, including gamma rays, neutrinos and cos-

*This project has received funding from the European Union ´s Horizon 2020 research and innovation programme under grant agreement No 800923.*

mic rays in nearby galaxies and galaxy clusters; attempts to directly produce WIMPs in colliders (such as the LHC) and direct detection experiments designed to measure the collision of WIMPs with nuclei in the laboratory.

Although most WIMPs encountering the Earth are expected to pass through without any effect, it is hoped that a large number of dark matter WIMPs crossing a sufficiently large detector will interact often enough to be seen. Interaction between WIMPs and normal matter are estimated to range from a few events/kg day for the most optimistic models, down to about $10^{-7}$event/kg day. Best accepted models typically provide event rates of a few $10^{-3}$ event/kg day or below.

### 3.9.2 *Double Beta Decay* ($0\nu\beta\beta$)

Neutrinos are currently one of the most puzzling types of particles described in the Standard Model. They are known to be electrically neutral fermions that interact only via the weak interaction and gravity. Since weak force has a very short range and the gravitational interaction is extremely weak, neutrinos typically pass through normal matter unimpeded and are therefore extremely difficult to detect.

Neutrinos undergo a quantum mechanical process known as oscillation, in which a neutrino created with a specific lepton family number can later be measured to have a different lepton family number[40]. The experimental confirmation of this process had special significance, because it established that at least one type of neutrino has non-zero mass.

A remaining relevant question is whether neutrinos and antineutrinos are identical (particles with such characteristic are often known as Majorana particles). If this is the case, and taking into the account the non-zero mass, it would be possible to demonstrate that the lepton number is not a symmetry of Nature. This will on turn provide an explanation of the Baryon Asymmetry of the Universe via Leptogenesis[41] and, in any case, will pave the way for an evolution of the Standard Model.

One important experimental path for validating or rejecting this hypothesis is the detection of double-$\beta$ decay processes[42]. Double $\beta$ decay is a type of radioactive decay in which two neutrons are simultaneously transformed into two protons (or the other way around) inside an atomic nucleus. As a result of this transformation, the nucleus emits two detectable $\beta$ particles, which are electrons or positrons. In ordinary double $\beta$ decay, which has been confirmed experimentally many times, two electrons and two electron antineutrinos are emitted from the decaying nucleus. In neutrinoless double

[40] Lepton number is a conserved quantum number representing the difference between the number of leptons and the number of antileptons in an elementary particle reaction. The probability of measuring a particular flavour for a neutrino varies between three known states, as it propagates through space. Experimental evidence for neutrino oscillation has been collected from many sources, over a wide range of neutrino energies and with many different detector technologies.

[41] Leptogenesis is the generic term for hypothetical physical processes that produced an asymmetry between leptons and antileptons in the very early universe. The lepton and baryon asymmetries affect the much better understood Big Bang period, during which light atomic nuclei formed. Successful synthesis of the light elements requires that there be an imbalance in the number of baryons and antibaryons to one part in a billion when the universe is a few minutes old.

[42] An updated introduction to the subject can be found in ref: (228).

*This project has received funding from the European Union´s Horizon 2020 research and innovation programme under grant agreement No 800923.*

beta $(0\nu\beta\beta)$ only two electrons are emitted. This can only occur if the neutrino and antineutrino are the same particle (i.e. Majorana neutrinos) so the same neutrino can be emitted and absorbed within the nucleus. In a $(0\nu\beta\beta)$ process total kinetic energy of the two electrons in the final state would be equal to the binding energy difference of the initial and final nuclei (generally referred to as Q-value, $(Q_{\beta\beta})$), and the nuclear recoil, which can be considered to be negligible. The study of the $(0\nu\beta\beta)$ could also allow for an estimation of the neutrino mass[43] (this would obviously require very accurate measurement of the sum of the kinetic energies of the two emitted electrons).

So far, there is no experimental evidence of $(0\nu\beta\beta)$. Within the natural isotopic composition of the different elements, there are 69 $\beta\beta$-unstable nuclides present, although only a small subset is of any practical experimental interest for the study of $(0\nu\beta\beta)$. Currently, only 9 isotopes are being considered ($^{48}Ca$, $^{76}Ge$, $^{82}Se$, $^{96}Zr$, $^{100}Mo$, $^{116}Cd$, $^{130}Te$, $^{136}Xe$ and $^{150}Nd$). The $\beta\beta$ decay mode is shared by all of the candidate isotopes, and is characterised by half-lives $\geq 10^{18}$ years, although $0\nu\beta\beta$ mode is an even more exotic variant of the already rare process, with an expected lifetimes longer than $10^{27}$years. This amount of time is many orders of magnitude larger that the Age of our Universe (which is around $13.8 \times 10^{9}$years). The only possible strategy for detecting such an event is to multiply the number of nuclei under monitoring: if one nucleus will disintegrate in $10^{27}$years, a collection of $10^{27}$years nuclei will allow to observe roughly 1 event per year. The amount of mass involved, is thus in the range of 1 metric ton of the isotope under observation.

The path for designing experiments is therefore rather clear and consist in gathering a sufficiently large amount of material whose nuclei can undergo such decay process, and place it inside a detector capable of detecting the products of the decay and the energies released in the process. In practice, the set up of $(0\nu\beta\beta)$ decay experiments is a decades long, tenths of million euro, process. Most of the effort is focused on: 1) purifying the selected material, so that it only contains the isotope that can undergo the decay and 2) building the detector using materials with very low radioactivity levels, so that these parasitic processes do not constitute an unbearable level of noise. The overall strategy is to develop very sensitive systems that can be scaled up to large volumes once validated.

Currently, several detecting concepts have been tested and validated[44], leading to a second generation of approximately 20 experiments, of which only the best performant are expected to reach a third generation where the cost of the experiment will be in the tenths of millions of euros range.

[43] The decay rate for this process is given by

$$\Gamma = G\,|M|^2\,|m_{\beta\beta}|^2$$

where $G$ is the two-body phase space factor, $M$ is the nuclear matrix element and $m_{\beta\beta}$ is the effective Majorana mass of the neutrino.

[44] An updated overview can be found in ref: (21).

*This project has received funding from the European Union´s Horizon 2020 research and innovation programme under grant agreement No 800923.*

### 3.9.3 *Technologies for Dark Matter and $(0\nu\beta\beta)$ detection*

The quests for experimental confirmation of the existence of dark matter and $(0\nu\beta\beta)$ decay are essentially different, although the instruments (detectors) employed shared a common ground. In principle, both types of research require instruments capable of detecting extremely small releases of energy, plus extra information that could allow to filter out those events which are also detected but correspond to naturally occurring processes (like environmental radioactivity or cosmic rays).

Several types of detectors are under test: Noble gas scintillators, crystal scintillators, bubble chambers, time projection chambers and cryogenic crystal detectors.

It is out of the scope of this report to discuss the advantages of each of these technologies[45] . We will rather focus attention on those where superconducting sensors are integrated. The later type (cryogenic crystal detectors) makes use of electromagnetic radiation sensors as part of the detection transduction chain.

Cryogenic detectors[46] are motivated by the fact that, at very low temperatures, the heat capacity approximately follows a Debye law with a $T^3$ dependence and it becomes possible to consider real calorimetric measurements down to very small energy deposition. In order to be able to detect the low energy nuclear recoils the target crystals are operated at temperatures of about 10 mK. The fundamental resolution of these detectors can be approximated by the thermodynamic fluctuations in the energy of the detector $\Delta E_{FWHM} \approx 2.35\sqrt{K_B C T^2}$where $K_B$ is Boltzmann constant, $C$ is the heat capacity of the detector, and $T$ is the operating temperature. Energy thresholds below 1 keV of recoil energy have already been demonstrated (at a temperature of 10 mK, a 1 keV energy deposited in a 100 g detector results in a typical temperature increase of about 1μK)(39).

These detectors are therefore very sensitive calorimeters, which measure the energy deposited by a single interacting particle through the corresponding temperature rise. Unlike other solid-state devices, bolometers are not ionisation detectors but phonon detectors. As a consequence they are almost equally sensitive to any kind of particle, despite the way energy is released. In other words electrons, α-particles and nuclear recoils, depositing the same amount of energy in the detector, produce a pulse with the same amplitude (and shape).

An important milestone for this technology has been the implementation of capacity to discriminate the background. This feature implicitly also brings information redundancy, which benefits the

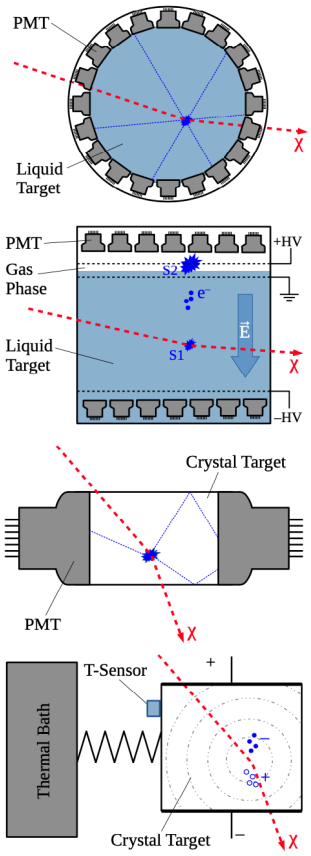


Figure 3.36: **Direct Dark Matter Detectors:** Noble Gas Scintillators (top) measure only the primary scintillation signal (single phase detectors); TCP (second from top) detect the primary scintillation light as well as the ionisation signal; Crystal scintillators (third from top) search for an annually modulating signal, but require extremely low intrinsic background levels. Cryogenic detectors (bottom) are cooled down to mK temperatures and weakly coupled to a thermal bath. Measured observables are heat (in form of phonons) and ionisation (or scintillation light). Source: (112).

*This project has received funding from the European Union´s Horizon 2020 research and innovation programme under grant agreement No 800923.*

[45] An introduction to the different types of particle detectors can be found in ref: (112).

[46] An introduction to the concept can be found in ref: (31), and an updated discussion in ref: (228).

reliability of data processing and is very convenient experiments where the interaction events are expected to be rare (a few counts per year). Real event-by-event identification allows to discriminate between electron recoils, associated with the $\gamma$, $\beta$ and $\alpha$ radioactive background, and nuclear recoils, observed in neutron and WIMP interactions.

The first discrimination method between electron recoils and nuclear recoils was based on their different ionisation efficiency, or quenching factor (these technology is usually referred to as charge-phonon type). This quenching factor is measured experimentally using neutron sources and tagged neutron beams. The energy dependence of this parameter is predicted theoretically by phenomenological models, such as the Lindhard model. Germanium detectors, for instance, with a gap energy at low temperatures of $\sim$ 0.7 eV, require in average $\sim$ 2.9 eV of deposited electron energy to produce an electron–hole pair. For nuclear recoils, the ionisation efficiency is typically a factor 3 lower than for electron recoils and depends on the deposited energy. Using cooled Field-Effect Transistors and SQUID electronics, these detectors present efficient discrimination performances down to recoil energies of $\sim$ 10 keV.

Charge phonon detectors have demonstrated excellent energy resolution (37), but face the important limitation due to surface events. $\alpha$-particles can loose a fraction of their initial energy while passing through the bulk of the material surrounding the detector before interacting in the bolometer. These so-called degraded $\alpha$-particles show a flat energy spectrum ranging from the Q-value of the $\alpha$-decay (several MeV) down to threshold energy, and therefore can potentially create background within the region of interest, close to the signal region where a large fraction of WIMP interactions are expected.

The only way to eliminate this $\alpha$-background is to identify the interacting particles. The discrimination can be obtained by measuring the Cherenkov light, as different particles (namely $\beta$, $\gamma$, $\alpha$ and neutrons) have also different scintillation yield (or scintillation Quenching Factor) and therefore can be very efficiently discriminated. $\alpha$-particles of few MeV have kinetic energies below the threshold for the creation of Cherenkov light, while the expected energy emitted in form of Cherenkov photons from electron interactions is in the order of 100eV(36).

This technique obviously requires integration of light detectors, which must have very low energy threshold and an excellent energy resolution. The incorporation of superconducting bolometers has allowed to develop an elegant solution. The energy deposited by an interacting particle is mainly converted into phonons, which are then detected with a transition edge sensor (TES) coupled directly to the

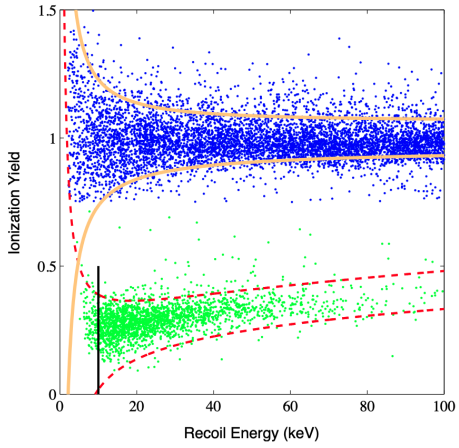


Figure 3.37: **Ionisation yield versus recoil energy** for calibration data with a $^{252}Cf$ gamma and neutron source for detectors showing the $\pm 2\sigma$ $\gamma$ band (solid curves) and the $\pm 2\sigma$ nuclear-recoil band (dashed curves). Source: (38).

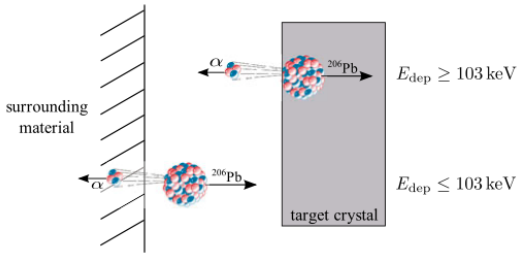


Figure 3.38: **Illustration of background events due to surface effects.** Source: (35).

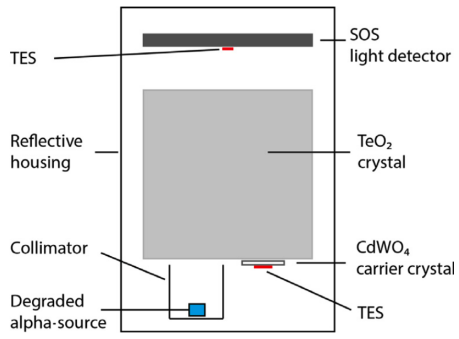


Figure 3.39: **Cryostat detector with TES technology.** In this scheme, an $\alpha$-particle source has been added for calibration purposes. Source: (34).

*This project has received funding from the European Union´s Horizon 2020 research and innovation programme under grant agreement No 800923.*

crystal (this assembly is usually named phonon detector). A second TES coupled to a light absorber (Silicon on sapphire - SOS), is used to detect Cherenkov radiation.

For each particle interaction, a detector module yields two coincident signals (one from the phonon and one from the light detector). While the phonon channel provides a sensitive measurement of the total energy deposition in the target (approximately independent of the type of interacting particle), the Cherenkov light signal can be used to discriminate different types of interactions. After the interaction, the crystal temperature relaxes back to the equilibrium state via a weak thermal coupling to the heat bath.

The most basic version of these detectors does not offer position tracking functionality, as light was detected using a single TES coupled to a SOS which covered the full surface of one side of the detector. A quadrant configuration (using four TES) allows to achieve position sensitivity down to the mm range.

TES technology competes with thermistor ones, mainly neutron transmutation doped Ge (27). With respect to semiconductor thermistors, TESs offer several advantages: 1) large arrays can be fully fabricated with standard micro-fabrication processes, 2) the larger electron-phonon coupling allows signal rising as fast as few microseconds, and 3) the low impedance reduces the sensitivity to environmental mechanical noise. The main drawbacks of TESs are the limited dynamic range(22), the adverse sensitivity to magnetic fields of TES and SQUID(24), and not yet fully understood sources of noise[47].

Apart form TES, other superconducting technologies are under test. In particular, both Magnetic Calorimeters(29) and KIDs (28; 25)are at early stages of development.

Careful choice of the scintillating crystal (as each have a characteristic quenching factor) can also lead to enhanced functionality of the bolometric sensors. Using, for instance, $CaMoO_4$ the thermal signal recorded by the TES displayed a different envelope, in depending of the type of particle interaction. This feature is very interesting because of the redundant information available for event discrimination, even without the need to detect the scintillation light(30).

The choice of different materials as scintillating crystals is also the mean for adapting this technique to the study a wide range of processes:

- In what concerns Dark Matter search, several of such devices have been and/or are under test. The aforementioned concept was developed and integrated into Cryogenic Dark Matter Search - CDMS in the US (current generation is being installed at SNOLAB in Canada)(33). The other, most relevant, experiment which

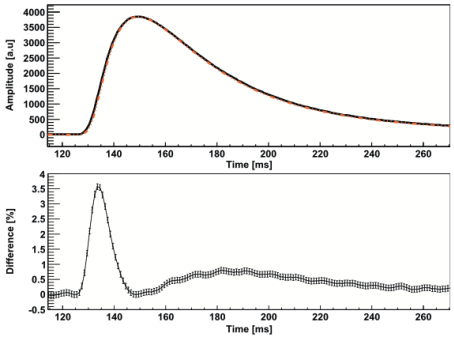


Figure 3.40: **Comparison of $\beta/\gamma$ and $\alpha$ thermal pulse shape.** Top graph shows (averaged) thermal pulses of $\gamma$-line (black continuous line) and $\alpha$ particles (red dotted line). Although these processes release a similar energy the difference between both signals (shown in bottom graph) makes it evident that pulse shapes are different and can therefore be discriminated. Source: (30).

[47] This issue is discussed in detail in section 2.7 of ref: (148).

*This project has received funding from the European Union´s Horizon 2020 research and innovation programme under grant agreement No 800923.*

integrates TES technology is the Cryogenic Rare Event Search with Superconducting Thermometers - CRESST (32). The use of SNSPDs have been proposed, but so far not demonstrated (2).

- For $0\nu\beta\beta$ search, ongoing experiments CUORE(**?** ), CUPID(20) and AMoRE(19) are building cryogenic detectors. Although currently Ge thermistors are the mainstream light detection technology, it is expected that superconducting sensors like TES or KID will eventually gain significance, for discrimination of the background signal(21).

- Direct measurement of neutrino mass has been also attempted on the light of the technological developments achieved in the aforementioned areas. Both experiments HOLMES[48] and NUMECS(26) integrate TES as part of the read out of cryogenic calorimeters.

In summary, the field of particle physics constitutes an interesting opportunity for the development of superconducting sensing technologies, as it poses very significant challenges. The size, cost, pace and intrinsic conditions of the experiments (ultra-low temperatures) imply that the barriers that are usually found in other applications, simply do not exist in this case.

[48] HOLMES experiment is funded by the European Research Council under the European Union's Seventh Framework Programme (FP7/2007-2013)/ERC Grant Agreement No. 340321.

*This project has received funding from the European Union´s Horizon 2020 research and innovation programme under grant agreement No 800923.*

# 4
# *Commercial Exploitation: Products, Business Models and Market Sizes.*

Commercial exploitation of a new technology will require its implementation in some short of product. This task will vary from straightforward industrialisation (i.e. definition of a manufacturing process that allows for replication of the device with controlled quality) up to complex integration together with other technologies (both hardware and software). Beyond the definition of a product, a full business model must be built, which will be the ultimate factor defining the success of the commercialisation.

This step must not be underestimated. Many interesting technologies have ended up with small or no penetration at all in the markets, either because they were implemented into unusable products (that did not solve customer problems) or because the business model built around it did not wok (as an example, for expensive technologies a renting model could be more appropriate than direct sale, as otherwise customers may not be able to afford it).

Both definition of products and business models requires an understanding about the structure of the value chain in each application, i.e. how the different industrial actors have organised themselves in order to be able to offer useful products to the end-users. The very basic structure of any value chain has three levels (raw materials, devices and systems). This, however, can become much more sophisticated if the complexity of the products is very high, requiring a lot of contributions from small ultra-specialised actors, or much simpler, if one single actor can integrate may capabilities.

Basic information about the value chain can be understood from an analysis of the type of companies and products that have been built in each case. We have tried to gather this type of information for some of the most important application which have been described in chapter 3.

Finally, an obvious interesting piece of information is the size of

the markets. Obtaining this information is, once more, a tricky business. Accurate estimation of market sizes can only be done after an in depth study of the actors present in this market, and the volume of their operations. Normally, this type of intelligence is built up slowly, after years of gathering information from many sources. This would have not been possible within the context of this project. Alternatively, it is possible to rely on technological analyst, which carry on this type of job. It is a rather well known fact that their estimations are very often overestimated[1] Even if future projections cannot be trusted, these analysis often contain historical data which has a higher degree of reliability, as it concerns the past, and show tendencies of the markets. The fact that analyst have devoted effort to gather information is already an indicative that there is a minimum level of industrial and entrepreneurial activity clustering around a technology. Because of this, we have also collected information regarding some of these reports.

[1] See, for instance, the presentation regarding markets for THz technologies of ref:(5).

## *4.1 Superconducting sensors and Analytical & Science Industry*

In this section we summarise all information related to products oriented to be integrated in scientific experimental set ups, or high-performance systems which can be used in analytical laboratories. Although it is worth mentioning that in many occasions the line separating both types of activities is thin (synchrotron or large academic laboratories, for instance, very often provide services to industry), from the point of view of product development the difference can be important:

- In a certain type of frontier research, like astrophysics or particle physics, the set ups are typically built from scratch and therefore the industry focuses on offering components. Technical performance is in this case the absolute top priority, and even new, unreliable, products can find their way as long as they can offer new functionalities or exceptional performance.
- In analytical facilities, on the other hand, priority is offer a stable and reliable service, and the usual tendency is to buy turn-key solutions that allow to establish such work-flow. Often the suppliers must therefore offer, as well as the systems, an adequate technical service and support, for maintenance and repair of systems which are often working in an intensive regime (so that they can provide return over investment.

Regarding quantum sensors, our sampling of the market reveals a rather asymmetric situation. There is a reasonable number of companies focuses on commercialisation of Superconducting Nanowire

*This project has received funding from the European Union´s Horizon 2020 research and innovation programme under grant agreement No 800923.*

Single Photon Detectors - SNSPDs, but none at all offering other, also well established, technologies such as TES and/or KID. The reason underneath is probably that SNSPD have been identified as backbone technologies for very powerful emerging technologies, such as quantum encryption, quantum computing or satellite optical communications, that can justify the investments in licensing. The situation with both TES and KID is probably more complicated because of: 1) the early involvement of large institutions like NIST, Stanford University, California Institute of Technology and the Jet Propulsion Laboratory, which may have controlled a large amount of the relevant IP, 2) the intense research activity which has publicly released a large fraction of information and 3) the restricted number of applications in which these technologies have been tested so far.

The companies that we are referring to are:

- **Single Quantum**[2] (Netherlands) offers at SNSPDs system level, including sensor head, cryostat, acquisition electronics and software.
- **PhotonSpot**[3] (US) offers SNSPD and closed cycle cryostats at components and system level.
- **Quantum Opus**[4] (US) offers SNSPD, read-out electronics, and turn-key systems.
- **Scontel**[5](Russia) offers SNSPD, Hot Electron Bolometers - HEB and cryogenic systems.

[2] Link to Single Quantum homepage.

[3] Link toPhotoSpot homepage.

[4] Link to Quantum Opus homepage

[5] Link to Scontel homepage.

All of them work with straightforward business models based on manufacturing and sale of key components and systems. All of the products can serve to scientific experiments, but will require further level of integration for being used as analytical systems. It is worth noting that all companies incorporate cryogenics as a core technology, which is obviously justified by the fact that the superconducting detectors cannot be used without and appropriate cryostat.

In what concerns instruments, the number of companies decreases drastically, as we have only found one:

- **Star Cryoelectronics**[6] (US) offers a large number of products, including sensors and cryostats, from component up to system level, as well as services (custom foundry). Their STJ X-ray Spectrometer integrates Superconducting Tunnelling Junction sensors with Ta electrodes(arrays between 36 and 112 pixels). Their X-ray microcalorimeter contains arrays of 2 x 8 TES, with different widths (350, 500 and 550 $\mu$m) and Bi absorbers.

[6] Link to Star Cryogenics homepage.

On top of the components, this company offers system level of integration, which means that the technology is sold within a module,

*This project has received funding from the European Union´s Horizon 2020 research and innovation programme under grant agreement No 800923.*

which contains all necessary elements, as well as software which makes it much easier and straightforward to use. This small size company competes in a market where several mid-size, well established companies[7] are offering alternative (and, in principle, less performant) technologies.

[7] An updated list of these, approximately 20 companies, can be found here.

## 4.2 *THz inspection*

As it has been described in section 3.6, the area of applications of spectroscopy and imaging in the THz range is very large and involves many different industrial fields. The volume of the market of THz radiation systems reached a size of 58.2 millions of dollars in 2018[8]. It must be taken into account, however, that such volume is shared between many different types of products (radiation sources, optics, electronics, software, etc).

[8] Sourcehere.

The number of companies developing some type of activity related to THz sensing is relatively large. We provide here a, very likely non-exhaustive, list:

- **Toptica**[9](Germany) offers a wide range of photonic products (mainly laser sources) in different wavelength ranges, part of which concern the THz range. This includes components, but also system level integrated solutions.

[9] Link to Toptica homepage.

- **Terasense**[10] (US) offers portable terahertz (THz) imaging systems, Terahertz imaging cameras, THz sources and THz detectors.

[10] Link to Terasense homepage.

- **Virginia Diodes**[11] (US) offers test and measurement equipment for mm-wave and THz applications.

[11] Link to Virginia Diodes homepage.

- **Swissto12**[12](Switzerland) offers 3D printed waveguides for THz and GHz range, as well as detecting assemblies (antennas and sensors).

[12] Link to Swissto12 homepage.

- **Euclid Techlabs**[13] (US) offers components with a focus on solutions for linear particle accelerators, ultrafast electron microscopy and advanced materials.

[13] Link to Euclid Techlabs homepage.

- **INO**[14](Canada) this Technology Center offers a range of products (camera, optics, radiation sources) for integration.

[14] Link toIno homepage.

- **Bridge12**[15] (US ) offers technology at components and system level for use in communications, defense, security and scientific applications, including high-frequency microwave sources, such as gyrotrons and vacuum electronic devices.

[15] Link to Bridge12 homepage.

- **TetechS**[16] (Canada) offers photoconductive antennas (which can

[16] Link to TetechS homepage.

*This project has received funding from the European Union´s Horizon 2020 research and innovation programme under grant agreement No 800923.*

be used both as sources and detectors) for imaging, spectroscopy and sensing applications.

- **Das-nano**[17] (Spain) offers solutions for counterfeit inspection, biometry and Non Destructive Inspection. In the later division, the company commercialises THz systems for inspection of 2D-materials (mainly graphene) and coatings.

[17] Link to Das-nano homepage.

- **Teraprobes**[18] (US) offers systems for fully-automated contact-free on-wafer testing solutions for high frequency devices and integrated circuits.

[18] Link to Teraprobes homepage.

- **Teraview**[19] offers a range of system for research, analysis (electro optical THz pulse reflectometry) and industrial (coatings) inspection

[19] Link to Teraview homepage.

- **Becker Photonik**[20] (Germany) offers portable solutions aiming industrial Non Destructive Testing.

[20] Link toBecker Photonik homepage.

- **Thruvision**[21] (UK) offers a range of systems for THz security inspection tasks.

[21] Link to Thruvision homepage.

- **Asqella**[22] (Finland) offers a range of systems for THz security surveillance tasks.

[22] Link to Asqella homepage.

- **Qinetiq**[23] (US) offers engineering capability for development of custom integrated solutions. The portfolio of the company shows an example[24] of passive surveillance systems in the THz range.

[23] Link toQinetiq homepage.

[24] Source here.

- **Leidos**[25] (US) offers advanced engineering for custom integrated solutions, with a focus on Defense and Security. The company commercialises several systems for passenger inspection at control points (in airports, public buildings, etc).

[25] Link to Leidos homepage.

- **Hubner Photonics**[26] (Germany) offers turn-key solutions for mail inspection.

[26] Link to Hubner Photonics homepage.

- **Smiths Detection**[27] (UK) offers integrated solutions for security applications, some of which are adapted to the THz range.

[27] Link toSmiths Detection homepage.

- **Neteera**[28] (Israel) offers solutions for remote monitoring of medical parameters (pulse rate, breathing, etc).

[28] Link to Neteera homepage.

- **Hypres**[29] (US) offers superconducting microelectronics for defence, wireless and optical network industries. Their portfolio of products includes, for instance, an integrated spectrometer for chemical and biological agent detection.

[29] Link to Hypres homepage.

*This project has received funding from the European Union´s Horizon 2020 research and innovation programme under grant agreement No 800923.*

An sticking fact extracted from an analysis of this list is that the vast majority of these companies are small in size despite a certain age, which is usually indicative of having their activity pinned down to small niche markets, where they can safely assure some income. THz markets seem nevertheless to lack a major application that will generate traction for major players to join. Probably the one with bigger potential, from this point of view, will be security monitoring and inspection.

## 4.3 *Satellite laser communications*

Although several analyst have released market reports, they do not seem to provide reliable information. Nevertheless, this sector is experiencing a large amount fo activity.

The following companies are currently testing and/or deploying infrastructure with commercial purposes:

- **SpaceX** is currently deploying a 10-strong fleet of polar satellites for laser communications[30].
- **Facebook,** through subsidiary PointView Tech[31] is currently testing communications between observatories[32].
- **Google,** through subsidiary Loon[33], has tried to deploy communication network using balloons as links to remote locations, mainly in african countries. This project seems to be halted as from 2020Source here..
- **Warpspace**, is a japanese star-up project, still at a very early stage of development[34].
- **Sitael and BridgeSat** are collaborating in the deployment of laser communication network [35]

[30] Source here.

[31] Source here.

[32] here

[33] Link toLoon homepage.

[34] Sourcehere.

[35] Source here..

Apart from these, also project Europe Data Relay System - EDRS (already operational), driven by German Aerospace Center, is testing this type of technology.

## 4.4 *Quantum key distribution*

The global quantum cryptography market size is estimated to be USD 89 million in 2020[36].

[36] Source here.

There are already several companies offering commercial quantum key distribution systems and components:

- **AegiQ**[37](UK) offers components (indistinguishable photon sources) for quantum encrypted communication and scalable quantum computing links.

[37] Link to AegiQ homepage.

*This project has received funding from the European Union ´s Horizon 2020 research and innovation programme under grant agreement No 800923.*

- **Agnostiq**[38] (Canada) specializes in providing cloud-based users with security software.

[38] Link to Agnostiq homepage.

- **Crypto Quantique**[39] (UK), focuses on development of Internet of Things security platform base on quantum cryptography technology.

[39] Link to Crypto Quantique homepage.

- **ID Quantique**[40] (Switzerland), offers quantum-safe network encryption, secure quantum key generation and quantum key distribution solutions and services to the financial industry, enterprises and government organisations. The company also commercialised components (quantum random number generator, photon counters and related electronics) for security, simulation and gaming industries.

[40] Link to ID Quantique homepage.

- **InfiniQuant**[41](Germany), offers turn key system for Quantum Key Distribution. Operates in project basis, with ongoing activity on metropolitan and satellite quantum communication.

[41] Link to InfiniQuant homepage.

- **ISARA**[42] (Canada), offers quantum-safe solutions for classical data security systems.

[42] Link to Isara homepage.

- **KETS Quantum Security** [43] (UK), offers hardware (system level) for Quantum Key Distribution and Quantum Random Number Generation.

[43] Link to KETS Quantum Security homepage.

- **Post-Quantum** [44] (UK), offers software based solutions for secure internet access, combining biometry and quantum cryptography.

[44] Link to Post-Quantum homepage.

- **PQShield** [45](UK) offers a products range from hardware and firmware for embedded devices, cryptographic Secure Key Distribution for mobile and server technologies, to encryption solutions for messaging platforms and apps. It has a focus on enabling transition from legacy systems, so that customers can leverage upcoming public-key cryptography standards across hardware, software and communication.

[45] Link to PQShield homepage.

- **Qabacus**[46] (US), mainly carries on R&D activity and offers IP regarding software based solutions for cybersecurity based on in areas like electronics, photonics, spintronics, classical cryptography and encryption systems.

[46] Link to Qabacus homepage.

- **Qaisec**[47] (Bulgaria), offers solutions based on quantum encrypted blockchain for financial markets and 5G telecom markets.

[47] Link to Qaisec homepage.

- **QaskyQuantum Technology**[48] (China) offers systems for quantum cryptography communication technology, quantum cryptography

[48] Link to Qasky Quantum Technology homepage.

*This project has received funding from the European Union´s Horizon 2020 research and innovation programme under grant agreement No 800923.*

communication networking technology and also quantum cryptography communication core devices (detectors, sources, clock generators, etc), both for applications and research markets.

- **QRATE**[49] Quantum Communications (Russia) offers systems industrial and academic systems, including a single-photon detector and a quantum random number generator.

[49] Link to Qrate homepage.

- **Qrypt**[50] (US) offers full full turn-key solution for indefinitely quantum cryptographic encoding.

[50] Link to Qrypt homepage.

- **Quantum Blockchains**[51](Poland) offers solutions for Quantum Blockchain based on quantum key distribution technology.

[51] Link to Quantum Blockchains homepage.

- **Quantum Dice**[52](UK) offers focuses on compact systems, offering self-certified quantum random number generator to provide security for encryption systems.

[52] Link to Quantum Dice homepage.

- **Quantum Xchange**[53] (US) offers key distribution systems.

[53] Link to Quantum Xchange homepage.

- **QuantumCTek**[54](China) offers quantum key distribution, quantum key management, and quantum secure communication networking at product and solution levels.

[54] Link to QuantumCtek homepage.

- **QuBalt**[55] (Germany) offers quantum- and cryptanalysis-secure cryptographic solutions to the automotive, aerospace and defence industries.

[55] Link to QuBalt homepage.

- **QuintessenceLabs**[56] (Australia), offers: 1) hardware (system level) for Quantum Random Number Generation, Quantum Entropy Enhancement, Key and Policy Management, Quantum Key Distribution and Encryption Solutions, 2) Software development kits for Key Management Interoperability Protocol, and 3) turn-key solutions application of these technologies to banking, cloud-storage and VMware (virtualisation).

[56] Link to Qunatessence Labs homepage.

- **QNu Labs**[57] (India), offers turn-key solutions for Quantum Key Distribution, Quantum Random Number Generation, Entropy as a Service, Post-Quantum Cryptography and Quantum security on AI PaaS.

[57] Link to QNu Labs homepage.

- **QuSecure**[58] (US) offers solutions for implementing quantum encrypted transport layer in Network Processes, Edge Computing and Personal Devices.

[58] Link to QuSecure homepage.

- **VeriQloud**[59](France) solution developer (mainly software based) for quantum network technologies.

[59] Link to VeriQloud homepage.

*This project has received funding from the European Union ´s Horizon 2020 research and innovation programme under grant agreement No 800923.*

- **MagiQ Technologies**[60] (US), offers solutions for mitigation of interference in military communications and wireless telecommunications, in-well sensing for oil&gas industries, and quantum cryptography.

Apart from these start-up/SME projects, several large corporations have established research programmes in this area: Toshiba[61], HP[62], IBM[63], Mitsubishi[64], NEC[65] and NTT[66].

[60] Link to MagiQ Technologies homepage.

[61] Link to Toshiba research program.
[62] Link to Hewlett Packard research program.
[63] Link to IBM research program.
[64] Link to Mitsubishi research program.
[65] Link to NEC research program.
[66] Link to NTT research program.

## 4.5 *Quantum computation*

The area of quantum computing is experiencing a hype, with very significant institutional investment from all technological powers. This situation induces a large distortion of the market, as many opportunistic actors gather around the funding opportunities. On the other hand, technology is still at a very unmature stage and the value chain is still rather undefined. It is expected that a consolidation of the market will follow.

Within this context, photonic quantum computing (the only one involving the sensing technologies studied in this report) will be competing with other alternatives, and it is unclear which ones will remain competitive.

It is worth mentioning, nevertheless, that several companies are adopting this type of technology:

- **NTT (Japan)** through its research centres at Bristol (UK) has developed photonic circuits with application is quantum computation (among others)[67].
- **PsiQuantum**[68] (US) aims to develop Si-based photonic quantum computers.
- **Xanadu Quantum Technologies**[69] (Canada) develops cloud accessible photonic quantum computers and develops open-source software for quantum machine learning and simulating quantum photonic devices.

[67] Details on the technology developed at NTT can be found in ref: (4).
[68] Link to PsiQuantum homepage.
[69] Link to Xanadu homepage.

*This project has received funding from the European Union´s Horizon 2020 research and innovation programme under grant agreement No 800923.*

# 5
# *Benchmarking*

## *5.1 Introduction*

When dealing with high technology solutions, performance will certainly play an important role as an argument for introducing them in markets, at least in the applications where high level of performance will have enabling character (like in most scientific research applications), or clearly help to differentiate products from competitors (like, for instance, in medical devices).

Gathering comparative information is always a tricky business. The main reason is that very rarely the different technologies are compared in equal conditions. Such an exercise, although undoubtedly interesting for the end-user choice, would be prohibitively expensive in most of the occasions. Alternatively, one can try to seek through bibliography, and try to gather relevant information that can be compared. This is the type of analysis that will be presented in the following tables. Information has been grouped by spectral ranges, since adaptation of the sensing technologies for each range will have an influence on its performance.

The degree of success of this type of search depends on the availability of relevant data. Sometimes more information, and for a larger number of technologies is available for specific spectral ranges. When possible, the comparison shows also information regarding the best performant technologies out of the superconducting sensors class.

A second, more specific type of comparison has been elaborated by several authors, mainly in the domain of astrophysics. The large timescale and elevated cost of these projects makes it very important to analyse the status of competing technologies and projects. This is done with the aim of avoiding the risk of investing effort in technologies that could become obsolete when ready. Comparison of key parameters is usually presented in a very clear manner through plots, some of which are reproduced here. These type of representation gives additional perspective as trends become apparent.

| Technology | Energy Resolution | Count Rates (per second) | Operating T | Decay Time | Detection range | Ref. |
|---|---|---|---|---|---|---|
| **Transition Edge Sensors** | 1.6 eV @5.9keV | $\sim 10^2$ | $\sim 100mK$ | $\sim 10^{-3}s$ | <10 keV | (174; 157; 156) |
| **Superconducting Tunnelling Junction** | 12 eV @5.9keV | $\sim 10^3 - \sim 10^4$ | $0.1 - 1.4K$ | $\sim 10^{-6}s$ | < 6 keV | (155; 16; 15) |
| **Kinetic Inductance Detectors** | 75 eV @5.9keV | $\sim 10^2$ | $\sim 100mK$ | $\sim 10^{-3}s$ | <10 keV | (14; 13) |
| **Superconducting Nanowire** | - | $\sim 16$ | $\sim 4K$ | $\sim 10^{-9}$ | 10 keV | (12; 11) |
| **Silicon Drift Detector** | ~150 eV | $\sim 13$ | $\sim 300K$ | $\sim 5 \times 10^{-6}s$ | <60 keV | (10) |

Table 5.1: **Benchmarking performance in the X-ray range.**

*This project has received funding from the European Union 's Horizon 2020 research and innovation programme under grant agreement No 800923.*

| Technology | Repetition Rate (Hz) | DK (Hz) | $\eta(\%)$ | NEP $(WHz^{-1/2})$ | $\lambda(nm)$ | $M_{noise}$ | $M_{max}$ | T(K) | Readout | Ref. |
|---|---|---|---|---|---|---|---|---|---|---|
| **Charge Integration Photodiode,** | 40 | - | 80 | - | 1550 | Yes | - | 4.2 | Cryogenic junction gate field-effect transistor | (169) |
| **Quantum Dot Field-Effect Transistor** | $2 \times 10^5$ | 0.4 | 1.3 | $2 \times 10^{-17}$ | 684 | Yes | 3 | 4.2 | Cryogenic metal epitaxial semiconductor field-effect transistor | (168; 167) |
| **Transition Edge Sensor** | $5 \times 10^4$ | 400 | 89 | $1 \times 10^{-19}$ | 1550 | Yes | 11 | <0.1 | SQUID array | (166; 165) |
| **Photomultiplier** | $6.7 \times 10^5$ | 400 | 7 | $1 \times 10^{-16}$ | 523 | Yes | 9 | 300 | Room T amplifiers | (164) |
| **Visible-Light Photon Counter** | $1.5 \times 10^4$ | $2 \times 10^4$ | 85 | $9 \times 10^{-17}$ | 543 | Yes | 10 | 6-7 | Cryogenic preamplifier | (163; 162) |
| **Multi-Pixel Photon Counter** | $1 \times 10^4$ | $1.4 \times 10^5$ | 25-65 | $7 \times 10^{-16}$ | 400 | Yes | 100-1600 | 300 | Room T amplifiers | (161) |
| **Avalanche Photo Diode** | $2 \times 14^4$ | $1.6 \times 10^8$ | 33 | $1 \times 10^{-14}$ | 1064 | No | 1024 | 246 | Multichannel | (160) |
| **Parallel Nanowire Detector** | $8 \times 10^7$ | 0.15 | 2 | $4 \times 10^{-18}$ | 1300 | No | 4 | 2 | Room T amplifiers | (170) |

**Table 5.2: Benchmarking performance for detectors with Photon Number Resolving capability in visible/IR range.**

*This project has received funding from the European Union 's Horizon 2020 research and innovation programme under grant agreement No 800923.*

| Sensing Technology | Instrument | Supercond. Material | Operating T | FOV (arcsec) | Array Size | Pixel Size ($\mu m^2$) | Wavelength Range (nm) | Maximum Count Rate (kHz) | Spectral Resolution (nm) | Ref. |
|---|---|---|---|---|---|---|---|---|---|---|
| **Transition Edge Sensor** | Stanford TES | W | 70 | $1.7 \times 1.7$ | $6 \times 6$ | 20 | 360-1700 | 30 | ~20 | (206) |
| **Superconducting Tunnelling Junction** | S-Cam 3 | Ta/Al | 285 | $9 \times 11$ | $10 \times 12$ | 33 | 330-750 | 5 | ~10 | (159) |
| **Microwave Kinetic Inductance Detectors** | MEC | TiN | 90 | $1.4 \times 1.44$ | $140 \times 144$ | 150 | 800-1400 | - | ~8 | (201) |

Table 5.3: **Benchmarking performance for superconductor detectors implemented in astrophysics applications in visible/IR.**

*This project has received funding from the European Union´s Horizon 2020 research and innovation programme under grant agreement No 800923.*

This project has received funding from the European Union 's Horizon 2020 research and innovation programme under grant agreement No 800923.

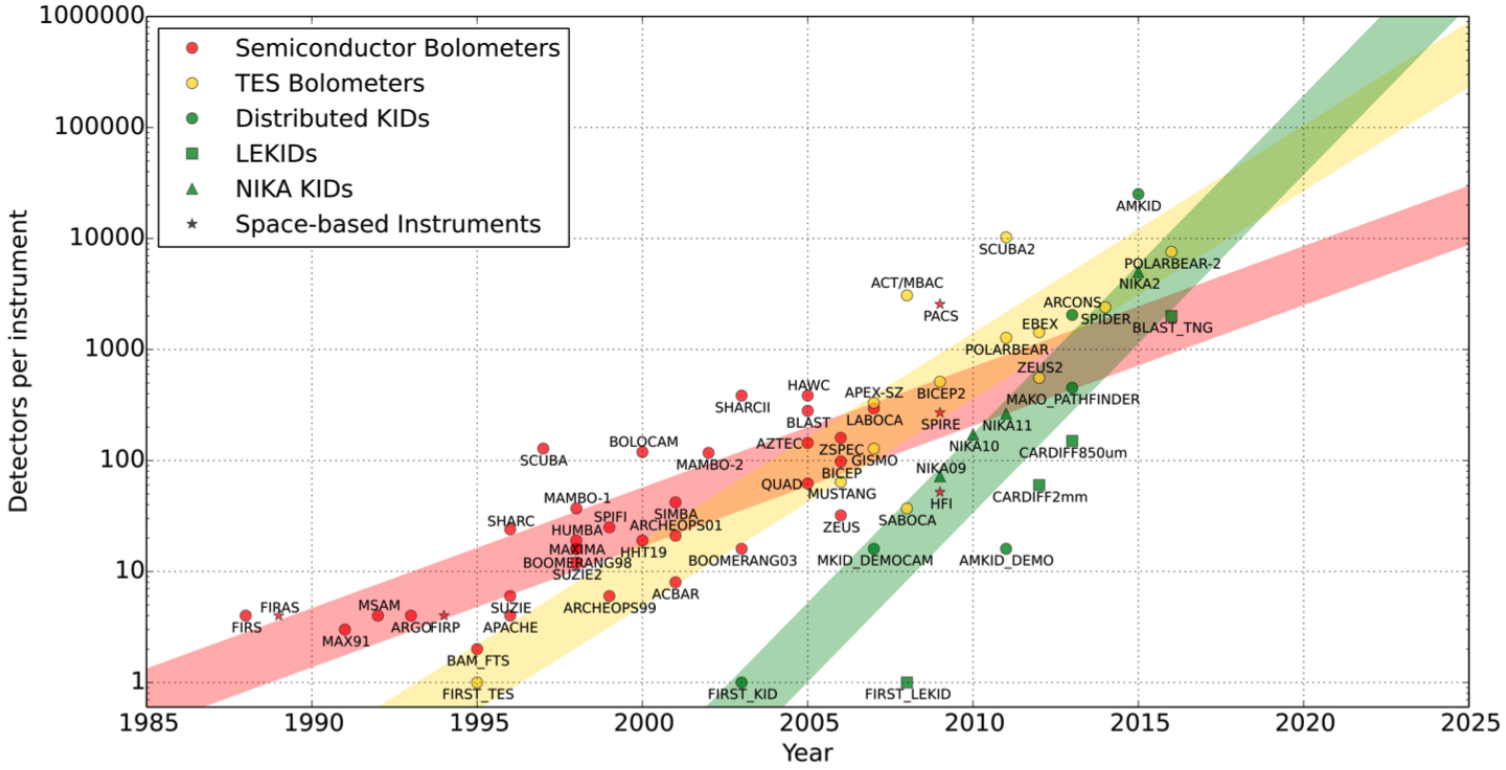


Figure 5.1: **Pixel counts in Astronomical receivers over the years.** The coloured areas indicate the potential for scaling up the different technologies. Source: (137).

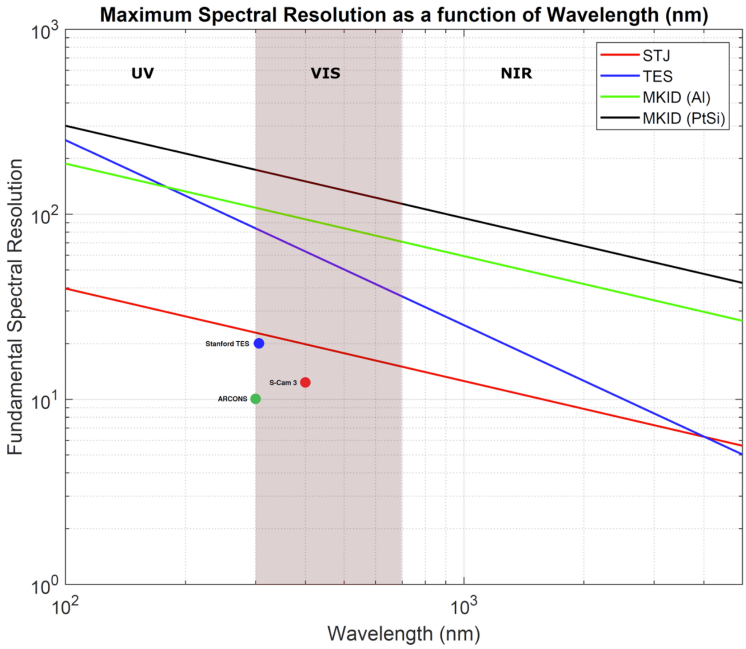


Figure 5.2: **Maximum Theoretical Spectral Resolution from 100 nm to 5000 nm:** For STJs and MKIDs the spectral energy resolution is limited by the bandgap of the superconductor. For comparison the best performing commissioned instruments, which have published observational results, are shown also on the plot. Source: (120).

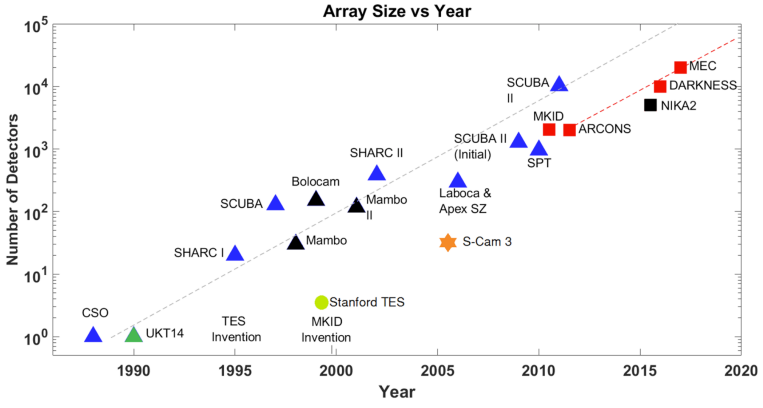


Figure 5.3: **Plot showing the array size growth of energy sensitive detectors from 1988 to 2020**. The triangular datapoints show single-pixel bolometers and TES arrays, the square datapoints show MKID-based arrays. The colors correspond to the region of the spectrum in which these detectors operate: Blue; Sub-mm, Green; mm and sub-mm, Black; mm, All others; UVOIR. Source: (120).

*This project has received funding from the European Union´s Horizon 2020 research and innovation programme under grant agreement No 800923.*

# 6
# *Conclusions*

The aim of this part of the document has been to collect all the information that can help put in perspective the competitiveness of the TED technology. This can only be done by comparing it with other competing technologies, and by looking at what are the needs of the applications.

TEDs exploit a physical phenomena which takes place when a material is in superconducting state. This is also the case of several other technologies (TES, KID, SNSPD, JTS, etc), and this is also the (physical) reason why all this class of superconducting sensors shows very high technical performance in terms or sensitivity, energy resolution, NEP, etc. These performances establish an upper limit, and currently no other technology has shown to do better.

There are subtle differences between these technologies, which make them more or less well adapted for a given application. Some of these technologies, for instance, are not easy to integrate into large focal plane arrays. Others are capable of operating at higher temperatures, thus reducing cost and complexity of the cryogenic system.

In what concerns non-superconducting technologies, the fact that they may show lower technical performance doesn't mean that they are excluded from the competition. This is because there are other important factors, like reliability, cost or complexity of maintenance and logistics, which have an important weight when evaluating the solutions.

It is out of the scope of this report to position the TED technology in a specific ranking. This task can only be completed once this new technology will be properly tested, hopefully by the end of SUPERTED project. An important bottomline message is, nevertheless, that this ranking is not unique, and will be application dependent.

In what concerns applications, TED technology can take advantage from the fact that many other of the superconducting sensing technologies have already been considered for a wide range of uses. We have been able to identify a large number of very different ap-

plications, and have tried to collect feedback regarding the use of superconducting sensors in them.

In principle, there are several scientific applications, mainly in the fields of astrophysics and particle physics, which constitute niches. These involve very small volumes, but they are very interesting testing grounds, where the sensing technologies will be exposed to very significant constrains. Adaptation of the technology for these applications can benefit from institutional R&D funding, and will certainly lead to improvements in reliability and performance.

There are many other applications which are linked to dynamic industrial and end-user applications. Some of these constitute emerging technological markets, like quantum computing and quantum cryptography, where the value chain is still under the process of formation. These, and some others, like beamline science and microbeam analysis, rely heavily in high performance of the sensors, and thus TED technology can be an interesting option. Some other applications, like THz image and sensing, or LIDAR, are very interesting markets, but the TED technology faces the challenge, as all other superconducting technologies, of becoming a deployable solution, which can be transported and installed at locations with lower infrastructure level that that found in scientific environments. The key issue in this case is cryogenics, and not the performance of the sensing technologies themselves.

We have finally had a look into the markets, to analyse their volume, type of actors and business models adopted. These first analysis is encouraging, as shows that many different types of companies populates these markets, and have found ways of exploiting other superconducting sensing technologies in an economically viable manner.

*This project has received funding from the European Union´s Horizon 2020 research and innovation programme under grant agreement No 800923.*

# 7
# Bibliography


[1] "European Space Agency: S-CAM 2", URL https://sci.esa.int/web/sci-fmi/-/33541-s-cam-2. 50

[2] Yonit Hochberg, et al., "Detecting Sub-GeV Dark Matter with Superconducting Nanowires", *Phys Rev Lett*, 123, 2019, p. 151802, URL https://link.aps.org/doi/10.1103/PhysRevLett.123.151802. 22, 109

[3] F. Ellrich, et al., "Terahertz Quality Inspection for Automotive and Aviation Industries", *Journal of Infrared, Millimeter, and Terahertz Waves*, 41(4), 2020, pp. 470–489, URL https://doi.org/10.1007/s10762-019-00639-4. 87

[4] Jacques Carolan, et al., "Universal linear optics", *Science*, 349(6249), 2015, pp. 711–716, URL https://science.sciencemag.org/content/349/6249/711. 119

[5] N; Deninger A.; Haring Bolivar P.; Globisch B.; Preu S. ; StöÌr A Leisching, P; Vieweg, "Photonic THz Systems meet Industrial Applications: Past, Present  Future", URL https://teraflag.eu/wp-content/uploads/2018/10/Keynote_THz-FlagShip_vfinal.pdf. 112

[6] S. M. Duff, et al., "Advanced ACTPol Multichroic Polarimeter Array Fabrication Process for 150 mm Wafers", *Journal of Low Temperature Physics*, 184(3), 2016, pp. 634–641, URL https://doi.org/10.1007/s10909-016-1576-y. 56

[7] J. Hubmayr, et al., "Low-Temperature Detectors for CMB Imaging Arrays", *Journal of Low Temperature Physics*, 193(3), 2018, pp. 633–647, URL https://doi.org/10.1007/s10909-018-2029-6. 56

[8] W. S. Holland, et al., "SCUBA-2: the 10 000 pixel bolometer camera on the James Clerk Maxwell Telescope", *Monthly No-*

*tices of the Royal Astronomical Society*, 430(4), 2013, pp. 2513–2533, URL https://doi.org/10.1093/mnras/sts612. 55

[9] Adam, R., et al., "The NIKA2 large-field-of-view millimetre continuum camera for the 30 m IRAM telescope", *A&A*, 609, 2018, p. A115, URL https://doi.org/10.1051/0004-6361/201731503. 56

[10] P. Lechner, et al., "Silicon drift detectors for high count rate X-ray spectroscopy at room temperature", *Nuclear Instruments and Methods in Physics Research Section A: Accelerators, Spectrometers, Detectors and Associated Equipment*, 458(1), 2001, pp. 281–287, URL https://www.sciencedirect.com/science/article/pii/S016890020000872X, proc. 11th Inbt. Workshop on Room Temperature Semiconductor X- and Gamma-Ray Detectors and Associated Electronics. 122

[11] K. Inderbitzin, et al., "An ultra-fast superconducting Nb nanowire single-photon detector for soft x-rays", *Applied Physics Letters*, 101(16), 2012, p. 162601, URL https://doi.org/10.1063/1.4759046. 122

[12] Xiaofu Zhang, et al., "Superconducting single X-ray photon detector based on $W_{0.8}Si_{0.2}$", *AIP Advances*, 6(11), 2016, p. 115104, URL https://doi.org/10.1063/1.4967278. 122

[13] M. Faverzani, et al., "Thermal kinetic inductance detectors for soft X-ray spectroscopy", *Nuclear Instruments and Methods in Physics Research Section A: Accelerators, Spectrometers, Detectors and Associated Equipment*, 936, 2019, pp. 197–198, URL https://www.sciencedirect.com/science/article/pii/S0168900218310854, frontier Detectors for Frontier Physics: 14th Pisa Meeting on Advanced Detectors. 122

[14] Gerhard Ulbricht, et al., "Highly multiplexible thermal kinetic inductance detectors for x-ray imaging spectroscopy", *Applied Physics Letters*, 106(25), 2015, p. 251103, URL https://doi.org/10.1063/1.4923096. 122

[15] S. Friedrich, et al., "112-Pixel Arrays of High-Efficiency STJ X-Ray Detectors", *Journal of Low Temperature Physics*, 176(3), 2014, pp. 553–559, URL https://doi.org/10.1007/s10909-014-1151-3. 122

[16] V. A. Andrianov, "Comment on "Observation of nuclear gamma resonance with superconducting tunnel junction detectors" [AIP Advances 6, 025315 (2016)]", *AIP Advances*, 9(5),

*This project has received funding from the European Union´s Horizon 2020 research and innovation programme under grant agreement No 800923.*

2019, p. 059101, URL https://doi.org/10.1063/1.5085756. 122

[17] R. C. Alig, et al., "Scattering by ionization and phonon emission in semiconductors", *Phys Rev B*, 22, 1980, pp. 5565–5582, URL https://link.aps.org/doi/10.1103/PhysRevB.22.5565. 22

[18] M. Blosch and J. Fenn, "Understanding Gartner's Hype Cycles", URL https://www.gartner.com/en/documents/3887767. 11

[19] Hyon-Suk Jo and, "Status of the AMoRE experiment", *Journal of Physics: Conference Series*, 888, 2017, p. 012232, URL https://doi.org/10.1088/1742-6596/888/1/012232. 109

[20] E. Armengaud, et al., "The CUPID-Mo experiment for neutrinoless double-beta decay: performance and prospects", *The European Physical Journal C*, 80(1), 2020, p. 44, URL https://doi.org/10.1140/epjc/s10052-019-7578-6. 109

[21] Michelle J. Dolinski, et al., "Neutrinoless Double-Beta Decay: Status and Prospects", *Annual Review of Nuclear and Particle Science*, 69(1), 2019, pp. 219–251, URL https://doi.org/10.1146/annurev-nucl-101918-023407. 105, 109

[22] M. Pyle, "Experimental Techniques to Search for Dark Matter throughout the Range of 1omeV < $M_{DM}$ < 10 GeV", URL https://conferences.pa.ucla.edu/ATI-2018/talks/pyle2.pdf. 108

[23] Federico Paolucci, et al., "Development of highly sensitive nanoscale transition edge sensors for gigahertz astronomy and dark matter search", *Journal of Applied Physics*, 128(19), 2020, p. 194502, URL https://doi.org/10.1063/5.0021996. 17

[24] R. A. Hijmering, et al., "Comparison of the Effects of Magnetic Field on Low Noise MoAu and TiAu TES Bolometers", *Journal of Low Temperature Physics*, 176(3), 2014, pp. 316–322, URL https://doi.org/10.1007/s10909-013-1061-9. 108

[25] H. Ishino, et al., "Development of Microwave Kinetic Inductance Detectors for a Detection of Phonons", *Journal of Low Temperature Physics*, 176(3), 2014, pp. 161–167, URL https://doi.org/10.1007/s10909-013-1025-0. 108

[26] M. P. Croce, et al., "Development of Holmium-163 Electron-Capture Spectroscopy with Transition-Edge Sensors", *Journal of*

*This project has received funding from the European Union´s Horizon 2020 research and innovation programme under grant agreement No 800923.*

*Low Temperature Physics*, 184(3), 2016, pp. 958–968, URL https://doi.org/10.1007/s10909-015-1451-2. 109

[27] D.R. Artusa, et al., "Enriched TeO2 bolometers with active particle discrimination: Towards the CUPID experiment", *Physics Letters B*, 767, 2017, pp. 321–329, URL https://www.sciencedirect.com/science/article/pii/S0370269317301016. 108

[28] Casali, N., et al., "Phonon and light read out of a $Li_2MoO_4$ crystal with multiplexed kinetic inductance detectors", *Eur Phys J C*, 79(8), 2019, p. 724, URL https://doi.org/10.1140/epjc/s10052-019-7242-1. 27, 108

[29] V. Alenkov, et al., "First results from the AMoRE-Pilot neutrinoless double beta decay experiment", *The European Physical Journal C*, 79(9), 2019, p. 791, URL https://doi.org/10.1140/epjc/s10052-019-7279-1. 108

[30] C. Arnaboldi, et al., "A novel technique of particle identification with bolometric detectors", *Astroparticle Physics*, 34(11), 2011, pp. 797–804, URL https://www.sciencedirect.com/science/article/pii/S0927650511000442. 108

[31] L. Gironi, "Scintillating bolometers: a powerful instrument for low background experiments", *Nuclear Physics B - Proceedings Supplements*, 215(1), 2011, pp. 262–264, URL https://www.sciencedirect.com/science/article/pii/S0920563211002647, proceedings of the 12th Topical Seminar on Innovative Particle and Radiation Detectors (IPRD10). 106

[32] G. Angloher, et al., "Results on low mass WIMPs using an upgraded CRESST-II detector", *The European Physical Journal C*, 74(12), 2014, p. 3184, URL https://doi.org/10.1140/epjc/s10052-014-3184-9. 109

[33] P. Cushman, "The Cryogenics Dark Matter Search: Status and Future Plans.", URL https://kicp-workshops.uchicago.edu/IDM2012/depot/plenary-talk-cushman-priscilla__1.pdf. 108

[34] K. Schäffner, et al., "Particle discrimination in TeO2 bolometers using light detectors read out by transition edge sensors", *Astroparticle Physics*, 69, 2015, pp. 30–36, URL https://www.sciencedirect.com/science/article/pii/S0927650515000481. 107

[35] G. Angloher, et al., "Results from 730 kg days of the CRESST-II Dark Matter search", *The European Physical Journal C*,

*This project has received funding from the European Union 's Horizon 2020 research and innovation programme under grant agreement No 800923.*

72(4), 2012, p. 1971, URL https://doi.org/10.1140/epjc/s10052-012-1971-8. 107

[36] T. Tabarelli de Fatis, "Cerenkov emission as a positive tag of double beta decays in bolometric experiments", *The European Physical Journal C*, 65(1), 2009, p. 359, URL https://doi.org/10.1140/epjc/s10052-009-1207-8. 107

[37] G. Gerbier, "Looking for SUSY with EDELWEISS I and II", *Nuclear Physics B - Proceedings Supplements*, 138, 2005, pp. 59–64, URL https://www.sciencedirect.com/science/article/pii/S0920563204005791, proceedings of the Eighth International Workshop on Topics in Astroparticle and Undeground Physics. 107

[38] D. S. Akerib, et al., "First Results from the Cryogenic Dark Matter Search in the Soudan Underground Laboratory", *Phys Rev Lett*, 93, 2004, p. 211301, URL https://link.aps.org/doi/10.1103/PhysRevLett.93.211301. 107

[39] S. Cebrián, et al., "First results of the ROSEBUD dark matter experiment", *Astroparticle Physics*, 15(1), 2001, pp. 79–85, URL https://www.sciencedirect.com/science/article/pii/S0927650500001389. 106

[40] Howard E. Haber and Laurel Stephenson Haskins, *Supersymmetric Theory and Models*, chap. 6, pp. 355–499, URL https://www.worldscientific.com/doi/abs/10.1142/9789813233348_0006. 103

[41] G. Chardin, *Dark Matter Direct Detection*, Springer Berlin Heidelberg, Berlin, Heidelberg, 2005, pp. 313–357, URL https://doi.org/10.1007/10933596_7. 103

[42] Erik Heinz, et al., "Toward high-sensitivity and high-resolution submillimeter-wave video imaging", *Optical Engineering*, 50(11), 2011, pp. 1 – 9, URL https://doi.org/10.1117/1.3654089. 95

[43] S. J. Smith, et al., "Toward 100,000-Pixel Microcalorimeter Arrays Using Multi-absorber Transition-Edge Sensors", *Journal of Low Temperature Physics*, 199(1), 2020, pp. 330–338, URL https://doi.org/10.1007/s10909-020-02362-0. 17

[44] Juha Hassel, et al., "Bolometric kinetic inductance detector technology for sub-millimeter radiometric imaging", in *Millimetre Wave and Terahertz Sensors and Technology VIII*, edited by Neil A. Salmon and Eddie L. Jacobs, International Society for Optics and Photonics, SPIE, 2015, vol. 9651, pp. 101 – 107, URL https://doi.org/10.1117/12.2197522. 95

*This project has received funding from the European Union 's Horizon 2020 research and innovation programme under grant agreement No 800923.*

[45] Norbert Palka, et al., "THz Screening for Civil and Military Security", in *THz and Security Applications*, edited by Carlo Corsi and Fedir Sizov, Springer Netherlands, Dordrecht, 2014, pp. 211–228. 94

[46] Samira Mansourzadeh, et al., "High-Power Lensless THz Imaging of Hidden Objects", *IEEE Access*, 9, 2021, pp. 6268–6276. 94

[47] J Du, et al., "A cryogen-free HTS Josephson junction detector for terahertz imaging", *Superconductor Science and Technology*, 28(8), 2015, p. 084001, URL https://doi.org/10.1088/0953-2048/28/8/084001. 32, 95

[48] A. V. Gordeeva, et al., "Record electron self-cooling in cold-electron bolometers with a hybrid superconductor-ferromagnetic nanoabsorber and traps", *Scientific Reports*, 10(1), 2020, p. 21961, URL https://doi.org/10.1038/s41598-020-78869-z. 30

[49] Leonid Kuzmin, "Superconducting cold-electron bolometer with proximity traps", *Microelectronic Engineering*, 69(2), 2003, pp. 309–316, URL https://www.sciencedirect.com/science/article/pii/S0167931703003149, proceedings of the Symposium and Summer School on: Nano and Giga Challenges in Microelectronics Research and Opportunities in Russia. 30

[50] Dmitri Golubev and Leonid Kuzmin, "Nonequilibrium theory of a hot-electron bolometer with normal metal-insulator-superconductor tunnel junction", *Journal of Applied Physics*, 89(11), 2001, pp. 6464–6472, URL https://doi.org/10.1063/1.1351002. 30

[51] Michael Tarasov and Leonid Kuzmin, "Normal Metal Cold-Electron Bolometer: Response, Noise, and Electron Cooling", in *Molecular Nanowires and Other Quantum Objects*, edited by Alexandre S. Alexandrov, et al., Springer Netherlands, Dordrecht, 2004, pp. 393–404. 30

[52] Leonid Kuzmin, et al., "Superconducting Cold-Electron Bolometers with JFET Readout for OLIMPO Balloon Telescope", *Journal of Physics: Conference Series*, 43, 2006, pp. 1298–1302, URL https://doi.org/10.1088/1742-6596/43/1/317. 30

[53] A. Kalabukhov, et al., "SQUID femtoamperemeter with cryogenic transformer for bolometer readout", , 2003. 30

*This project has received funding from the European Union´s Horizon 2020 research and innovation programme under grant agreement No 800923.*

[54] A. N. Vystavkin, "Comparison of Two Types of Andreev Reflection Hot-Electron Microbolometer for Submillimeter Radio Astronomy", in *Proceedings of the Eleventh International Symposium on Space Terahertz Technology,*, University of Michigan Solid-State Electronics Laboratory., 2000, p. 197. 30

[55] A Luukanen, et al., "Applications of superconducting bolometers in security imaging", *Journal of Physics: Conference Series*, 400(5), 2012, p. 052018, URL https://doi.org/10.1088/1742-6596/400/5/052018. 94

[56] S S Dhillon, et al., "The 2017 terahertz science and technology roadmap", *Journal of Physics D: Applied Physics*, 50(4), 2017, p. 043001, URL https://doi.org/10.1088/1361-6463/50/4/043001. 75

[57] V.P. Wallace, et al., "Terahertz pulsed imaging of basal cell carcinoma ex vivo and in vivo", *British Journal of Dermatology*, 151(2), 2004, pp. 424–432, URL https://onlinelibrary.wiley.com/doi/abs/10.1111/j.1365-2133.2004.06129.x. 90

[58] T May, et al., "Next generation of a sub-millimetre wave security camera utilising superconducting detectors", *Journal of Instrumentation*, 8(01), 2013, pp. P01014–P01014, URL https://doi.org/10.1088/1748-0221/8/01/p01014. 94

[59] Leili Afsah-Hejri, et al., "A Comprehensive Review on Food Applications of Terahertz Spectroscopy and Imaging", *Comprehensive Reviews in Food Science and Food Safety*, 18(5), 2019, pp. 1563–1621, URL https://onlinelibrary.wiley.com/doi/abs/10.1111/1541-4337.12490. 87

[60] Proceedings of the Conference on Lasers and Electro-Optics (CLEO) and Quantum Electronics and Laser Science Conference (QELS), 2010, *High-Rate Quantum Key Distribution with Superconducting Nanowire Single Photon Detectors*, Institute of Electrical and Electronics Engineers (IEEE), 2010. 67

[61] T. Honjo, et al., "Long-distance entanglement-based quantum key distribution over optical fiber", *Opt Express*, 16(23), 2008, pp. 19118–19126, URL http://www.opticsexpress.org/abstract.cfm?URI=oe-16-23-19118. 67

[62] D Stucki, et al., "High rate, long-distance quantum key distribution over 250 km of ultra low loss fibres", *New Journal of Physics*, 11(7), 2009, p. 075003, URL https://doi.org/10.1088/1367-2630/11/7/075003. 67

*This project has received funding from the European Union 's Horizon 2020 research and innovation programme under grant agreement No 800923.*

[63] Matthäus Halder, et al., "Entangling independent photons by time measurement", *Nature Physics*, 3(10), 2007, pp. 692–695, URL https://doi.org/10.1038/nphys700. 67

[64] Devin H. Smith, et al., "Conclusive quantum steering with superconducting transition-edge sensors", *Nature Communications*, 3(1), 2012, p. 625, URL https://doi.org/10.1038/ncomms1628. 67

[65] Thomas Gerrits, et al., *Superconducting Transition Edge Sensors for Quantum Optics*, Springer, Berlin, -1, 2015, URL https://tsapps.nist.gov/publication/get_pdf.cfm?pub_id=917980. 67

[66] Jens Neu and Charles A. Schmuttenmaer, "Tutorial: An introduction to terahertz time domain spectroscopy (THz-TDS)", *Journal of Applied Physics*, 124(23), 2018, p. 231101, URL https://doi.org/10.1063/1.5047659. 73

[67] Wei Zhang, et al., "Recent Developments in Spectroscopic Techniques for the Detection of Explosives", *Materials (Basel, Switzerland)*, 11(8), 2018, p. 1364, URL https://pubmed.ncbi.nlm.nih.gov/30082670. 94

[68] Hiromichi Hoshina, et al., "Noninvasive Mail Inspection System with Terahertz Radiation", *Applied Spectroscopy*, 63(1), 2009, pp. 81–86, URL https://doi.org/10.1366/000370209787169713, pMID: 19146722. 94

[69] Pütz, P., et al., "Terahertz hot electron bolometer waveguide mixers for GREAT", *A&A*, 542, 2012, p. L2, URL https://doi.org/10.1051/0004-6361/201218916. 19

[70] M. Shcherbatenko, et al., "Nonequilibrium interpretation of DC properties of NbN superconducting hot electron bolometers", *Applied Physics Letters*, 109(13), 2016, p. 132602, URL https://doi.org/10.1063/1.4963691. 18, 19

[71] Denis Büchel, et al., "4.7-THz Superconducting Hot Electron Bolometer Waveguide Mixer", *IEEE Transactions on Terahertz Science and Technology*, 5(2), 2015, pp. 207–214. 19

[72] de Graauw, Th., et al., "The Herschel-Heterodyne Instrument for the Far-Infrared (HIFI)*", *A&A*, 518, 2010, p. L6, URL https://doi.org/10.1051/0004-6361/201014698. 19

[73] A Shurakov, et al., "Superconducting hot-electron bolometer: from the discovery of hot-electron phenomena to practical

*This project has received funding from the European Union´s Horizon 2020 research and innovation programme under grant agreement No 800923.*

applications", *Superconductor Science and Technology*, 29(2), 2015, p. 023001, URL https://doi.org/10.1088/0953-2048/29/2/023001. 18

[74] Anthony D. Turner, et al., "Silicon nitride micromesh bolometer array for submillimeter astrophysics", *Appl Opt*, 40(28), 2001, pp. 4921–4932, URL http://ao.osa.org/abstract.cfm?URI=ao-40-28-4921. 55

[75] P. L. Richards, "Bolometers for infrared and millimeter waves", *Journal of Applied Physics*, 76(1), 1994, pp. 1–24, URL https://doi.org/10.1063/1.357128. 55

[76] J.C. Webber and M.W. Pospieszalski, "Microwave instrumentation for radio astronomy", *IEEE Transactions on Microwave Theory and Techniques*, 50(3), 2002, pp. 986–995. 55

[77] F. Sizov, "THz radiation sensors", 18(1), 2010, pp. 10–36, URL https://doi.org/10.2478/s11772-009-0029-4. 73

[78] R A Lewis, "A review of terahertz detectors", *Journal of Physics D: Applied Physics*, 52(43), 2019, p. 433001, URL https://doi.org/10.1088/1361-6463/ab31d5. 73

[79] Hai-Bo Liu, et al., "Terahertz Spectroscopy and Imaging for Defense and Security Applications", *Proceedings of the IEEE*, 95(8), 2007, pp. 1514–1527. 94

[80] *International Migration 2019: Report (ST/ESA/SER.A/438).*, Tech. rep., United Nations, Department of Economic and Social Affairs, Population Division, 2019. 91

[81] *European Union Terroris Situation and Trend Report 2020*, Tech. rep., EUROPOL, 2020. 91

[82] Ruth Wasem, et al., "Border Security: Inspections Practices, Policies, and Issues", , 2004, p. 69. 91

[83] John F Federici, et al., "THz imaging and sensing for security applications—explosives, weapons and drugs", *Semiconductor Science and Technology*, 20(7), 2005, pp. S266–S280, URL https://doi.org/10.1088/0268-1242/20/7/018. 93

[84] J. Trontelj and A. Sešek, "Electronic terahertz imaging for security applications", in *Terahertz, RF, Millimeter, and Submillimeter-Wave Technology and Applications IX*, edited by Laurence P. Sadwick and Tianxin Yang, International Society for Optics and Photonics, SPIE, 2016, vol. 9747, pp. 161 – 166, URL https://doi.org/10.1117/12.2217574. 94

*This project has received funding from the European Union 's Horizon 2020 research and innovation programme under grant agreement No 800923.*

[85] B. S.-Y. Ung, et al., "Towards quality control of food using terahertz", in *BioMEMS and Nanotechnology III*, edited by Dan V. Nicolau, et al., International Society for Optics and Photonics, SPIE, 2007, vol. 6799, pp. 380 – 383, URL https://doi.org/10.1117/12.759825. 87

[86] Yan Peng, et al., "Terahertz spectroscopy in biomedical field: a review on signal-to-noise ratio improvement", *PhotoniX*, 1(1), 2020, p. 12, URL https://doi.org/10.1186/s43074-020-00011-z. 90

[87] I Hosako and N Oda, "Terahertz imaging for detection or diagnosis", . 90

[88] Nagendra Paradad Yadav, et al., "Diagnosis of dental problem by using terahertz technology", *Journal of Electronic Science and Technology*, 2021, p. 100082, URL https://www.sciencedirect.com/science/article/pii/S1674862X21000033. 89

[89] Zohreh Vafapour, et al., "The potential of terahertz sensing for cancer diagnosis", *Heliyon*, 6(12), 2020, p. e05623, URL https://www.sciencedirect.com/science/article/pii/S240584402032466X. 89

[90] Young Bin Ji, et al., "A miniaturized fiber-coupled terahertz endoscope system", *Opt Express*, 17(19), 2009, pp. 17082–17087, URL http://www.opticsexpress.org/abstract.cfm?URI=oe-17-19-17082. 89

[91] Moumita Dutta, et al., "THz Imaging of Skin Burn: Seeing the Unseen-An Overview", *Advances in wound care*, 5(8), 2016, pp. 338–348, URL https://pubmed.ncbi.nlm.nih.gov/27602253. 89

[92] Nick Rothbart, et al., "Analysis of Human Breath by Millimeter-Wave/Terahertz Spectroscopy", *Sensors*, 19(12), 2019, URL https://www.mdpi.com/1424-8220/19/12/2719. 88

[93] Shuting Fan, et al., "Use of Terahertz Waves To Monitor Moisture Content in High-Pressure Natural Gas Pipelines", *Energy & Fuels*, 33(9), 2019, pp. 8026–8031, URL https://doi.org/10.1021/acs.energyfuels.9b01112. 87

[94] Li N. Ge, et al., "Optical Characterization of the Principal Hydrocarbon Components in Natural Gas Using Terahertz Spectroscopy", *Energy & Fuels*, 29(3), 2015, pp. 1622–1627, URL https://doi.org/10.1021/ef5028235. 86

*This project has received funding from the European Union 's Horizon 2020 research and innovation programme under grant agreement No 800923.*

[95] Liu Yang, et al., "Toxic chemical compound detection by terahertz spectroscopy: a review", *Reviews in Analytical Chemistry*, 37(3), 2018, p. 20170021, URL https://app.dimensions.ai/details/publication/pub.1104587905andhttps://www.degruyter.com/document/doi/10.1515/revac-2017-0021/pdf. 86

[96] Ryan M. Smith and Mark A. Arnold, "Selectivity of Terahertz Gas-Phase Spectroscopy", *Analytical Chemistry*, 87(21), 2015, pp. 10679–10683, URL https://doi.org/10.1021/acs.analchem.5b03028. 85

[97] Ming Yin, et al., "The application of terahertz spectroscopy to liquid petrochemicals detection: A review", *Applied Spectroscopy Reviews*, 51(5), 2016, pp. 379–396, URL https://doi.org/10.1080/05704928.2016.1141291. 85

[98] Décio Alves-Lima, et al., "Review of Terahertz Pulsed Imaging for Pharmaceutical Film Coating Analysis", *Sensors*, 20(5), 2020, URL https://www.mdpi.com/1424-8220/20/5/1441. 78

[99] Álvaro Cordón, et al., "THz to Inspect Graphene and Thin Film Materials", in *2019 44th International Conference on Infrared, Millimeter, and Terahertz Waves (IRMMW-THz)*, 2019, pp. 1–2. 84

[100] A. J. Huber, et al., "Terahertz Near-Field Nanoscopy of Mobile Carriers in Single Semiconductor Nanodevices", *Nano Letters*, 8(11), 2008, pp. 3766–3770, URL https://doi.org/10.1021/nl802086x. 83

[101] Masatsugu Yamashita, et al., "THz emission characteristics from p/n junctions with metal lines under non-bias conditions for LSI failure analysis", *Opt Express*, 19(11), 2011, pp. 10864–10873, URL http://www.opticsexpress.org/abstract.cfm?URI=oe-19-11-10864. 82

[102] Kiarash Ahi, et al., "Quality control and authentication of packaged integrated circuits using enhanced-spatial-resolution terahertz time-domain spectroscopy and imaging", *Optics and Lasers in Engineering*, 104, 2018, pp. 274–284, URL https://www.sciencedirect.com/science/article/pii/S0143816617303913, optical Tools for Metrology, Imaging and Diagnostics. 83

[103] L. Liebelt, et al., "Influence of bandwidth and dynamic range on thickness determination using terahertz time-domain spectroscopy", in *2019 44th International Conference on Infrared, Millimeter, and Terahertz Waves (IRMMW-THz)*, 2019, pp. 1–2. 77

*This project has received funding from the European Union 's Horizon 2020 research and innovation programme under grant agreement No 800923.*

[104] Bernd M. Fischer, et al., "Investigating Material Characteristics and Morphology of Polymers Using Terahertz Technologies", *IEEE Transactions on Terahertz Science and Technology*, 3(3), 2013, pp. 259–268. 76

[105] David Zimdars, et al., "Technology and Applications of Terahertz Imaging NonâDestructive Examination: Inspection of Space Shuttle Sprayed On Foam Insulation", *AIP Conference Proceedings*, 760(1), 2005, pp. 570–577, URL https://aip.scitation.org/doi/abs/10.1063/1.1916726. 77

[106] Antonio D. Córcoles, et al., "Challenges and Opportunities of Near-Term Quantum Computing Systems", *Proceedings of the IEEE*, 108(8), 2020, pp. 1338–1352. 64

[107] John M. Martinis, "Saving superconducting quantum processors from qubit decay and correlated errors generated by gamma and cosmic rays", . 69

[108] J. Orrell and B. Loer, "Sensor-assisted fault mitigation in quantum computation", , 2020. 69

[109] Evan D. Walsh, et al., "Josephson junction infrared single-photon detector", *Science*, 372(6540), 2021, pp. 409–412, URL https://science.sciencemag.org/content/372/6540/409. 32

[110] Antti P. Vepsäläinen, et al., "Impact of ionizing radiation on superconducting qubit coherence", *Nature*, 584(7822), 2020, pp. 551–556, URL https://doi.org/10.1038/s41586-020-2619-8. 68, 69

[111] Hua-Lei Yin, et al., "Measurement-Device-Independent Quantum Key Distribution Over a 404 km Optical Fiber", *Phys Rev Lett*, 117, 2016, p. 190501, URL https://link.aps.org/doi/10.1103/PhysRevLett.117.190501. 65

[112] Marc Schumann, "Direct detection of WIMP dark matter: concepts and status", *Journal of Physics G: Nuclear and Particle Physics*, 46(10), 2019, p. 103003, URL https://doi.org/10.1088/1361-6471/ab2ea5. 106

[113] M. A. Diagne, et al., "Integrated array of 2-$\mu$m antimonide-based single-photon counting devices", *Opt Express*, 19(5), 2011, pp. 4210–4216, URL http://www.opticsexpress.org/abstract.cfm?URI=oe-19-5-4210. 97

[114] Aongus McCarthy, et al., "Kilometer-range, high resolution depth imaging via 1560 nm wavelength single-photon detection", *Opt Express*, 21(7), 2013, pp. 8904–8915, URL http:

*This project has received funding from the European Union 's Horizon 2020 research and innovation programme under grant agreement No 800923.*

//www.opticsexpress.org/abstract.cfm?URI=oe-21-7-8904. 96, 97

[115] Don M. Boroson and Bryan S. Robinson, *The Lunar Laser Communication Demonstration: NASA's First Step Toward Very High Data Rate Support of Science and Exploration Missions*, Springer International Publishing, Cham, 2015, pp. 115–128, URL https://doi.org/10.1007/978-3-319-18717-4_6. 99

[116] Lixing You, et al., "Superconducting nanowire single photon detection system for space applications", *Opt Express*, 26(3), 2018, pp. 2965–2971, URL http://www.opticsexpress.org/abstract.cfm?URI=oe-26-3-2965. 101

[117] Matthew Shaw, et al., "Superconducting nanowire single photon detectors for deep space optical communication (Conference Presentation)", in *Free-Space Laser Communication and Atmospheric Propagation XXIX*, edited by Hamid Hemmati and Don M. Boroson, International Society for Optics and Photonics, SPIE, 2017, vol. 10096, pp. 145 – 145, URL https://doi.org/10.1117/12.2255836. 101

[118] Nathan R Gemmell, et al., "A miniaturized 4 K platform for superconducting infrared photon counting detectors", *Superconductor Science and Technology*, 30(11), 2017, p. 11LT01, URL https://doi.org/10.1088/1361-6668/aa8ac7. 98, 101

[119] Hamid Hemmati, et al., "Deep-Space Optical Communications: Future Perspectives and Applications", *Proceedings of the IEEE*, 99(11), 2011, pp. 2020–2039. 99

[120] E.G.P. O'Connor, et al., "Energy-sensitive detectors for astronomy: Past, present and future", *New Astronomy Reviews*, 87, 2019, p. 101526, URL https://www.sciencedirect.com/science/article/pii/S1387647320300038. 126

[121] B.A. Mazin, *Kinetic Inductance Detectors*, Ph.D. thesis, California Institute of Technology, 2004. 26

[122] Peter W. A. Roming, et al., "Scaling Kinetic Inductance Detectors (KIDs)", in *2018 IEEE Aerospace Conference*, 2018, pp. 1–11. 23

[123] Artem Kuzmin, et al., "Terahertz Transition-Edge Sensor With Kinetic-Inductance Amplifier at 4.2 K", *IEEE Transactions on Terahertz Science and Technology*, 8(6), 2018, pp. 622–629. 17

[124] D Salvoni, et al., "Lidar techniques for a SNSPD-based measurement", *Journal of Physics: Conference Series*, 1182, 2019, p.

*This project has received funding from the European Union 's Horizon 2020 research and innovation programme under grant agreement No 800923.*

012014, URL https://doi.org/10.1088/1742-6596/1182/1/012014. 97

[125] Hao Li, et al., "Superconducting nanowire single photon detector at 532 nm and demonstration in satellite laser ranging", *Opt Express*, 24(4), 2016, pp. 3535–3542, URL http://www.opticsexpress.org/abstract.cfm?URI=oe-24-4-3535. 97

[126] Jiang Zhu, et al., "Demonstration of measuring sea fog with an SNSPD-based Lidar system", *Scientific Reports*, 7(1), 2017, p. 15113, URL https://doi.org/10.1038/s41598-017-15429-y. 97

[127] Li Xue, et al., "Satellite laser ranging using superconducting nanowire single-photon detectors at 1064  nm wavelength", *Opt Lett*, 41(16), 2016, pp. 3848–3851, URL http://ol.osa.org/abstract.cfm?URI=ol-41-16-3848. 97

[128] O. Novotný, et al., "Cryogenic micro-calorimeters for mass spectrometric identification of neutral molecules and molecular fragments", *Journal of Applied Physics*, 118(10), 2015, p. 104503, URL https://doi.org/10.1063/1.4930036. 28

[129] D. Gray, et al., "The First Tests of a Large-Area Light Detector Equipped with Metallic Magnetic Calorimeters for Scintillating Bolometers for the LUMINEU Neutrinoless Double Beta Decay Search", *Journal of Low Temperature Physics*, 184(3), 2016, pp. 904–909, URL https://doi.org/10.1007/s10909-016-1535-7. 28

[130] L. Gastaldo, et al., "The Electron Capture $$^{163}$$Ho Experiment ECHo", *Journal of Low Temperature Physics*, 176(5), 2014, pp. 876–884, URL https://doi.org/10.1007/s10909-014-1187-4. 28

[131] M. Loidl, et al., "Metallic Magnetic Calorimeters for Absolute Activity Measurement", *Journal of Low Temperature Physics*, 151(3), 2008, pp. 1055–1060, URL https://doi.org/10.1007/s10909-008-9793-7. 28

[132] C. R. Bates, et al., "Development of MMC Gamma Detectors for Nuclear Analysis", *Journal of Low Temperature Physics*, 176(5), 2014, pp. 631–636, URL https://doi.org/10.1007/s10909-013-1063-7. 28

[133] D Hengstler, et al., "Towards FAIR: first measurements of metallic magnetic calorimeters for high-resolution x-ray spec-

*This project has received funding from the European Union 's Horizon 2020 research and innovation programme under grant agreement No 800923.*

troscopy at GSI", *Physica Scripta*, T166, 2015, p. 014054, URL https://doi.org/10.1088/0031-8949/2015/t166/014054. 28

[134] Pretzl1990, "Superconducting Granule Detectors", *Particle World*, 1(6), 1990, pp. 153–162. 32

[135] Andrew Blaikie, et al., "A fast and sensitive room-temperature graphene nanomechanical bolometer", *Nature Communications*, 10(1), 2019, p. 4726, URL https://doi.org/10.1038/s41467-019-12562-2. 31

[136] J. Hubmayr, et al., "Photon-noise limited sensitivity in titanium nitride kinetic inductance detectors", *Applied Physics Letters*, 106(7), 2015, p. 073505, URL https://doi.org/10.1063/1.4913418. 24

[137] S. Doyle, "An overview of Kinetic Inductance Detectors and applications.", URL http://www.astro.cardiff.ac.uk/~spxsmd/KIDs_Lecture_for_Dan.pdf. 125

[138] "An Introduction to Kinetic Inductance Detectors", URL http://www-ecole-drtbt.grenoble.cnrs.fr/userfiles/file/drtbt2012/Introduction_to_KIDs_DRTBT_2012.pdf. 26

[139] P. D. Mauskopf, "Transition Edge Sensors and Kinetic Inductance Detectors in Astronomical Instruments", *Publications of the Astronomical Society of the Pacific*, 130(990), 2018, pp. 1–28, URL https://www.jstor.org/stable/26660634. 15, 26

[140] Naohito Yoshioka, et al., "Current-Biased Kinetic Inductance Detector Using $MgB_2$ Nanowires for Detecting Neutrons", *IEEE Transactions on Applied Superconductivity*, 23(3), 2013, pp. 2400604–2400604. 25

[141] S. Doyle, et al., "Lumped Element Kinetic Inductance Detectors", *Journal of Low Temperature Physics*, 151(1), 2008, pp. 530–536, URL https://doi.org/10.1007/s10909-007-9685-2. 25

[142] B. A. Steinbach, et al., "Thermal Kinetic Inductance Detectors for Ground-Based Millimeter-Wave Cosmology", *Journal of Low Temperature Physics*, 193(3), 2018, pp. 88–95, URL https://doi.org/10.1007/s10909-018-2016-y. 25

[143] Benjamin A. Mazin, et al., "A Position sensitive X-ray spectrophotometer using microwave kinetic inductance detectors", *Appl Phys Lett*, 89, 2006, p. 222507. 24, 27

[144] Liu Wei, et al., "Application of terahertz spectroscopy in biomolecule detection", *Frontiers in Laboratory Medicine*, 2(4), 2018,

*This project has received funding from the European Union´s Horizon 2020 research and innovation programme under grant agreement No 800923.*

pp. 127–133, URL https://www.sciencedirect.com/science/article/pii/S2542364919300111. 80

[145] L. Li, et al., "Quasiparticle nonequilibrium dynamics in a superconducting Ta film", *Journal of Applied Physics*, 93(2), 2003, pp. 1137–1141, URL https://doi.org/10.1063/1.1533106. 24

[146] Peter K. Day, et al., "A broadband superconducting detector suitable for use in large arrays", *Nature*, 425(6960), 2003, pp. 817–821, URL https://doi.org/10.1038/nature02037. 23, 24

[147] Didier D. E. Martin and Peter Verhoeve, "Superconducting tunnel junctions", *ISSI Scientific Reports Series*, 9, 2010, pp. 441–457. 19

[148] K.D. Irwin and G.C. Hilton, *Transition-Edge Sensors*, Springer Berlin Heidelberg, Berlin, Heidelberg, 2005, pp. 63–150, URL https://doi.org/10.1007/10933596_3. 15, 108

[149] J. Uhlig, et al., "High-resolution X-ray emission spectroscopy with transition-edge sensors: present performance and future potential", *Journal of Synchrotron Radiation*, 22(3), 2015, pp. 766–775, URL https://onlinelibrary.wiley.com/doi/abs/10.1107/S1600577515004312. 61, 62

[150] J.N. Ullom, et al., "Transition-Edge Sensor Microcalorimeters for X-ray Beamline Science", *Synchrotron Radiation News*, 27(4), 2014, pp. 24–27, URL https://doi.org/10.1080/08940886.2014.930806. 60

[151] S. Shiki, et al., "X-ray Detection Performance of 100-pixel Superconducting Tunnel Junction Array Detector in the Soft X-ray Region", *Journal of Low Temperature Physics*, 167(5), 2012, pp. 748–753, URL https://doi.org/10.1007/s10909-012-0526-6. 60

[152] Reithmaier G.M., *Superconducting detectors for semiconductor quantum photonics*, Ph.D. thesis, Technischen Universität München, 2015. 14

[153] Brice Calkins, et al., "High quantum-efficiency photon-number-resolving detector for photonic on-chip information processing", *Opt Express*, 21(19), 2013, pp. 22657–22670, URL http://www.opticsexpress.org/abstract.cfm?URI=oe-21-19-22657. 67, 68

[154] Simone Ferrari, et al., "Waveguide-integrated single- and multi-photon detection at telecom wavelengths using superconducting nanowires", *Applied Physics Letters*, 106(15), 2015, p. 151101, URL https://doi.org/10.1063/1.4917166. 68

*This project has received funding from the European Union´s Horizon 2020 research and innovation programme under grant agreement No 800923.*

[155] Victor V Samedov, "Influence of the proximity effect on the energy resolution of STJs", *Nuclear Instruments and Methods in Physics Research Section A: Accelerators, Spectrometers, Detectors and Associated Equipment*, 520(1), 2004, pp. 257–259, URL https://www.sciencedirect.com/science/article/pii/S0168900203032133, proceedings of the 10th International Workshop on Low Temperature Detectors. 122

[156] Joel N Ullom and Douglas A Bennett, "Review of superconducting transition-edge sensors for x-ray and gamma-ray spectroscopy", *Superconductor Science and Technology*, 28(8), 2015, p. 084003, URL https://doi.org/10.1088/0953-2048/28/8/084003. 122

[157] K D Irwin, et al., "Code-division multiplexing of superconducting transition-edge sensor arrays", *Superconductor Science and Technology*, 23(3), 2010, p. 034004, URL https://doi.org/10.1088/0953-2048/23/3/034004. 122

[158] Benjamin A. Mazin, et al., "A superconducting focal plane array for ultraviolet, optical, and near-infrared astrophysics", *Opt Express*, 20(2), 2012, pp. 1503–1511, URL http://www.opticsexpress.org/abstract.cfm?URI=oe-20-2-1503. 27

[159] *ESA SP-1288 Report on the activities of the Research and Scientific Support Department 2003-2004*, Tech. rep., European Space Agency - ESA, 2004. 124

[160] Leaf A. Jiang, et al., "Photon-number-resolving detector with 10 bits of resolution", *Phys Rev A*, 75, 2007, p. 062325, URL https://link.aps.org/doi/10.1103/PhysRevA.75.062325. 123

[161] K. Yamamoto, et al., "Development of Multi-Pixel Photon Counter (MPPC)", in *2007 IEEE Nuclear Science Symposium Conference Record*, 2007, vol. 2, pp. 1511–1515. 123

[162] Edo Waks, et al., "Direct Observation of Nonclassical Photon Statistics in Parametric Down-Conversion", , 92(11), 2004, p. 113602. 123

[163] E. Waks, et al., "High-efficiency photon-number detection for quantum information processing", *IEEE Journal of Selected Topics in Quantum Electronics*, 9(6), 2003, pp. 1502–1511. 123

[164] Guido Zambra, et al., "Counting photoelectrons in the response of a photomultiplier tube to single picosecond light pulses", *Review of Scientific Instruments*, 75(8), 2004, pp. 2762–2765, URL https://doi.org/10.1063/1.1777407. 123

*This project has received funding from the European Union´s Horizon 2020 research and innovation programme under grant agreement No 800923.*

[165] Aaron J. Miller, et al., "Demonstration of a low-noise near-infrared photon counter with multiphoton discrimination", *Applied Physics Letters*, 83(4), 2003, pp. 791–793, URL https://doi.org/10.1063/1.1596723. 123

[166] Danna Rosenberg, et al., "Noise-free high-efficiency photon-number-resolving detectors", *Phys Rev A*, 71, 2005, p. 061803, URL https://link.aps.org/doi/10.1103/PhysRevA.71.061803. 123

[167] B. E. Kardynał, et al., "An avalancheâphotodiode-based photon-number-resolving detector", *Nature Photonics*, 2(7), 2008, pp. 425–428, URL https://doi.org/10.1038/nphoton.2008.101. 123

[168] E. J. Gansen, et al., "Photon-number-discriminating detection using a quantum-dot, optically gated, field-effect transistor", *Nature Photonics*, 1(10), 2007, pp. 585–588, URL https://doi.org/10.1038/nphoton.2007.173. 123

[169] Mikio Fujiwara and Masahide Sasaki, "Direct measurement of photon number statistics at telecom wavelengths using a charge integration photon detector", *Appl Opt*, 46(16), 2007, pp. 3069–3074, URL http://ao.osa.org/abstract.cfm?URI=ao-46-16-3069. 123

[170] Aleksander Divochiy, et al., "Superconducting nanowire photon-number-resolving detector at telecommunication wavelengths", *Nature Photonics*, 2(5), 2008, pp. 302–306, URL https://doi.org/10.1038/nphoton.2008.51. 123

[171] Jan Philipp Höpker, et al., "Integrated transition edge sensors on titanium in-diffused lithium niobate waveguides", *APL Photonics*, 4(5), 2019, p. 056103, URL https://doi.org/10.1063/1.5086276. 65, 68

[172] Robin Cantor and Hideo Naito, "Practical X-ray Spectrometry with Second-Generation Microcalorimeter Detectors", *Microscopy Today*, 20(4), 2012, pp. 38–42. 59

[173] Del Redfern, et al., "The Microcalorimeter for Industrial Applications", *Journal of research of the National Institute of Standards and Technology*, 107(6), 2002, pp. 621–626, URL https://pubmed.ncbi.nlm.nih.gov/27446756. 59

[174] D. A. WOLLMAN, et al., "High-resolution, energy-dispersive microcalorimeter spectrometer for X-ray microanalysis", *Journal of Microscopy*, 188(3), 1997, pp. 196–223, URL https:

*This project has received funding from the European Union ´s Horizon 2020 research and innovation programme under grant agreement No 800923.*

//onlinelibrary.wiley.com/doi/abs/10.1046/j.1365-2818.1997.2670824.x. 58, 122

[175] George F. Smoot, "Nobel Lecture: Cosmic microwave background radiation anisotropies: Their discovery and utilization", *Reviews of Modern Physics*, 79(4), 2007, pp. 1349–1379. 54

[176] Andrew S. Hoover, et al., "Measurement of the 240Pu/239Pu Mass Ratio Using a Transition-Edge-Sensor Microcalorimeter for Total Decay Energy Spectroscopy", *Analytical Chemistry*, 87(7), 2015, pp. 3996–4000, URL https://doi.org/10.1021/acs.analchem.5b00195. 42

[177] V. Merlo, et al., "Superconducting thermal neutron detectors", *Journal of Physics: Conference Series*, 746, 2016, p. 012019, URL https://doi.org/10.1088/1742-6596/746/1/012019. 42

[178] Hiroaki Shishido, et al., "Neutron detection using a current biased kinetic inductance detector", *Applied Physics Letters*, 107(23), 2015, p. 232601, URL https://doi.org/10.1063/1.4937144. 26, 42

[179] M. Loidl, et al., "First measurement of the beta spectrum of 241Pu with a cryogenic detector", *Applied Radiation and Isotopes*, 68(7), 2010, pp. 1454–1458, URL https://www.sciencedirect.com/science/article/pii/S096980430900743X, proceedings of the 17th International Conference on Radionuclide Metrology and its Applications (ICRM 2009). 42

[180] Robert D. Horansky, et al., "Superconducting calorimetric alpha particle sensors for nuclear nonproliferation applications", *Applied Physics Letters*, 93(12), 2008, p. 123504, URL https://doi.org/10.1063/1.2978204. 42

[181] B. Alpert, et al., "HOLMES", *The European Physical Journal C*, 75(3), 2015, p. 112, URL https://doi.org/10.1140/epjc/s10052-015-3329-5. 42

[182] R. Ardito, et al., "The CUORICINO and CUORE double beta decay experiments", *Progress in Particle and Nuclear Physics*, 57(1), 2006, pp. 203–216, URL https://www.sciencedirect.com/science/article/pii/S0146641005001250, international Workshop of Nuclear Physics 27th course. 42

[183] Andrew S. Hoover, et al., "Uncertainty of Plutonium Isotopic Measurements with Microcalorimeter and High-Purity Germanium Detectors", *IEEE Transactions on Nuclear Science*, 61(4), 2014, pp. 2365–2372. 41

*This project has received funding from the European Union´s Horizon 2020 research and innovation programme under grant agreement No 800923.*

[184] Dmitri K. Efetov, et al., "Fast thermal relaxation in cavity-coupled graphene bolometers with a Johnson noise read-out", *Nature Nanotechnology*, 13(9), 2018, pp. 797–801, URL https://doi.org/10.1038/s41565-018-0169-0. 31

[185] S. R. Bandler, et al., "Magnetically Coupled Microcalorimeters", *Journal of Low Temperature Physics*, 167(3), 2012, pp. 254–268, URL https://doi.org/10.1007/s10909-012-0544-4. 28

[186] Sebastian Kempf, et al., "Demonstration of a scalable frequency-domain readout of metallic magnetic calorimeters by means of a microwave SQUID multiplexer", *AIP Advances*, 7(1), 2017, p. 015007, URL https://doi.org/10.1063/1.4973872. 29

[187] Duc T Vo, "FRAMÂŽs Isotopic Uncertainty Analysis.", , 2005, URL https://www.osti.gov/biblio/977985. 40

[188] R. Winkler, et al., "256-pixel microcalorimeter array for high-resolution $\gamma$-ray spectroscopy of mixed-actinide materials", *Nuclear Instruments and Methods in Physics Research Section A: Accelerators, Spectrometers, Detectors and Associated Equipment*, 770, 2015, pp. 203–210, URL https://www.sciencedirect.com/science/article/pii/S0168900214010778. 40

[189] N. Jethava, et al., "Improved Isotopic Analysis With a Large Array of Gamma-Ray Microcalorimeters", *IEEE Transactions on Applied Superconductivity*, 19(3), 2009, pp. 536–539. 40

[190] Taro YAMASHITA, et al., "Recent Progress and Application of Superconducting Nanowire Single-Photon Detectors", *IEICE Transactions on Electronics*, E100.C(3), 2017, pp. 274–282. 21

[191] Martin A. Wolff, et al., "Superconducting nanowire single-photon detectors integrated with tantalum pentoxide waveguides", *Scientific Reports*, 10(1), 2020, p. 17170, URL https://doi.org/10.1038/s41598-020-74426-w. 22

[192] Misael Caloz, et al., "High-detection efficiency and low-timing jitter with amorphous superconducting nanowire single-photon detectors", *Applied Physics Letters*, 112(6), 2018, p. 061103, URL https://doi.org/10.1063/1.5010102. 21

[193] Chandra M. Natarajan, et al., "Superconducting nanowire single-photon detectors: physics and applications", *Supercond Sci Technol*, 25, 2012, p. 063001. 21

[194] Masahiro Ukibe, et al., "Modification of Layer Structures of Superconducting Tunnel Junctions to Improve X-ray Energy

*This project has received funding from the European Union´s Horizon 2020 research and innovation programme under grant agreement No 800923.*

Resolution", *Journal of Low Temperature Physics*, 184(1), 2016, pp. 200–205, URL https://doi.org/10.1007/s10909-016-1488-x. 20

[195] *Anisotropies in the CMB*, 1999. 55

[196] D. C. Moore, et al., "Quasiparticle Trapping in Microwave Kinetic Inductance Strip Detectors", *AIP Conference Proceedings*, 1185(1), 2009, pp. 168–171, URL https://aip.scitation.org/doi/abs/10.1063/1.3292307. 25, 52

[197] R. A. Hijmering, et al., "First results of a cryogenic optical photon-counting imaging spectrometer using a DROID array", , 511, 2010, p. A59. 50

[198] A. Peacock, et al., "Single optical photon detection with a superconducting tunnel junction", *Nature*, 381(6578), 1996, pp. 135–137, URL https://doi.org/10.1038/381135a0. 50

[199] Benjamin A. Mazin, et al., "KRAKENS: a superconducting MKID integral field spectrograph concept for the Keck I telescope", in *Ground-based and Airborne Instrumentation for Astronomy VII*, edited by Christopher J. Evans, et al., International Society for Optics and Photonics, SPIE, 2018, vol. 10702, pp. 108 – 127, URL https://doi.org/10.1117/12.2312221. 52

[200] Kieran O'Brien, et al., "KIDSpec: an MKID based medium resolution integral field spectrograph", in *Ground-based and Airborne Instrumentation for Astronomy V*, edited by Suzanne K. Ramsay, et al., International Society for Optics and Photonics, SPIE, 2014, vol. 9147, pp. 143 – 150, URL https://doi.org/10.1117/12.2056297. 52

[201] Frantz Martinache, et al., "Closed-loop focal plane wavefront control with the SCExAO instrument", , 593, 2016, p. A33. 51, 124

[202] Seth R. Meeker, et al., "DARKNESS: A Microwave Kinetic Inductance Detector Integral Field Spectrograph for High-contrast Astronomy", *PASP*, 130(988), 2018, p. 065001. 51

[203] M. J. Strader, et al., "Excess Optical Enhancement Observed with ARCONS for Early Crab Giant Pulses", , 779(1), 2013, p. L12. 51

[204] J. Schlaerth, et al., "A Millimeter and Submillimeter Kinetic Inductance Detector Camera", *Journal of Low Temperature Physics*, 151(3), 2008, pp. 684–689, URL https://doi.org/10.1007/s10909-008-9728-3. 24, 55

*This project has received funding from the European Union 's Horizon 2020 research and innovation programme under grant agreement No 800923.*

[205] R. Romani, et al., "Phase-resolved Crab Studies with a Cryogenic Transition-Edge Sensor Spectrophotometer", (563), 2001. 49

[206] R. Romani, et al., "First Astronomical Application of a Cryogenic Transition Edge Sensor Spectrophotometer", (521), 1999. 49, 124

[207] Michael Lesser, "A Summary of Charge-Coupled Devices for Astronomy", *Publications of the Astronomical Society of the Pacific*, 127(957), 2015, pp. 1097–1104, URL https://doi.org/10.1086/684054. 49

[208] BA Smith, "Astronomical imaging applications for CCDs Astronomical imaging applications for CCDs", URL https://ntrs.nasa.gov/citations/19770010339. 48

[209] A. Boksenberg, "Performance of the UCL image photon counting system.", in *Auxiliary Instrumentation for Large Telescopes*, 1972, pp. 295–316. 48

[210] W. S. Boyle and G. E. Smith, "Charge Coupled Semiconductor Devices", *Bell System Technical Journal*, 49(4), 1970, pp. 587–593, URL https://onlinelibrary.wiley.com/doi/abs/10.1002/j.1538-7305.1970.tb01790.x. 48

[211] Frederick Scott Porter, et al., "The Astro-E2 X-ray spectrometer/EBIT microcalorimeter x-ray spectrometer", *Review of Scientific Instruments*, 75(10), 2004, pp. 3772–3774, URL https://doi.org/10.1063/1.1781758. 47

[212] P. Szypryt, et al., "A transition-edge sensor-based x-ray spectrometer for the study of highly charged ions at the National Institute of Standards and Technology electron beam ion trap", *Review of Scientific Instruments*, 90(12), 2019, p. 123107, URL https://doi.org/10.1063/1.5116717. 47

[213] E. Figueroa-Feliciano, et al., "Update on the Micro-X Sounding Rocket payload", in *Space Telescopes and Instrumentation 2012: Ultraviolet to Gamma Ray*, edited by Tadayuki Takahashi, et al., International Society for Optics and Photonics, SPIE, 2012, vol. 8443, pp. 387 – 403, URL https://doi.org/10.1117/12.927167. 47

[214] Richard L. Kelley, et al., "The Astro-H high resolution soft x-ray spectrometer", in *Space Telescopes and Instrumentation 2016: Ultraviolet to Gamma Ray*, edited by Jan-Willem A. den Herder, et al., International Society for Optics and Photonics, SPIE,

*This project has received funding from the European Union´s Horizon 2020 research and innovation programme under grant agreement No 800923.*

2016, vol. 9905, pp. 229 – 245, URL https://doi.org/10.1117/12.2232509. 47

[215] *Handbook of X-ray Astronomy*, Cambridge Observing Handbooks for Research Astronomers, Cambridge University Press, 2011. 45

[216] J. U. Ness, et al., "Helium-like triplet density diagnostics. Applications to CHANDRA-LETGS X-ray observations of Capella and Procyon", , 367, 2001, pp. 282–296. 45

[217] S. H. Moseley, et al., "Thermal detectors as xâray spectrometers", *Journal of Applied Physics*, 56(5), 1984, pp. 1257–1262, URL https://doi.org/10.1063/1.334129. 46

[218] Stephan Friedrich, "Nuclear diagnostics with cryogenic spectrometers", *Nuclear Instruments and Methods in Physics Research Section A: Accelerators, Spectrometers, Detectors and Associated Equipment*, 579(1), 2007, pp. 157–160, URL https://www.sciencedirect.com/science/article/pii/S0168900207005992, proceedings of the 11th Symposium on Radiation Measurements and Applications. 38

[219] R. Kouzes, et al., "Naturally occurring radioactive materials in cargo at US borders", *Packaging, Transport, Storage & Security of Radioactive Material*, 17(1), 2006, pp. 11–17, URL https://doi.org/10.1179/174651006X95556. 39

[220] M. K. Bacrania, et al., "Large-Area Microcalorimeter Detectors for Ultra-High-Resolution X-Ray and Gamma-Ray Spectroscopy", *IEEE Transactions on Nuclear Science*, 56(4), 2009, pp. 2299–2302. 39

[221] D. A. Bennett, et al., "A high resolution gamma-ray spectrometer based on superconducting microcalorimeters", *Review of Scientific Instruments*, 83(9), 2012, p. 093113, URL https://doi.org/10.1063/1.4754630. 39

[222] Omid Noroozian, et al., "High-resolution gamma-ray spectroscopy with a microwave-multiplexed transition-edge sensor array", *Applied Physics Letters*, 103(20), 2013, p. 202602, URL https://doi.org/10.1063/1.4829156. 38

[223] W. B. Doriese, et al., "14-pixel, multiplexed array of gamma-ray microcalorimeters with 47eV energy resolution at 103keV", *Applied Physics Letters*, 90(19), 2007, p. 193508, URL https://doi.org/10.1063/1.2738371. 38

*This project has received funding from the European Union 's Horizon 2020 research and innovation programme under grant agreement No 800923.*

[224] M. F. Cunningham, et al., "High-resolution operation of frequency-multiplexed transition-edge photon sensors", *Applied Physics Letters*, 81(1), 2002, pp. 159–161, URL https://doi.org/10.1063/1.1489486. 38

[225] Daniel T. Chow, et al., "High-resolution gamma-ray spectrometers using bulk absorbers coupled to Mo/Cu multilayer superconducting transition-edge sensors", in *Hard X-Ray, Gamma-Ray, and Neutron Detector Physics II*, edited by Ralph B. James and Richard C. Schirato, International Society for Optics and Photonics, SPIE, 2000, vol. 4141, pp. 67 – 75, URL https://doi.org/10.1117/12.407605. 38

[226] Eric H. Silver, et al., "NTD germanium-based microcalorimeters for hard x-ray spectroscopy", in *X-Ray and Gamma-Ray Instrumentation for Astronomy XI*, edited by Kathryn A. Flanagan and Oswald H. W. Siegmund, International Society for Optics and Photonics, SPIE, 2000, vol. 4140, pp. 397 – 401, URL https://doi.org/10.1117/12.409135. 38

[227] Kaixuan Ni, "Dark Matter Direct Detection: A Status Review", URL https://indico.cern.ch/event/782953/contributions/3414267/attachments/1887848/3112634/DarkMatterDetection-Review-DPF2019.pdf. 37

[228] Chiara Brofferio, et al., "Neutrinoless Double Beta Decay Experiments With TeO2 Low-Temperature Detectors", *Frontiers in Physics*, 7, 2019, p. 86, URL https://www.frontiersin.org/article/10.3389/fphy.2019.00086. 37, 104, 106

[229] A. S. Hoover, et al., "Microcalorimeter arrays for ultra-high energy resolution X- and gamma-ray detection", *Journal of Radioanalytical and Nuclear Chemistry*, 282(1), 2009, p. 227, URL https://doi.org/10.1007/s10967-009-0223-3. 37

[230] Micah Zenko, "Intelligence Estimates of Nuclear Terrorism", *The ANNALS of the American Academy of Political and Social Science*, 607(1), 2006, pp. 87–102, URL https://doi.org/10.1177/0002716206290862. 37

[231] Adriana E. Lita, et al., "Counting near-infrared single-photons with 95% efficiency", *Opt Express*, 16(5), 2008, pp. 3032–3040, URL http://www.opticsexpress.org/abstract.cfm?URI=oe-16-5-3032. 16

[232] N Tralshawala, et al., "Design and fabrication of superconducting transition edge X-ray calorimeters", *Nuclear Instruments and Methods in Physics Research Section A: Accelerators, Spectrometers,*

*This project has received funding from the European Union ´s Horizon 2020 research and innovation programme under grant agreement No 800923.*

*Detectors and Associated Equipment*, 444(1), 2000, pp. 188–191, URL https://www.sciencedirect.com/science/article/pii/S0168900299013558. 17

[233] D Rosenberg, et al., "Near-unity absorption of near-infrared light in tungsten films", *Nuclear Instruments and Methods in Physics Research Section A: Accelerators, Spectrometers, Detectors and Associated Equipment*, 520(1), 2004, pp. 537–540, URL https://www.sciencedirect.com/science/article/pii/S0168900203032364, proceedings of the 10th International Workshop on Low Temperature Detectors. 17

[234] J. M. Gildemeister, et al., "A fully lithographed voltage-biased superconducting spiderweb bolometer", *Applied Physics Letters*, 74(6), 1999, pp. 868–870, URL https://doi.org/10.1063/1.123393. 17

[235] M. D. Audley, et al., "Microstrip-coupled TES bolometers for CLOVER", in *Proceedings of the 19th International Symposium on Space Terahertz Technology, ISSTT 2008*, 2008, pp. 124–133, 19th International Symposium on Space Terahertz Technology, ISSTT 2008 ; Conference date: 28-04-2008 Through 30-04-2008. 17

[236] S. M. Stanchfield, et al., "Development of a Microwave SQUID-Multiplexed TES Array for MUSTANG-2", *Journal of Low Temperature Physics*, 184(1), 2016, pp. 460–465, URL https://doi.org/10.1007/s10909-016-1570-4. 16

[237] K. D. Irwin and K. W. Lehnert, "Microwave SQUID multiplexer", *Applied Physics Letters*, 85(11), 2004, pp. 2107–2109, URL https://doi.org/10.1063/1.1791733. 16

[238] M. D. Niemack, et al., "Code-division SQUID multiplexing", *Applied Physics Letters*, 96(16), 2010, p. 163509, URL https://doi.org/10.1063/1.3378772. 16

[239] John Ruhl, et al., "The South Pole Telescope", *Proc SPIE*, 5498, 2004, pp. 11 – 29, URL https://doi.org/10.1117/12.552473. 16

[240] Asad M. Aboobaker, et al., "The EBEX Balloon-borne Experiment—Optics, Receiver, and Polarimetry", *The Astrophysical Journal Supplement Series*, 239(1), 2018, p. 7, URL https://doi.org/10.3847/1538-4365/aae434. 16

[241] Adam L. Woodcraft, et al., "Electrical and optical measurements on the first SCUBA-2 prototype 1280pixel submillimeter superconducting bolometer array", *Review of*

*This project has received funding from the European Union ´s Horizon 2020 research and innovation programme under grant agreement No 800923.*

*Scientific Instruments*, 78(2), 2007, p. 024502, URL https://doi.org/10.1063/1.2436839. 16

[242] J.A Chervenak, et al., "Performance of multiplexed SQUID readout for Cryogenic Sensor Arrays", *Nuclear Instruments and Methods in Physics Research Section A: Accelerators, Spectrometers, Detectors and Associated Equipment*, 444(1), 2000, pp. 107–110, URL https://www.sciencedirect.com/science/article/pii/S016890029901339X. 16

[243] M. K. Maul, et al., "Excess Noise in Superconducting Bolometers", *Phys Rev*, 182, 1969, pp. 522–525, URL https://link.aps.org/doi/10.1103/PhysRev.182.522. 16

[244] K. D. Irwin, "An application of electrothermal feedback for high resolution cryogenic particle detection", *Applied Physics Letters*, 66(15), 1995, pp. 1998–2000, URL https://doi.org/10.1063/1.113674. 16

[245] D. H. Andrews, et al., "Attenuated Superconductors I. For Measuring InfraRed Radiation", *Review of Scientific Instruments*, 13(7), 1942, pp. 281–292, URL https://doi.org/10.1063/1.1770037. 15

*This project has received funding from the European Union 's Horizon 2020 research and innovation programme under grant agreement No 800923.*

# Part II

# Collaborative Platforms

# 8
# *Introduction*

Adoption of a technology as a solution for a given application is a complex process in which the technology will have to be adapted to the constrains imposed by the new environment. New and very useful feedback information will be generated during this period, as it will set guidelines for improving the original concept and focus the new research efforts.

At SUPERTED project we wanted to include the first steps of this process within the project agenda. Once TED technology has been developed through the project, we have planned to make it available for researchers from outside the SUPERTED Consortium, so that they can have a first contact with the technology while having the opportunity to discuss with the partners.

Letting alone the information that such experience can bring, we also see it as an opportunity for establishing new links with research communities whose activity is closer to interesting applications. Hopefully this can eventually consolidate onto collaborations that will help the technology to continue evolving and rise funding for this task.

Unfortunately, making the TED technology available is not straightforward, for a number of reasons:

- The superconductor material require operating temperatures of 10mK, which can only be achieved with deep cryogenics techniques. These are expensive systems (in the range of hundreds of thousands of euros), which are also expensive to run.
- As the demonstrator systems cannot be installed and running indefinitely (due to the stated above), they must be stored disassembled (i.e. the sensor, together with the antennas/absorbers, must be extracted from the cryostat) and stored under controlled conditions which prevent it from being damaged (this could happen because of exposure of the sensor to the atmosphere).
- Development of the technology is still ongoing, and it is still un-

clear if the performance could be enough for testing under the constraints imposed by applications.

Because of this difficulties, we have adopted a mixed approach, which includes two types of activities:

- On the one hand, two different testing set ups will be implemented by partners of the SUPERTED Consortium, thus granting enough resources through the financial planning of the project. One of this set ups, installed at University of Jyväskylä (Finland) will be focused on testing TED technology for detection of X-rays, and the second set up, installed at Institute Néel in Grenoble (France) will be focused on the testing the sensors for detecting radiation in the THz/GHz range.

- On the other hand, we have maintained a series of contacts with different institutions across Europe, and chosen a collaboration that both offered the possibility to develop a potential application where TED technology could gain significance, but also that granted that a number of resources would be committed by the external collaborators, so that the effort was shared. We have found particularly interesting the possibility of collaborating with Dr Francesc Monrabal (current Technical Coordinator of NEXT $0\nu$**fifi** experiment) and the underground facility Laboratorio Subterraneo de Canfranc (LSC, Spain) which have proposed to explore the viability of using TED as the core technology for direct dark matter detection.

All these three opportunities will be discussed in some detail in the following sections. Altogether, they should offer a rather comprehensive sampling of the performance of the TED sensors, as they will be exposed to environments which are very similar to those found in the main applications.

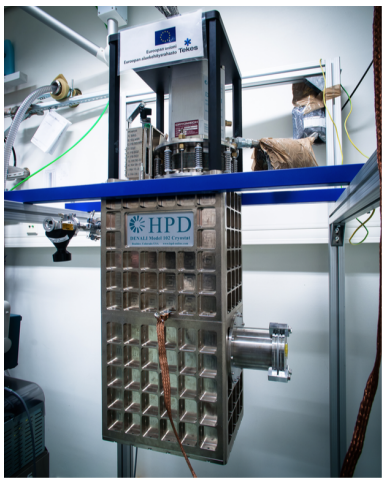


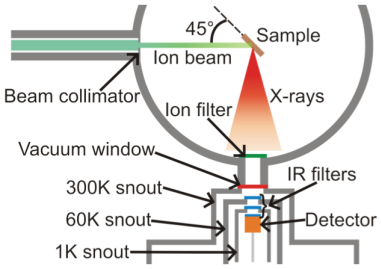


Figure 8.1: **X-ray spectroscopy at University of Jyväskylä:** Sensors are hosted in a cryogen-free pulse tube ADR cryostat, shown on top. Radiation can be guided inside and towards the sample through a window and a series of filters, as shown on the bottom scheme. Alternatively, low activity radiation sources can be placed inside for calibration.

## *8.1 TED applied to X-ray detection at University of Jyväskylä*

The Coordinating partner of SUPERTED project (University of Jyväskylä) has state-of-the-art facilities for Time Resolved X-ray spectroscopy, which already operate using TES. The integration of TED technology in these setup will therefore to directly compare both technologies, and provides a testing environment which corresponds to that of main applications like X-ray and $\gamma-$ray spectroscopies for Nuclear Material Analysis, Beamline Science and Microbeam Analysis (See part I for details). The high-end instruments for such applications are in principle very similar to this testing bench.

*This project has received funding from the European Union´s Horizon 2020 research and innovation programme under grant agreement No 800923.*

The key components of the set up (apart from the sensors) are HPD Denali 102 cryogen-free pulse tube ADR cryostat and a 256 channel multiplexed SQUID readout.

TED sensor will be integrated with absorbers made of either Sn or Au (both are currently under test), and with SQUID read-out.

Calibration of the sensors will be carried out through exposure to radiation from $^{55}Fe$ source, that emits 6 keV photons. Characterization at lower energies will be carried out by interposing crystals (like, for instance, NaCl) between this source and the sensors, in order to generate secondary fluorescent X-rays.

## 8.2 *TED applied to THz/GHz detection at Institut Néel*

Parter CNRS (Institut Néel) has very large experience in the integration of superconducing technologies (TES and KID) into Astrophysics instruments. Several of these systems have been commissioned to Telescopes worldwide, after being assembled and tested at the facilities in Grenoble. These facilities will be used for the testing of the TED sensors.

This provides an interesting environment because the cryostats have ruggedised design (so that they can stand the harsh conditions of high altitude Telescopes) and so the TED technology will be exposed, not only to constraints found in Astrophysics applications, but also to very similar conditions found in any application which requires field- deployment of the system (like, for instance LIDAR, surveillance and inspection in the THz range).

TED sensor will be integrated with meanders and micro-lenses, in order to couple THz/GHz radiation into the sensors. Read-out will be based on iKID concept (3).

Calibration of the sensors will be done using warm sources. If needed, realistic conditions can be achieved using techniques developed for calibration of other types of sensors for telescope instruments. In order to compensate the absence of the telescope optics, a corrective lens is added at the cryostat input window. This lens is creating an image of the focal planes onto a workbench know as Sky Simulator[1], which basically consist on a black disk with the same dimensions as the telescope focal plane, which is cooled down. This cold disk simulates the background temperature in ordinary ground-based observing conditions[2]. A sub-beam- sized, i.e. point-like, warm source, moved in front of the sky simulator by means of an X-Y stage, allows beams shape and array geometry (e.g. pixel-per-pixel pointing) characterisation. The sensitivity is calculated by executing calibrated temperature sweeps of the sky simulator, and measuring the signal-to- noise ratio.

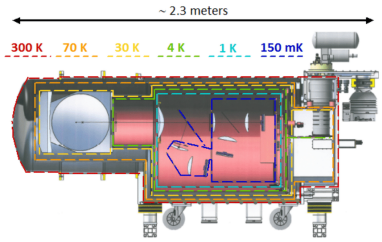


Figure 8.2: **THz/GHz detection at Institut Néel:** Sensors are hosted in cryostats designed for deployment in Telescopes, as the one shown on top. Radiation is guided inside and towards the sample through the different temperature stages using polyethilene (DHPE) lenses.

[1] Details about the Sky Simulator can be found in ref: (4).

[2] On a telescope the main contributions to the background are the atmospheric residual opacity, which is weather depen-dent, and the emissivities of the mirrors.

*This project has received funding from the European Union´s Horizon 2020 research and innovation programme under grant agreement No 800923.*

## 8.3 TED applied to Dark Matter Detection at LSC

In order to explore the possibility of applying TED technology into the frontier-research field of Dark Matter search, we have established a first contact with Dr Francesc Monrabal (Technical Coordinator of NEXT experiment for detection of $0\nu\beta\beta$) and Dr Carlos Peña (Director of LSC underground laboratory at Canfranc, Spain). Both have expressed their interest with letters that are attached at the end of this section. As part of this collaboration LSC has offered some underground space and a cryostat that can host the sensors for the validation tests. We hereby the the chance to thank them for their constructive discussions and support on the development of the collaboration.

As described in section 3.9, several concepts of detectors are currently being explored, from which cryogenic detectors seem an interesting option. These systems consist on a mass of a given crystal, which is monitored in order to detect interactions of these material with WIMPs. The monitoring is done through direct detection of phonons propagating within the crystal and photons resulting either from scintillation and/or Cherenkov radiation. TED, same as other types of superconducting detectors, seem interesting for this tasks, because in principle they can be adapted both for the detection of phonons and photons (a dedicated sensor is devoted to each one of this tasks).

In order to validate the possibility of using TED for this purpose, we intend to carry on a first simple experiment, based on the work initially proposed for testing of TES (2) and which has been used recently for demonstration of most sensitive sensor so far(1). The proposed device acts as a quasiparticle-trap-assisted sensor for phonon-mediated particle detection. The quasiparticle trapping mechanism makes it possible to instrument large surface areas without increasing sensor heat capacity, thus allowing larger absorbers and reducing phonon collection times.

In this intended experiment, TED detector could be built on top of a Si wafer, and coupled to an Al thin film and a network of W lines. Athermal phonons generated by events in the substrate propagate with high efficiency to the Al/substrate interface, where they are either transmitted or reflected. The transmitted phonons break Cooper pairs in the Al creating free, athermal quasiparticles - QPs, which diffuse through the fin from the initial event and towards the FI/S structure of the TED and are drained away through the junction. In principle, the same read-out set up used for detection of X-rays can be used.

Calibration of the device can be carried out at low energies by

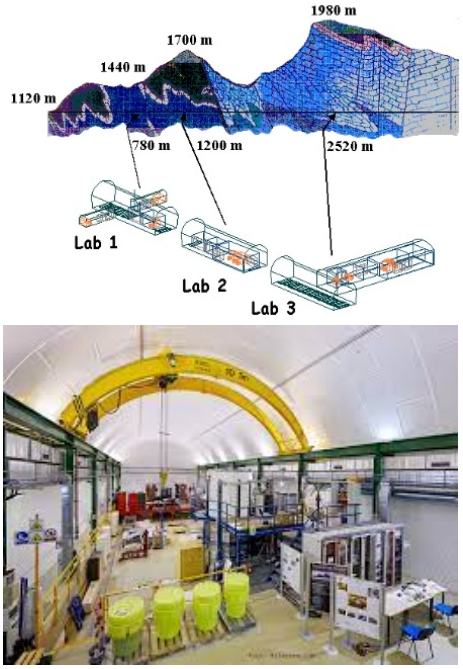


Figure 8.3: **LSC Facilities at Canfranc (Spain).** This underground laboratory is located below Tobazo peak, and was built expanding and old train tunnel between Spain and France. Currently it hosts several experiments for neutrino and dark matter search, among others.


Figure 8.4: **TED for Dark Matter Detection:** The cross section scheme shows the structure of the detector. Phonons (represented by arrows) generated in the Si substrate will eventually generate quasiparticles (represented by yellow spheres) inside an Al thin film. This can be collected through the TED.

*This project has received funding from the European Union´s Horizon 2020 research and innovation programme under grant agreement No 800923.*

exposing the Si substrate to pulsed laser radiation in the visible range (as long as pulse duration will be much shorter than rise time of sensors), and at higher energies by insertion of a radioactive source ($^{55}Fe$ or $^{57}Co$) nearby the device.

*This project has received funding from the European Union ´s Horizon 2020 research and innovation programme under grant agreement No 800923.*

To Whom May it Concern,

I had the chance to learn about the Thermoelectric Detector (TED) which is currently being developed at SUPERTED project, funded under the H2020 program.

Through discussions with Celia Rogero and Francisco Lopez, we came to the conclusion that it would be interesting to test this new sensors for direct detection of Dark Matter. In principle, this area of research is in need of cryogenic sensing technologies capable of reaching energy thresholds below the eV scale and allowing for some scalability.

We would therefore propose to carry on a first validation experiment, using methodology similar to that presented by K. Irwin et al in Rev. Sci. Instrum. 66 (II), November 1995; for the case of TES technology, and which is still the basis of work for calibration purposes.

This experiment will be carried on at the underground facilities of Laboratorio Subterráneo de Canfranc (LSC) where we have been granted access to a 10 mK dilution refrigerator.

We are looking forward to initiate this interesting collaboration.

Sincerely,

Frances Monrabal Capilla
Ikerbasque Research Fellow
Technical Coordinator NEXT experiment

*This project has received funding from the European Union´s Horizon 2020 research and innovation programme under grant agreement No 800923.*

Canfranc-Estación on May 27th, 2021,

The Laboratorio Subterráneo de Canfranc (LSC) is one of the Spanish National Research and Technology Installations, a modern 1600 square metres space which is the second largest deep underground laboratory in Europe. As a Director of the LSC, I hereby underline the strongest interest of the LSC in hosting the new dark matter direct detection experiment proposed by the SUPERTED consortium and based on new TED technologies which would require access to a 10 mK dilution refrigerator.

The search for rare events produced by dark matter or neutrino interactions, one of the most important research and technology areas in physics, requires the access to underground facilities with much reduced cosmic radiation. The LSC is equipped with several services which can be used by the collaboration like the clean room, the HPGe gamma spectrometers and the radon abatement system. The underground lab hosts a 10 mK dilution refrigerator housing the CROSS experiment scintillating bolometers and is purchasing another 10 mK dilution refrigerator for new experiments. The LSC agrees on supporting without charges the electrical power, nitrogen and radon-free air. Moreover, the LSC offers office space and meeting rooms that will be available to the researchers and engineers working at the LSC.

I look forward to receiving great news from the SUPERTED consortium and having the budget approved to come to the LSC.

Sincerely,

Carlos Peña Garay
Director
Laboratorio Subterráneo de Canfranc

*This project has received funding from the European Union´s Horizon 2020 research and innovation programme under grant agreement No 800923.*

# 9
# *Conclusions*

The TED technology will be demonstrated by its first time in the SUPERTED project. During this period, the core of the activity is focused in overcoming the many technical challenges, but we also find it very important to rise awareness and take the technology to testing grounds where it can be presented to researchers from outside of SUPERTED Consortium. In order to grant the success of this task, this activity has been included as part of the agenda of the project.

Two testing sites will be set up during the project lifetime by partners of the Consortium. One of the (at University of Jyväskylä) will be devoted to detection of X-radiation. The second one (at Institute Néel) will focus on detection of radiation in the THz/GHz range.

It is important to outline that both facilities indeed correspond to real environments (as opposed to experiments built on purpose for testing the TED technology only). The Cryogenic X-ray spectrometer set up at University of Jyväskylä is an instrument analogue to those found in beamline science, microbeam analysis and nuclear material analysis environments. The THz/GHz testing workbenches at Institute Néel are equipped with rugged cryostats which are used for testing instruments for astrophysics experiments, and then deployed in the observation sites.

A third and complementary approach has been to establish an external collaboration, for directly linking with new research groups and applications. We have decided to consolidate a collaboration focused on the detection of dark matter. The reasons for this choice are: 1) that through this collaboration we were granted access to underground facilities and cryostat equipment, and 2) that this is a challenging frontier research area.

Altogether, these three opportunities will expose the TED technology to relevant operating constrains, helping to expose both its strength and vulnerabilities. At the same time, it will allow to rise its profile among research communities whose interest in the technology can be determining for approaching it towards the applications.

# 10
# Bibliography


[1] R. Ren, et al., "Design and Characterization of a Phonon-Mediated Cryogenic Particle Detector with an eV-Scale Threshold and 100 keV-Scale Dynamic Range", , 2021. 160

[2] K. D. Irwin, et al., "A quasiparticleâtrapâassisted transitionâedge sensor for phononâmediated particle detection", *Review of Scientific Instruments*, 66(11), 1995, pp. 5322–5326, URL https://doi.org/10.1063/1.1146105. 160

[3] A. Kher, et al., "Kinetic Inductance Parametric Up-Converter", *Journal of Low Temperature Physics*, 184(1), 2016, pp. 480–485, URL https://doi.org/10.1007/s10909-015-1364-0. 159

[4] A. Monfardini, et al., "A dual-band millimeter-wave kinetic inductance camera for the IRAM 30-meter telescope", *The Astrophysical Journal Supplement Series*, 194(2), 2011, p. 24, URL https://doi.org/10.1088/0067-0049/194/2/24. 159

# Part III

# Management of Technology Transfer

# 11
# *Introduction*

European Commission Framework Programs have established themselves as a powerful tool, providing solid funding coverage and promoting large multidisciplinary collaborations that would probably not be possible to establish otherwise. The outcome of such activity is advanced knowledge and technologies. Paradoxically, this may increase the difficulty of the next step (the transfer of these knowledge for its exploitation).

There are two sources of this difficulty:

- The project consortiums are powerful workgroups that put together world-class research units of very different backgrounds in a collaborative mode. All their skills, background knowledge and cutting-edge infrastructures are put to the service of developing the new (foreground) knowledge. For any actor interested in exploiting these results, and specially if it is an small player (i.e. start-up company), it becomes a real challenge even to put together the resources required to reproduce the results once more (as a starting point for, for instance, an industrialisation process).

- Since Consortiums are relatively large heterogeneous groups (of academic and industrial partners), and even if the rules for management of the intellectual property are clear, any third party interested in exploiting the results will face engaging negotiations with several partners, who may have very different interests and objectives when licensing technology. Time consumed by these negotiations is an important and critical factor, specially if patents are involved, since the patenting process eventually demands large investments.

Because of this vulnerabilities, in SUPERTED project we have considered necessary to have a proactive approach, both in organising and promoting the transfer of the technology. The ongoing state of these activities is listed in the upcoming sections.

## 11.1 Organisation of the Technology Transfer.

The TED sensing technology has required many advances in different fields, which can, in first approach, be classified as follows:

- **Material Fabrication:** The TED technologies deeply relies in the manufacturing of layered structures at the nano-scale, comprising Ferromagnetic Insulating and Superconducting materials. The fabrication of these materials (and their interfaces) with enough quality is far from trivial, and has constituted a major achievement of this project.
- **Sensor Design :** The structure of the sensor (form factor, geometrical dimensions of the layered materials, etc) which is ultimately underpinned by the physics governing the device, has been optimised through iterative modelling and experimental characterisation.
- **X-ray Coupling :** Adaptation of the device for detection on the X-ray range requires design of appropriate absorbers and means of coupling them to the sensor.
- **X-ray read-out :** Design of the different stages of electronics used for extracting the signal from the sensor (inside the cryostat) to the amplification stages (at room temperature).
- **THz/GHz coupling:** Adaptation of the device for detection on the THz/GHz range requires design of appropriate couplers (antennas, optics).
- **THz/GHz read-out :** The main applications within this range require development of multiplexing technology that could allow construction of focal plane arrays. On top of this, the read-out system must as well take the signal out from the cryogenic environment.
- **Cryostat design:** While currently available cryogenic technology is sufficient for reaching TED operational temperatures, progress have been made in development of rugged cryostats, which are of special interest in applications where the sensing technology has to be deployed away from laboratory environment.
- **Software :** is being developed for data processing and visualisation, system control and set up.

The development of these elements has been carried on in a collaborative manner, but only the partners with required skills have contributed to each. Table 11.1 summarises the contribution to each element

*This project has received funding from the European Union´s Horizon 2020 research and innovation programme under grant agreement No 800923.*

from the partners of the Consortium. Such contributions obviously generate Intellectual Property rights.

This information has been detailed so that external third parties who are interested only in a set of elements can understand who will be the partners involved in the negotiations. This should be the most likely scenario, as the TED technology has different fields of application (a third party interested in, for instance, applying the technology for THz sensing will not require access to the X-ray related elements). Taking into account these many possible fields of application of the TED technology (as described in Part I of this report), and following the recommendations given by the European Commission[1], exclusive licences granted without any limitation to a specific field of use will, in principle, be avoided.

[1] Commission Recommendation C(2008) 1329.

| | JYU | CSIC | CNR | NEEL | ADVA |
|---|---|---|---|---|---|
| **Material Fabrication** | | ✓ | | | |
| **Sensor Design** | ✓ | ✓ | ✓ | | |
| **X-ray Coupling** | ✓ | | | | |
| **X-ray read-out** | ✓ | | | | |
| **THz/GHz coupling** | | | ✓ | ✓ | |
| **THz/GHz read-out** | | | ✓ | ✓ | |
| **Cryostat design** | | | | ✓ | ✓ |
| **Software** | | | | | ✓ |

Table 11.1: **Distribution of Intellectual Property.** The table indicates which partners have been involved in the development of the main parts of the TED technology. In principle, these also corresponds to the distribution of the Intellectual Property generated for each element. This table has no contractual value, and has been presented for informative purposes only. Final distribution (once project is completed) may be different.

In the event of interest in licensing the TED technology, and assuming that SUPERTED project may already be completed, we find it important that the contact persons are clearly identified and easy to reach. This information has been summarised in Table 11.2. Technical contacts refer to researchers from the SUPERTED consortium who have played a relevant role and can provide detailed information about the technology, if needed. Technology Transfer contacts are members of the different partners' administrations who are aware of the project and can provide information regarding licensing terms and policies.

## 11.2 *Exploitation of the technologies*

SUPERTED Consortium proactively seeks to drive the technologies developed within the project towards successful commercial exploitation. As part of this policy, we have identified key technologies which have been produced during the project, and then try to set in plans specific actions for promoting these technologies outside of the Consortium. If the maturity of the technology allows for it, we try to set

*This project has received funding from the European Union´s Horizon 2020 research and innovation programme under grant agreement No 800923.*

| Partner | Technical Contact | Technology Transfer Contact |
|---|---|---|
| **JYU** | Tero Heikkilä<br>tero.t.heikkila@jyu.fi | Riikka Reitzer<br>riikka.reitzer@jyu.fi |
| **CSIC** | Sebastian Bergeret<br>sebastian_bergeret@ehu.es | Sheila González<br>sheila.gonzalez@csic.es |
| **CNR** | Elia Strambini<br>elia.strambini@sns.it | Giulio Bollino<br>giulio.bollino@cnr.it |
| **NEEL** | Alessandro Monfardini<br>alessandro.monfardini@neel.cnrs.fr | Nathalie Argoud<br>nathalie.argoud@dr11.cnrs.fr |
| **ADVA** | Francisco Lopez<br>francisco.gejo@advacam.com | Juha Kalliopuska<br>juha.kalliopuska@advacam.com |

Table 11.2: **Contact Directory:** Third parties external to the SUPERTED Consortium are advised to get in touch with the people listed in this directory for discussing about the possibility of licensing the technology. JYU: University of Jyväskylä, CSIC:Agencia Estatal Consejo Superior de Investigaciones Científicas, CNR:Consiglio Nazionale delle Ricerche, NEEL: Institut Néel, ADVA: Advacam Oy

in place an strategy for attracting funding that will allow to approach it to the markets.

## 11.3 *Exploitation of TED technology as a whole*

While the exploitation of TED as a whole (an ultra–sensitive thermoelectric sensor both for X-ray and THz radiation for multi-pixel imaging) should be an obvious target, the development of this technology up to a level where it could become usable will not be reached until the end of the project. Only at that point it will be possible to gain perspective about the performance in comparison with other competing technologies, such as those discussed in Part I.

In order to reinforce this stage, gather as much information as possible and maximise the chances of presenting the technology outside the Consortium, we have scheduled the set up of the different demonstration facilities, as described in Part II. All three planned activities will expose the TED to relevant constraints imposed by applications, and will be good opportunities for open discussion with potential end-users.

## 11.4 *Exploitation of key knowledge on fabrication of new materials*

Some of the most remarkable technological achievements of SUPERTED project concern the domain of Materials Science. The group from partner CSIC lead by Celia Rogero has been the first in Europe and second worldwide[2] which has been able to generate layered structures of ferromagnetic insulators and superconducting materials of enough quality to observe the giant thermoelectric effect. Such milestone is backed by the construction of an extensive knowledge

[2] Before SUPERTED project, the only group capable of fabricating layered structures was the one led by J. Moodera at MIT (US).

*This project has received funding from the European Union´s Horizon 2020 research and innovation programme under grant agreement No 800923.*

regarding several material growth technologies and the physics governing the material and their interfaces (see, for instance ref (**?** ) ).

This knowledge has a much larger range of applications than the manufacturing of the TED sensors, and indeed it will play an essential role on the development of strategic emerging technologies, and in particular in quantum computing and spintronics(**?** ). One of the key difficulties to solve, which is currently hindering the development of this technology, is the loss of quantum coherence which takes place at the interfaces(**?** ).

Although all this knowledge concerns mainly fundamental material sciences, the rapid development of applications like quantum computing is creating a need for actors who can provide both engineering and manufacturing services. With this idea in mind, we are currently trying to attract some institutional funding that could allow to further study the market, define the business model and prepare strategic documentation that can be used for presenting the project to investors.

This work is been done under the supervision of BIC Gipuzkoa[3]. This organisation, directly dependent from Basque Government (regional government) and Diputacion Foral (Province Administration) has the mission of fostering the creation of new entrepreneurial projects, particularly with a technological competitive edge. At the moment of submission of this report, we are submitting a proposal for funding in the range of 30.000€, that will be employed in market analysis and promotion of the project.

[3] Link to BIC Gipuzkoa homepage.

*This project has received funding from the European Union´s Horizon 2020 research and innovation programme under grant agreement No 800923.*

# 12
# *Conclusions*

The new sensing technology developed in the SUPERTED project has required several key achievements in many fields, including materials science, sensor design and signal processing. Reaching these milestones has been possible through collaborative work, in which several world-class research groups with different sets of skills and background have joined forces. As a result from this collaboration, the Intellectual Property - IP which has been generated will be shared among different partners, and therefore any party interested on licensing the technology will need to engage a round of negotiations with different institutions.

As this negotiation can be a complex task, we have found it important to ease as much as possible the contact, by establishing a clear map of the distribution of IP, and listing all relevant contacts.

We are also proactively seeking for ways of exploiting the key results of the project. The most relevant example so far concerns material fabrication. The processes required for building the layered structure of ferromagnetic insulating and superconducting materials are indeed useful for many other emerging fields, specially in the domain of quantum information technologies. We are currently working with regional institutions on the study of the market needs and the definition of a business model that can exploit this outcome.